Title
GDF10 is a signal for axonal sprouting and functional recovery after stroke

Journal
Nature Neuroscience, 18(12)

ISSN
1097-6256

Authors
Li, Songlin
Nie, Esther H
Yin, Yuqin
et al.

Publication Date
2015-12-01

DOI
10.1038/nn.4146

Peer reviewed

GDF10 Is a Signal for Axonal Sprouting and Functional Recovery after Stroke

Li S[1], Nie EH[1], Yin Y[2], Benowitz LI[2], Tung S[3], Vinters HV[3], Bahjat FR[4], Stenzel-Poore MP[4], Kawaguchi R[5], Coppola G[5], Carmichael ST[1,6]

1- Department of Neurology, David Geffen School of Medicine at UCLA, Los Angeles, CA
2-Laboratories for Neuroscience Research in Neurosurgery, Children's Hospital, Boston, MA
3-Department of Pathology and Laboratory Medicine (Neuropathology), David Geffen School of Medicine at UCLA, Los Angeles, CA
4- Department of Molecular Microbiology & Immunology, Oregon Health & Science University, Portland, OR
5- Program in Neurogenetics, Department of Neurology and Department of Psychiatry, Semel Institute for Neuroscience and Human Behavior, Los Angeles, CA
6 – Corresponding author. scarmichael@mednet.ucla.edu

ABSTRACT

Stroke produces a limited process of neural repair. Axonal sprouting in cortex adjacent to the infarct is part of this recovery process, but the signal that initiates axonal sprouting is not known. Growth and Differentiation Factor 10 (GDF10) is induced in peri-infarct neurons in mouse, non-human primate and human. GDF10 promotes axonal outgrowth *in vitro* in mouse, rat and human neurons through TGFβRI/II signaling. Using pharmacogenetic gain and loss of function studies, GDF10 produces axonal sprouting and enhanced functional recovery after stroke; knocking down GDF10 blocks axonal sprouting and reduces recovery. RNA-seq from peri-infarct cortical neurons indicates that GDF10 downregulates PTEN and upregulates PI3 kinase signaling and induces specific axonal guidance molecules. Unsupervised genome-wide association analysis of the GDF10 transcriptome shows that it is not related to neurodevelopment but may partially overlap with other CNS injury patterns. GDF10 is a stroke-induced signal for axonal sprouting and functional recovery.

Stroke is the leading cause of adult disability due to the brain's limited capacity for repair. Stroke induces axonal sprouting and the formation of new connections in peri-infarct cortex that link premotor, motor, somatosensory and association areas[1-4]. In humans, good functional recovery after stroke is associated with remapping of sensorimotor function in motor, somatosensory and premotor circuits[5,6] and is accompanied by increases in cortical thickness in these reorganizing areas[7]. In rodent and primate models of stroke, axonal sprouting and the formation of new connections occurs in motor, somatosensory and premotor areas[1-4]. These new connections are causally associated with functional recovery[4]. A better understanding of the mechanisms of axonal sprouting may allow the development of therapies to stimulate recovery after stroke. We previously used transcriptional profiling of single sprouting neurons to identify a unique gene expression profile, a post-stroke sprouting transcriptome[3]. The molecular networks in this transcriptome involve coordinated signaling systems from secreted growth factors and cytokines to cell surface receptors, intermediary cytoplasmic cascades, and transcriptional control molecules[3]. Within the post-stroke axonal sprouting transcriptome, Growth and Differentiation Factor 10 (GDF10) is one of the most highly upregulated genes during the initiation of axonal sprouting in peri-infarct cortical neurons in the aged brain.

There have been many studies of the molecules that block axonal sprouting after CNS injury, such as myelin proteins or chondroitin sulfate proteoglycans (CSPGs)[8-10], but the factor(s) that are triggered by stroke to promote the initiation of a molecular growth program and axonal sprouting are unknown. As a secreted growth factor, GDF10 is a

leading candidate for such a growth promoting signal after stroke. GDF10 is a divergent member of the bone morphogenetic protein (BMP)/transforming growth factor-β (TGFβ) superfamily[11-14] (Supplementary Fig. 1). Compared to other GDFs, GDF10 has a unique gene structure[12] and signals through TGFβ receptors (TGFβR)[14,15]. Though GDF10 mRNA is strongly expressed in the developing brain[16,17], a role for GDF10 in the adult brain or after CNS injury has not been described.

Here, we show that GDF10 upregulation after stroke is conserved across mice, non-human primates and humans. GDF10 promotes axonal sprouting through TGFβR I and II. *In vivo*, GDF10 enhances axonal sprouting in peri-infarct cortex and improves motor recovery after stroke; knockdown of GDF10 blocks this axonal sprouting and behavioral recovery. RNA-seq analyses indicate that GDF10 coordinately regulates several molecular signaling systems to induce a neuronal growth state that is distinct from other developmental, CNS- injury and adult plasticity phenotypes. These mechanistic insights into GDF10 begin to advance our understanding for its potential as a therapeutic target after stroke.

RESULTS

GDF10 expression in peri-infarct cortex after stroke

GDF10 is induced in sprouting neurons from aged rats during the initiation phase of axonal sprouting, 7 days after stroke[3]: 1.32x with microarray and 3x with confirmatory qPCR ($p<0.0009$) at 7d after stroke[3]. To confirm the universality of GDF10 induction, GDF10 was localized in peri-infarct tissue in mouse, non-human primate and human. There is a very low level of GDF10 present in neurons in non-stroke cortex (Fig. 1c,k,s). After stroke, GDF10 is induced in cells with markers of neurons and in brain tissue surrounding these neurons (Fig. 1, Supplementary Fig. 2a,b,d). GDF10 immunoreactivity within peri-infarct cortex is not present in cells with markers of microglia and astrocytes, but is seen in the extracellular matrix, as expected of a secreted protein in the peri-infarct cortex (Fig. 1, Supplementary Fig. 2d,e). By Western blot, GDF10 protein is significantly elevated in peri-infarct cortex (Supplementary Fig. 3). In these studies, GDF10 is induced in rodents (7 days after stroke), non-human primates (2 days) and humans (chronic period) indicating a large range of species and a broad time period for upregulation after stroke. GDF10 may serve as a paracrine signal for axonal sprouting.

GDF10 enhances axonal length of primary cortical neurons

A role for GDF10 in axonal outgrowth has not been previously established. In mouse primary cortical neurons, GDF10 produces an increase in axonal outgrowth, with the dose of 500ηg/ml producing equivalent axonal outgrowth to similar doses of the well-

described axonal sprouting growth factors braid derived growth factor (BDNF) and fibroblast growth factor 2 (FGF2) (Fig. 2a). GDF10 siRNA significantly knocks down GDF10 protein levels (Supplementary Figs. 3a,c) and inhibits axonal outgrowth from cortical neurons (Fig. 2b). To understand the effects of GDF10 on other neurons, we tested the effects of this molecule on FACS-isolated adult rat retinal ganglion cells (RGCs)[18]. GDF10 stimulates axonal outgrowth of RGCs compared to negative control. The relative proportion of this axonal outgrowth effect is independent of treatments that separately induce axonal outgrowth, such as elevation in cAMP with forskolin (Fig. 2e). These studies show that GDF10 enhances axonal outgrowth and knockdown of GDF10 blocks axonal outgrowth in several neuronal types, with a dose effect that is similar to other growth promoting factors.

Axonal outgrowth in the adult brain after stroke occurs in an environment inhibitory to axonal sprouting, with prominent induction of glial scar molecules such as CSPGs[5,6]. CSPGs inhibit axonal outgrowth of P4 cortical neurons in culture medium alone or with a protein control (Supplementary Fig. 3b). Significantly, GDF10 has a dose-dependent promotion of outgrowth in the presence of CSPGs (Fig. 2c).

GDF10 promotes axonal outgrowth *in vitro* via TGFβRs

Unlike other GDFs, GDF10 signals through TGFβRI and RII and downstream transcription factors Smad2/3, and not BMPRI/II and Smad1/5[15] (Supplementary Figure 1). To identify the molecular signaling systems for GDF10's axonal outgrowth effect,

neurons were treated with the TGFβRI antagonist SB431542, or TGFβRII or TGFβRIII siRNA. All siRNAs knockdown their respective protein target (Supplementary Fig. 3c,d) in this culture model system where GDF10 is expressed in neurons that have undergone the plating process (Supplementary Fig. 4). The axonal growth-promoting effect of GDF10 was significantly reduced either with blockade of TGFβRI or knockdown of TGFβRII (Fig. 3a). No statistical difference was noted between the groups treated with TGFβRIII siRNA+GDF10 and scrambled siRNA control+GDF10 (Fig. 3a). Knockdown of Smad2 or Smad3 significantly inhibited the axonal outgrowth effect of GDF10 on primary neurons. No significant difference in axonal length was noted between the groups of the scrambled siRNA+GDF10 and Smad1 or 5 siRNA treated with GDF10 (Fig. 3b). Furthermore, *in vivo* pharmacological blockade of TGFβRI/II using SB431542 and losartan[19,20] decreases Smad2/3 signaling in the peri-infarct tissue (Supplementary Fig. 5) during the period of GDF activity after stroke. In total, these studies show that TGFβRI/II and Smad 2/3 mediate the effects of GDF10 in enhancing axonal outgrowth.

These findings raise the question of whether TGFβ itself will promote axonal outgrowth from cortical neurons. This has been described with other primary neuronal systems[21,22], as well as the opposite—that Smad2 blocks axonal sprouting[23,24]. Administration of TGFβ1 to cortical neurons promotes axonal outgrowth. However, the axonal outgrowth effect of TGFβ is weaker than that of GDF10, as well as BDNF, and has a ceiling effect (Fig. 3g). Smad2 was directly transfected into P4 cortical neurons to test its effect on axonal outgrowth. This produces a significant increase in axonal outgrowth compared to control plasmid transfection (Fig. 3f). These data provide independent confirmation that

Smad2 downstream signaling from TGFβRI/II promotes axonal sprouting, but suggest that additional elements in GDF10 action play a role in the full axonal sprouting effect.

GDF10 stimulates axonal outgrowth of human iPS-neurons

Human and rodent cells may respond differently to TGFβ/BMP signaling[25]. To determine if GDF10 has axonal growth-promoting effects on human neurons, human induced pluripotent stem cell derived neurons (hiPS-neurons) [26,27] were tested. GDF10 promotes significant axonal outgrowth of hiPS-neurons (Figs. 3c,e,f) and blockade of TGFβRI or knockdown of TGFβRII in the presence of GDF10 prevents GDF10-induced axonal outgrowth (Fig. 3c). Also, the growth-promoting effect of GDF10 is blocked by knockdown of Smad 2/3 (Fig. 3d). This data indicates that GDF10 has a common signaling pathway for axonal outgrowth in human and rodent neurons.

GDF10 increases axonal connections in peri-infarct cortex

A candidate signal for axonal sprouting in peri-infarct cortex after stroke would be induced at the stroke site and promote the formation of new connections. To test this hypothesis, GDF10 gain and loss of function was produced directly from the stroke through sustained release via biopolymer hydrogel, which produces release over 2-3 weeks from the stroke site[3,4,28] without altering local inflammation, gliosis, neuronal or vascular structure[4]. As previously shown in other gene systems[3,4], nucleotide-modified siRNA delivered directly into the infarct core produces protein knockdown over at least 2

weeks after stroke with GDF10 (Supplementary Fig. 3a).

Mice received a stroke in forelimb motor cortex, followed 7 days later by injection of GDF10/hydrogel or GDF10 siRNA. This 7 day period is when GDF10 is induced in peri-infarct cortex in the rodent[3] (Fig. 1). Twenty-one days later the neuronal tracer biotinylated dextran amine (BDA) was microinjected into the intact forelimb motor cortex anterior to the stroke site. New connections in peri-infarct cortex can be detected after stroke within this timeframe[3,4,29]. The BDA-labeled connections of the forelimb motor cortex were quantitatively mapped and registered to functional cortical areas using the somatosensory body map[3,4,28,29] and to the location of corticospinal neurons in motor, premotor and somatosensory areas retrogradely labeled from the spinal cord (Supplementary Fig. 6a). There is no significant difference in BDA injection location and volumes, or in infarct volumes across all experimental conditions (Supplementary Fig. 7a,b). As reported previously[3,4,28,29], stroke alone modestly but significantly induces axonal sprouting in the motor cortex adjacent to the stroke site compared to normal motor system connections (Supplementary Fig. 6b). This post-stroke axonal sprouting occurs from motor cortex, posteriorly towards immediate peri-infarct motor and somatosensory areas.

Two control conditions were utilized for GDF10 protein and siRNA delivery: stroke+scrambled siRNA and stroke+protein control (cytochrome C). These produced the same pattern of connections as stroke-alone (n = 8-9 per group, Supplementary Figs. 8 and 9). Quantitative connectional mapping shows that stroke+GDF10 induces a

statistically significant change in cortical connections compared to stroke alone and stroke+protein control, with a robust projection from motor cortex anteriorly to premotor and prefrontal cortex (n = 8-9 per group, Fig. 4a-c). This is a non-isotropic increase in projections, with a unique frontally-projecting axonal connection with GDF10 delivery after stroke. To further quantify the location of individual neuronal projections the number of labeled axons was counted in a linear distribution in each tangential section through the injection site, extending across the cortical hemisphere (Fig. 4c). This shows a significant increase in neuronal projections with GDF10 delivery, particularly anterior to the motor cortex. Furthermore, colocalization analysis of the pre- and post-synaptic markers VGLUT2 and Homer1 indicate that BDA-labeled sprouting neurons contain the pre-synaptic glutamatergic marker in tight association with the post-synaptic marker Homer1 (Supplementary Fig 10). siRNA knockdown of GDF10 significantly inhibits cortical axonal sprouting after stroke (Fig. 4d,e), producing a pattern of motor system axonal connections that resembles the non-stroke, normal brain (Fig 4d; Supplementary Figs 8, 13). These data show that GDF10 induces substantial axonal sprouting and synapse formation after stroke into premotor and prefrontal areas, and blocking GDF10 eliminates the normal pattern of axonal sprouting seen in stroke to produce a pattern of motor system connections that is not statistically different from that of the normal brain.

GDF10 increases angiogenesis and gliosis after stroke

TGFβ family members stimulate astrocyte responses and modify angiogenesis and neuroinflammation[30,31]. To determine what tissue changes occur concomitantly to enhanced axonal outgrowth with GDF10, we analyzed markers for these processes

following GDF10 delivery or knockdown in stroke at the time of increased axonal sprouting. As previously reported[4], stroke alone produced increased levels of GFAP, CD31/PECAM and IBA-1, makers for astrocytes, endothelial cells and microglia/macrophages, respectively (Fig. 5). GDF10 significantly increased astrocytosis, as indicated by an increase in the area of GFAP+ processes, and in blood vessel area, as indicated by an increase in PECAM+ endothelial cell area, above that seen in stroke, with no significant effect on microglial staining (Fig. 5). GDF10 knockdown decreased vascular, astrocyte and microglial staining compared with stroke-alone. The delivery of control protein or scrambled siRNA had no effect on these processes. These data indicate that GDF10 delivery not only enhances axonal sprouting, but also induces vascular remodeling and astrocytosis. The GDF10 knockdown effect indicates that in the normal process of post-stroke tissue reorganization, GDF10 is partially responsible for post-stroke astrocyte, blood vessel and microglial changes.

GDF10 improves functional recovery after stroke

To determine if GDF10-induced axonal sprouting promotes functional recovery, we tested mice on forelimb motor tasks using the same forelimb motor cortex stroke in which axonal sprouting was measured. The grid walking, cylinder and pasta handing tasks measure gait, exploratory forelimb use and skilled control of thin pasta pieces[4,29,32,33]. GDF10 and GDF10 siRNA were delivered as in the axonal sprouting studies (Fig. 4).

Stroke produces impairments in forelimb motor control for an extended period: at least 11 weeks (pasta handling) or 15 weeks after stroke (cylinder, gridwalking) (Fig. 6).

Delivery of GDF10 starting 1 week after stroke enhances recovery beginning from 3 weeks post-stroke (Fig. 6). With GDF10 delivery, mice performed at the level of non-stroke motor control by 5 weeks after the infarct. Remarkably, GDF10 siRNA produces a significant reduction in the normal process of recovery after stroke, beginning 1-3 weeks after delivery. No significant changes in motor performance were observed among animals treated with protein or siRNA delivery controls. Thus, administration of GDF10 protein improves motor recovery after stroke and knocking down GDF10 levels significantly decreases functional recovery. These behavioral data indicate that endogenous GDF10 has an important role in normal recovery after stroke and that the neuronal sprouting mapped *in vivo* may represent formation of neural circuits that cause behavioral improvement.

Systems biology of GDF10 in the CNS

To understand the molecular program induced by GDF10 during axonal sprouting and functional recovery after stroke, we FACS-isolated cortical neurons (based on NCAM) (Fig. 7a) from GDF10+stroke, stroke-alone, normal control and at age P4, a time in which cortical neurons are forming new connections during development[34]. The number of reads ranged from 64,602,785 to 107,291,640 and the uniquely mapped reads ranged from 43,087,682 to 85,407,243. The differentially expressed genes were analyzed after a cutoff for a false discovery rate (FDR) of <0.1.

The greatest difference in the transcriptomes among conditions is between adult cortical neurons, from control, stroke and stroke+GDF10, compared to the developmental age of

P4 (Fig. 7b). This indicates that the biggest alteration in the neuronal transcriptome is between adult and developmental states, rather than with the presence of a stroke or with GDF10 delivery. Unsupervised cluster analysis of these transcriptomes confirms that the adult vs. neonatal gene expression changes cluster together (Fig. 7c). After this distinction, the most unique transcriptome is stroke+GDF10 vs. stroke. Thus, GDF10 delivery in stroke regulates a unique transcriptome that consists of a smaller set of genes from that seen during the initial process of axonal sprouting in neurodevelopment. An open question in the field of neural repair is if the molecular program stimulated by tissue regeneration resembles that seen in neurodevelopment, i.e. if "regeneration recapitulates development". These results indicate that GDF10 delivery in stroke, which promotes axonal sprouting in the adult, regulates a dramatically different and smaller set of genes from that seen during the initial process of axonal sprouting in neurodevelopment and in the adult state, GDF10 induces a unique transcriptome after stroke.

Stroke+GDF10 significantly regulates specific canonical pathways in post-stroke neurons (Supplementary Table 2). Among the most highly regulated are Axonal Guidance, PTEN and PI3K signaling (Fig. 8a). PTEN canonical signaling (8 genes in class) is downregulated, and PI3K canonical signaling (12 genes in class) is upregulated with GDF10 in stroke (Supplementary Tables 3-6). Axonal guidance molecules that are differentially regulated by GDF10 in stroke include Ephrin A3, Tα1tubulin, Beta-II-tubulin, VEGFd, neuropilin 1, SOCS3 and downstream molecules in the Rho and Rac pathways (Supplementary Tables 7, 8). PTEN and SOCS3 inhibition induce axonal sprouting in multiple adult CNS systems, including optic nerve and spinal cord injury[8,35].

The differential control of PTEN, PI3K and SOCS3 signaling by GDF10 represents a potential mechanism of action in axonal sprouting after stroke.

Axonal sprouting after stroke shares similarities with the neuronal morphology changes in learning and memory paradigms, optic nerve and spinal cord regeneration and neurodevelopment[36,37]. We used unsupervised genome-wide association analysis to compare our data from GDF10 and stroke to transcriptomes from cortical neuronal outgrowth during development; the cortical critical period; mouse growth cones; P7 to P28 mouse neurons; motor cortex after spinal cord injury; retina after optic nerve crush; contralateral cortex after stroke; and learning and memory paradigms in hippocampus and medial prefrontal cortex (Supplementary Table 9). The data from 180 microarray or RNA-seq studies were analyzed from original array files, normalized, controlled for batch effect (Supplementary Fig. 11) and statistically compared to the present data sets for cortical neurons from stroke, stroke+GDF10, control and P4. There is a variance in statistical spread across transcriptomes, even from the same cell population in the same experiment (Fig. 8c), which likely has to do with the fact that these transcriptional profiles are mostly from specific cell types, rather than from large in vitro preparations or tissue-level sources. For example, in layer V/VI from motor cortex after spinal cord injury, transcriptomes from the same condition can vary across 30 units in statistical space; similar variance is seen with cortical efferent neurons, such as callosal neurons at P4 and in adult optic nerve injury. Within the variance in gene expression in these conditions of axonal sprouting, injury or learning and memory, stroke and stroke+GDF10 transcriptomes are separated by the largest difference from cortical P4 neurons,

confirming the cluster analysis within this data set (Fig. 8c). Stroke and stroke+GDF10 transcriptomes cluster closely together with a relationship to retina 12 hours after optic nerve crush. Mouse growth cone, mouse cortical critical period and corticospinal and callosal postnatal neuronal transcriptomes cluster together but not near stroke+GDF10 or stroke-alone. These data indicate that GDF10 induces a unique transcriptional profile after stroke, more closely related to stroke alone than to the transcriptomes seen in several contexts of neuronal development, CNS injury or of learning and memory.

DISCUSSION

Axonal sprouting in the adult occurs in a limited manner after stroke, optic nerve lesions, spinal cord injury and in models of neurodegenerative diseases[8,9]. After stroke, axonal sprouting has been demonstrated in mice, rats and non-human primates[1-4,10,38]. In humans, the initial cloning studies of GAP43, the paradigmatic neuronal growth cone marker , showed that it is induced in peri-infarct cortex after stroke[39] and increases cortical thickness in regions of cortical map plasticity during recovery[7]. The induction of axonal sprouting in adult cortex after stroke and the formation of new patterns of connections suggests that neurons have been placed into a growth state. Much scientific study has focused on the molecular components of the injury response that block axonal sprouting, such as the glial growth inhibitors NogoA and the chondroitin sulfate proteoglycans[8-10]. However, there has been comparatively less research on the molecular signals for a neuronal growth program after stroke. The present data indicate that GDF10 is induced after stroke in a wide range of species, promotes axonal outgrowth *in vitro* in human, mouse and rat neurons, and induces axonal sprouting and functional recovery after stroke *in vivo*. Knockdown of endogenous GDF10 after stroke reduces axonal sprouting and recovery. GDF10 controls a unique transcriptional profile with differential regulation of PTEN, PI3K and axonal outgrowth molecules. These findings suggest that GDF10 is a post-stroke axonal sprouting signal that induces functional recovery.

Stroke normally produces a limited pattern of axonal sprouting from motor or somatosensory cortex posteriorly to areas adjacent to or caudal to the stroke[2-4,28,29].

GDF10 delivery induces a unique connectional pattern—substantial projections anterior from motor cortex to premotor and prefrontal areas. We localized these connections topographically using retrograde back-labeling of the corticospinal neurons to identify primary somatosensory, motor and premotor areas and with histological demonstration of the rodent whisker cortex for mouse primary somatosensory areas. This anterior projection from motor cortex to premotor cortex is causally associated with functional recovery in this model of stroke[4]. The magnitude of post-stroke axonal sprouting induced by GDF10 exceeds that seen with the blockade of several axonal growth inhibitory systems, such as ephrin-A5[4] and Nogo/NgR1[3]. Further, knockdown of GDF10 after stroke abolishes the normal process of post-stroke axonal sprouting and reduces functional recovery. These results indicate that the normal release of stroke-induced GDF10 participates in the limited motor recovery that occurs naturally in stroke.

GDF10 signals through TGFβ receptors. In other *in vitro* systems, TGFβ promotes axonal outgrowth of injured neurons[21,22,39,40] and blockade of TGFβRII alters neuronal polarity and leads to shorter axons[42]. However, activation of Smad2 signaling has also been reported to occur with myelin axonal growth inhibition, and direct activation of Smad2 reduces axonal outgrowth in some preparations[22,24]. These discrepant findings of both axonal sprouting and axonal growth inhibition with TGFβ may stem from non-canonical signaling or context-specific signaling. Though TGFβ and GDF10 both signal through TGFβRI/II[12-14], we show that their signaling levels are not equivalent. These growth factors may produce non-canonical signaling outside of the Smad transcription factors, such as through the MAPK pathway[40,41].

The action of TGFβRI/II signaling in axonal outgrowth may be context specific in terms of the local tissue environment and differ between local axonal sprouting in peri-infarct cortex and distant axonal sprouting from corticospinal neurons after spinal cord injury. We find that the transcriptomes for these two sprouting conditions are very different (Fig. 8b). Such context-specific signaling is a hallmark of TGFβ in its role in cancer, where it switches from inhibition of tumor growth and metastasis to promotion of endothelial to mesenchymal transition and metastasis as the local tumor environment evolves[14,43].

GDF10 activates a coordinated upregulation of genes in the PI3kinase pathway, downregulation of genes in the PTEN pathway and control of specific axonal guidance molecules, including a downregulation of SOCS3. PTEN inhibition potentiates axonal sprouting in optic nerve injury and spinal cord injury, through induction of PI3kinase signaling and activation of mTOR. Inhibition of SOCS3 further promotes axonal sprouting on top of PTEN inhibition[8,37,38]. Detailed analysis of the GDF10 transcriptome in stroke will provide further insights into mechanisms for the GDF10 trigger for post-stroke axonal sprouting. In all, GDF10 represents a significant regulator of axonal outgrowth and functional recovery after stroke and may present a valuable target for therapeutic intervention. With such a therapy in mind, systemic delivery of TGFβ would activate its signaling systems in all tissue of the body. TGFβ promotes tissue fibrosis and has potential direct deleterious effects on kidney, liver and immune function[14]. A possible approach to a GDF10 or TGFβ therapeutic in stroke is either short term systemic delivery to minimize non-CNS effects or site-specific delivery, as achieved in the present

approach with tissue bioengineering, to produce a GDF10 effect specifically in peri-infarct cortex.

ACKNOWLEDGMENTS

This research was supported by US National Institutes of Health grants NS085019 and NS086431, American Heart Association grant 09SDG2310180, Richard Merkin Foundation for Neural Repair at UCLA, the Dr. Miriam and Sheldon G. Adelson Medical Research Foundation and the Edwin W. and Catherine Davis Foundation. We thank Dr. William Lowry (UCLA) for human iPS-neural precursor cells and the NINDS Informatics Center for Neurogenetics and Neurogenomics (P30 NS062691) at UCLA for deep sequencing, alignment and RNA-seq analysis.

AUTHOR CONTRIBUTIONS

S.T.C, S.L. and E.H.N conceived the project. S.T.C., S.L., and E.H.N designed the experiments. S.L. performed most of the experiments. E.H.N. performed immunohistochemical characterization of GDF10 expression, FACS, RNA isolation, synapse analyses, and in vivo TGFβ blockade experiments. Y.Y. and L.I.B. performed rat neuronal experiments. S.T. and H.V.V. performed human tissue preparation. FRB and M.P.S-P. performed primate stroke experiments. R.K. and C.G. performed RNA-seq and bioinformatics experiments. S.T.C., E.H.N. and S.L. wrote the manuscript.

COMPETING FINANCIAL INTERESTS

The authors declare no competing financial interests.

REFERENCES

1. Dancause N, Barbay S, Frost SB, Plautz EJ, Chen D, Zoubina EV, Stowe AM, Nudo RJ. Extensive cortical rewiring after brain injury. J Neurosci. 2005 Nov 2;25(44):10167-79.
2. Brown CE, Aminoltejari K, Erb H, Winship IR, Murphy TH. In vivo voltage-sensitive dye imaging in adult mice reveals that somatosensory maps lost to stroke are replaced over weeks by new structural and functional circuits with prolonged modes of activation within both the peri-infarct zone and distant sites. J Neurosci. 2009;29:1719-34.
3. Li S, Overman JJ, Katsman D, Kozlov SV, Donnelly CJ, Twiss JL, et al. An age-related sprouting transcriptome provides molecular control of axonal sprouting after stroke. Nat Neurosci. 2010;13:1496-504.
4. Overman JJ, Clarkson AN, Wanner IB, Overman WT, Eckstein I, Maguire JL, et al. A role for ephrin-A5 in axonal sprouting, recovery, and activity-dependent plast icity after stroke. Proc Natl Acad Sci U S A. 2012;33:1-22.
5. Favre I, Zeffiro TA, Detante O, Krainik A, Hommel M, Jaillard A. Upper limb recovery after stroke is associated with ipsilesional primary motor cortical activity: a meta-analysis. Stroke. 2014;45:1077-83
6. Kantak SS, Stinear JW, Buch ER, Cohen LG. Rewiring the brain: potential role of the premotor cortex in motor control, learning, and recovery of function following brain injury. Neurorehabil Neural Repair. 2012;6:282-92

7. Schaechter JD, Moore CI, Connell BD, Rosen BR, Dijkhuizen RM. Structural and functional plasticity in the somatosensory cortex of chronic stroke patients. Brain. 2006; 129:2722-33.
8. Liu K, Tedeschi A, Park KK, He Z. Neuronal intrinsic mechanisms of axon regeneration. Annu Rev Neurosci. 2011;34:131-52.
9. Soleman S, Filippov MA, Dityatev A, Fawcett JW. Targeting the neural extracellular matrix in neurological disorders. Neuroscience. 2013;253:194-213.
10. Wahl AS, Omlor W, Rubio JC, Chen JL, Zheng H, Schroter A, et al. Neuronal repair. Asynchronous therapy restores motor control by rewiring of the rat corticospinal tract after stroke. Science. 2014;344:1250-5.
11. Cunningham NS, Jenkins NA, Gilbert DJ, Copeland NG, Reddi AH, Lee SJ. Growth/differentiation factor-10: a new member of the transforming growth factor-beta superfamily related to bone morphogenetic protein-3. Growth Factors. 1995;12:99-109.
12. Katoh Y, Katoh M. Comparative integromics on BMP/GDF family. Int J Mol Med. 2006;17:951-5.
13. Carreira AC, Lojudice FH, Halcsik E, Navarro RD, Sogayar MC, Granjeiro JM. Bone morphogenetic proteins: facts, challenges, and future perspectives. J Dent Res. 2014;93:335-45.
14. Akhurst RJ, Hata A. Targeting the TGFβ signalling pathway in disease. Nat Rev Drug Discov. 2012;11:790-811.
15. Upadhyay G, Yin Y, Yuan H, Li X, Derynck R, Glazer RI. Stem cell antigen-1 enhances tumorigenicity by disruption of growth differentiation factor-10

(GDF10)-dependent TGF-beta signaling. Proc Natl Acad Sci U S A. 2011;108:7820-5.

16. Soderstrom S, Ebendal T. Localized expression of BMP and GDF mRNA in the rodent brain. J Neurosci Res. 1999;56:482-92.
17. Zhao R, Lawler AM, Lee SJ. Characterization of GDF-10 expression patterns and null mice. Dev Biol. 1999;212:68-79
18. Yin Y, Cui Q, Li Y, Irwin N, Fischer D, Harvey AR, et al. Macrophage-derived factors stimulate optic nerve regeneration. J Neurosci. 2003;23:2284-93
19. Bar-Klein G, Cacheaux LP, Kamintsky L, Prager O, Weissberg I, Schoknecht K, Cheng P et al. Losartan prevents acquired epilepsy via TGF-b signaling suppression. Ann Neuol 2014;75:864–875.
20. Waghabi MC, de Souza EM, de Oliveira GM, Keramidas M, Feige J-J, Arau´jo-Jorge TC, Bailly S. Pharmacological inhibition of Transforming Growth Factor β signaling decreases infection and prevents heart damage in acute Chagas' Disease. Antimicrobial Agents Chemo 2009;53: 4694–4701
21. Ishihara A, Saito H, Abe K. Transforming growth factor-beta 1 and -beta 2 promote neurite sprouting and elongation of cultured rat hippocampal neurons. Brain Res. 1994;639:21-5.
22. Knöferle J, Ramljak S, Koch JC, Tönges L, Asif AR, Michel U, Wouters FS, Heermann S, Krieglstein K, Zerr I, Bähr M, Lingor P. TGF-beta 1 enhances neurite outgrowth via regulation of proteasome function and EFABP. Neurobiol Dis. 2010 Jun;38(3):395-404.

23. Hannila SS, Siddiq MM, Carmel JB, Hou J, Chaudhry N, Bradley PM, et al. Secretory leukocyte protease inhibitor reverses inhibition by CNS myelin, promotes regeneration in the optic nerve, and suppresses expression of the transforming growth factor-beta signaling protein Smad2. J Neurosci. 2013;33:5138-51.
24. Stegmuller J, Huynh MA, Yuan Z, Konishi Y, Bonni A. TGFbeta-Smad2 signaling regulates the Cdh1-APC/SnoN pathway of axonal morphogenesis. J Neurosci. 2008;28:1961-9.
25. Vallier L, Pedersen RA. Human embryonic stem cells: an in vitro model to study mechanisms controlling pluripotency in early mammalian development. Stem Cell Rev. 2005;1:119-30.
26. Chin MH, Pellegrini M, Plath K, Lowry WE. Molecular analyses of human induced pluripotent stem cells and embryonic stem cells. Cell Stem Cell. 2010 Aug 6;7(2):263-9.
27. Pasca SP, Portmann T, Voineagu I, Yazawa M, Shcheglovitov A, Pasca AM, et al. Using iPSC-derived neurons to uncover cellular phenotypes associated with Timothy syndrome. Nat Med. 2011;17:1657-62.
28. Clarkson AN, Lopez-Valdes HE, Overman JJ, Charles AC, Brennan KC, Thomas Carmichael S. Multimodal examination of structural and functional remapping in the mouse photothrombotic stroke model. J Cereb Blood Flow Metab. 2013;33:716-23.

29. Clarkson AN, Overman JJ, Zhong S, Mueller R, Lynch G, Carmichael ST. AMPA receptor-induced local brain-derived neurotrophic factor signaling mediates motor recovery after stroke. J Neurosci. 2011;31:3766-75.
30. Smith GM, Strunz C. Growth factor and cytokine regulation of chondroitin sulfate proteoglycans by astrocytes. Glia. 2005;52:209-18.
31. Wang J, Wang Y, Wang Y, Ma Y, Lan Y, Yang X. Transforming growth factor β-regulated microRNA-29a promotes angiogenesis through targeting the phosphatase and tensin homolog in endothelium. J Biol Chem. 2013 Apr 12;288(15):10418-26.
32. Tennant KA, Asay AL, Allred RP, Ozburn AR, Kleim JA, Jones TA. The vermicelli and capellini handling tests: simple quantitative measures of dexterous forepaw function in rats and mice. J Vis Exp. 2010 Jul 21;(41). pii: 2076.
33. Clarkson AN, Huang BS, Macisaac SE, Mody I, Carmichael ST. Reducing excessive GABA-mediated tonic inhibition promotes functional recovery after stroke. Nature. 2010;468:305-9.
34. Dye CA, El Shawa H, Huffman KJ. A lifespan analysis of intraneocortical connections and gene expression in the mouse I. Cereb Cortex. 2011; 21:1311-30.
35. Sun F, Park KK, Belin S, Wang D, Lu T, Chen G, Zhang K, Yeung C, Feng G, Yankner BA, He Z. Sustained axon regeneration induced by co-deletion of PTEN and SOCS3. Nature. 2011;480:372-5.
36. Carmichael ST. Translating the frontiers of brain repair to treatments: starting not to break the rules. Neurobiol Dis. 2010;37:237-42.

37. Liu K, Tedeschi A, Park KK, He Z. Neuronal intrinsic mechanisms of axon regeneration. Annu Rev Neurosci. 2011;34:131-52.

38. Zai L, Ferrari C, Subbaiah S, Havton LA, Coppola G, Strittmatter S, et al. Inosine alters gene expression and axonal projections in neurons contralateral to a cortical infarct and improves skilled use of the impaired limb. J Neurosci. 2009;29:8187-97.

39. Ng SC, de la Monte SM, Conboy GL, Karns LR, Fishman MC. Cloning of human GAP-43: growth association and ischemic resurgence. Neuron. 1988;1:133-9.

40. Abe K, Chu PJ, Ishihara A, Saito H. Transforming growth factor-beta 1 promotes re-elongation of injured axons of cultured rat hippocampal neurons. Brain Res. 1996;723:206-9.

41. Walshe TE, Leach LL, D'Amore PA. TGF-beta signaling is required for maintenance of retinal ganglion cell differentiation and survival. Neuroscience. 2011;189:123-31.

42. Yi JJ, Barnes AP, Hand R, Polleux F, Ehlers MD. TGF-beta signaling specifies axons during brain development. Cell. 2010;142:144-57.

43. Lenferink AE, Cantin C, Nantel A, Wang E, Durocher Y, Banville M, et al. Transcriptome profiling of a TGF-beta-induced epithelial-to-mesenchymal transition reveals extracellular clusterin as a target for therapeutic antibodies. Oncogene. 2010;29:831-44.

FIGURE LEGENDS

Figure 1. GDF10 expression in peri-infarct cortex after stroke in mice, macaques and humans. Top section shows immunohistochemical staining in peri-infarct cortex in mice 7 days after stroke (n=5). GD10 staining (red) is apparent in peri-infarct tissue, overlapping with NeuN staining (green). Arrows in bottom right panel show representative NeuN+/GDF10+ cells. Schematic at right shows location of stroke as red shaded area; box is position of photomicrographs. The panels below the mouse schematic are higher magnification of GDF10 (red) co-localizing to neurons whose dendrites are MAP2+ (white), denoted by arrows. Middle section shows immunohistochemical staining in peri-infarct cortex in non-human primate (n = 2 stroke, n = 3 control) 2 days after stroke. Same conventions as in mouse panels. Arrows in bottom right show double labeled NeuN+/GDF10+ neurons after stroke. Bottom section shows mmunohistochemical staining in human control (n = 4) and stroke (n = 7). Arrows show double labeled NeuN+/GDF10+ neurons after stroke. In this human case the stroke is chronic, or greater than 3 months after the event. Scale bar = 50 μm and applies to all photomicrographs.

Figure 2. GDF10 enhances axonal outgrowth in primary neurons *in vitro*. (**a-c)** Axonal outgrowth in P4 mouse primary cortical neurons. Axon length was measured after 3 days in culture. Cyto C = cytochrome C, a protein control for the addition of growth factor, used in the *in vivo* studies (Fig. 4a). In (**c**), wells are plated with CSPG prior to cell growth. (**d**) P4 cortical neurons stained with SMI-312 after 2 additional days culture in medium alone or medium+GDF10 (500 ηg /ml). Scale bar = 20 μm. (**e**) Rat adult RGCs

cultured in presence of GDF10, forskolin or mannitol. n=7 in culture medium only; n=8 the other 3 groups. Two independent cultures per condition and in each culture 4 wells repeating the condition. * = P<0.05, ** = P<0.01, compared to Medium only; ^ = P<0.05 compared to Medium+GDF10; # = P<0.05, ## = P<0.01 compared to Scrambled+GDF10; @ = P<0.05, @@ = P<0.01 compared to Protein control Cyto C. All conditions were tested in quadruplicate, in two separate experiments. In (a) F (6, 105) = 7.220; (b) F (6, 105) = 8.384; (c) F (6, 105) = 22.44; (e) medium vs GDF10: t=2.852 df=13; fosk/mann vs fosk/man GDF10:t=2.371 df=14. Error bars are SEM. All observations are normalized to the number of NeuN positive cells in each sample (Supplementary Figure 12). Statistical testing is repeated-measures ANOVA followed by Tukey-Kramer's post hoc test (a-c) or one tail unpaired T test (e).

Figure 3. GDF10 enhances axonal outgrowth in human neurons via TGFβ signaling.

(**a**, **b**) P4 mouse cortical neuron culture with TβRI/II and Smad blockade. SB431542 is a TGFβRI antagonist, added at initial plating. (**c, d**) human iPS-neurons cultured in the presence of GDF10, SB431542, or TβRII, Smad2 and Smad3 siRNA. Each condition is 2-4 observations in 2-3 independent experiments. (**e**,**f**) iPS-NPCs in culture with GDF10 for 2 days, stained with SMI-312 for axons. Scale bar = 20 μm. (**g**) TGFβ1 and smad2 enhance axonal outgrowth of P4 primary cortical neurons. Axon length with treatment of TGFβ1 at ascending concentrations. N=3 for each experiment. (**h**) Axonal outgrowth with transfection of Smad2 expression plasmid. Conventions as in (g). * =P<0.05, ** =P<0.01, *** = P<0.005 compared to Medium only; ^ = P<0.05 compared to Medium+GDF10; # = P<0.05, ## = P<0.01 compared to Scrambled+GDF10; @ =

P<0.05, @@ = P<0.01 compared to Protein control Cyto C. All conditions were tested in quadruplicate, in two separate experiments. In (a) F (5, 186) = 10.28; (b) F (2, 93) = 6.138; (c) F (4, 155) = 10.23; (d) F (4, 155) = 11.49; (g) F (2, 93) = 4.435; (h) t test, two-tailed t = 3.073 df = 62. Error bars are SEM. All observations are normalized to the number of NeuN positive cells in each sample (Supplementary Figure 12). Statistical testing is repeated-measures ANOVA followed by Tukey-Kramer's post hoc test (a-d,g) or one tail unpaired T test (h).

Figure 4. GDF10 promotes axonal connections in peri-infarct cortex after stroke. (**a**) Quantitative cortical mapping of connections in layers II/III of the flattened mouse cortical hemisphere ipsilateral to the forelimb motor cortex in stroke with protein control (Cyto C) (blue, n=8), GDF10+Stroke (red, n=8), and areas of dense overlap of these two conditions (dark blue). X and Y axes are distances in millimeters from the center of the BDA tracer injection (empty circle). P value is Hotellings T^2. The horizontal line shows the position in which neuronal label was quantified within the ipsilateral hemisphere (**c**). (**b**) Polar plot of connections of forelimb motor cortex projections relative to the tracer injection in forelimb motor cortex as the origin. Filled polygons represent the 70th percentile of the distances of all BDA labeled connections from the injection site in each segment of the graph. Weighted polar vectors represent the median vector multiplied by the median of the normal distribution of the number of points in a given segment of the graph. P value is Watson's nonparametric two-sample U^2 test. (**c**) Projections from forelimb motor cortex after stroke with GDF10 delivery (red) and protein control (Cyto C) (red) taken from counts along the line in (**a**). * = P<0.05, **=P<0.01. Inset shows

schematic mouse brain with the location of the BDA injection (black dot) and the linear quantification construct (line). (**d**) Quantitative cortical mapping of GDF10 knockdown in stroke. Same conventions as in (**a**). (**e**) Polar plots of GDF10 siRNA and scrambled siRNA after stroke with same conventions as in (**b**). (**f**) Linear quantification of neuronal connections in treatment groups of GDF10 siRNA+Stroke and scrambled siRNA+Stroke. Same conventions as in (**c**). In (c) F (1, 10) = 12.03; (f) F (1, 10) = 20.24. In (b) $U^2$647.176, df 90939, df2 180911; (e) U^2 78.616, df 38554, df2 5906. Error bars are SEM. The circle in (a) and (d) indicates the center of the stroke site.

Figure 5. Astrocyte, endothelial and inflammatory responses in peri-infarct cortex with GDF10 after stroke. All data are 28 days after stroke. (**a**) GFAP immunoreactivity is increased in all stroke conditions compared to control (* = $p< 0.05$, ** = $p<0.01$ vs. control, ^, # = $p< 0.05$ vs. stroke only, stroke+protein control, respectively) and significantly decreased in GDF10 siRNA+stroke compared to the scrambled siRNA ($=$p<0.05 vs scrambled siRNA+stroke). (**b**) Photomicrographs of GFAP immunostaining in stroke and Stroke+GDF10. (**c**) PECAM/CD31 immunoreactivity for endothelial cells in control and gain and loss of function in GDF10 after stroke. Conventions as in (**a**). GDF10 induces an increase and GDF10 siRNA reduces a decrease in PECAM immunoreactive vessels in peri-infarct cortex after stroke. (**d**) PECAM staining in peri-infarct cortex in stroke and stroke+GDF10. (**e,f**) IBA-1 immunoreactivity for microglia/macrophages in peri-infarct cortex. Stroke increases the microglial staining in peri-infarct cortex. GDF10 knockdown significantly reduces ($ = $p<0.05$) the staining of microglia/macrophages compared to scrambled siRNA+stroke. ($ = $p<0.05$).

However, there is a significant difference in IBA-1 immunoreactive signal between groups of GDF10+Stroke and cyto C+Stroke. Bar in (f)=50μm. See Supplementary Table 11 for sample size and ANOVA statistics.

Figure 6. GDF10 improves behavioral recovery after stroke. (**a**) Cylinder test of forelimb symmetry in exploratory rearing (n=7 all conditions in behavioral testing). Y axis shows bilaterally symmetric rearing as 0.0 and percent of left (unaffected) forelimb rearing as negative values. Left graph: Stroke causes a significant increase in the number of rears with the left forelimb. GDF10 treatment produces a significant recovery compared to stroke+vehicle (# = $P<0.05$) and stroke+cyto C (^ = $P<0.05$). Right graph: Stroke+GDF10 siRNA impairs the normal recovery seen in stroke+vehicle (# = $p<0.01$) and in stroke+scrambled siRNA ($ = $P<0.05$). (**b**) Gridwalking test of forelimb function in gait. Y axis is the number of footfaults of the forelimb contralateral to the stroke (right forelimb). Left graph: Stroke+GDF10 produces a significant recovery in forelimb function compared to stroke+cyto C (^ = $P<0.05$). Right graph: Stroke+GDF10 siRNA reduces the normal process of motor recovery after stroke (** = $P<0.01$, compared with stroke+vehicle) and impairs the forelimb function compared with stroke+scrambled siRNA ($ = $P<0.05$). (**c**) Pasta handling task after stroke. Y axis is the Y axis is the percentage of handling time using right forepaw relative to both paws. Delivery of GDF10 results in a significant recovery in forepaw use compared to delivery of protein control cyto C (^ = $P<0.05$). Injection of GDF10 siRNA complex significantly reduces right forepaw function compared to injection of the scrambled siRNA ($ = $p<0.05$). In (a) $F (1.958, 11.75) = 22.07$; (b) $F (1.869, 11.21) = 10.70$; (c) $F (2.101, 12.61) = 9.382$. Error

bars are SEM. Statistics are multiple comparisons ANOVA followed by Tukey-Kramer's post hoc test

Figure 7. GDF stroke transcriptome. Genes differentially regulated at false discovery rate (FDR)<0.1 analyzed for relationship across stroke conditions, developmental state and molecular pathway. (**a**) Schematic of experimental approach of neuron isolation and deep sequencing (n=3 sample for each condition of 2 pooled brains per sample) (**b**). Differences in gene expression among conditions. Red is upregulated and green is downregulated greater than 1.2 fold. (**c**) Heat map and unsupervised clustering of transcriptomes. Green is downregulated and red is upregulated. Differentially expressed genes were identifed using the Bioconductor package EdgeR which are then considered and ranked based on adjusted p-values (FDR) of < 0.1. For hierarchical cluster analysis the distances between clusters were computed using the complete linkage clustering method (R hclust function).

Figure 8. GDF10 canonical signaling pathways and genome-wide associations. (**a**) Top canonical pathways significantly regulated in Stroke+GDF10 vs Stroke. Y axis is inverse log of p value corrected for multiple comparisons in Benjamini-Hochberg (B-H) test. Significance is set to a B-H p<0.05 = -log(B-H p-value) of 1.3. Red is net upregulation of this genes in this pathway; green is net downregulation. Grey is mixed up or downregulation in pathway genes such that there is not net trend. (**b**) Genome wide associations of Stroke+GDF10 transcriptome to learning and memory, neurodevelopmental and CNS injury transcriptomes. Statistical testing was Fisher's exact p value, Benjamini-Hochberg correction for multiple comparisons (a) and principle component analysis of 180 transcriptomes (Supplementary Figure 11).

ONLINE METHODS

Mouse model of stroke

Animal procedures were performed in accordance with the US National Institutes of Health Animal Protection Guidelines and the University of California Los Angeles Chancellor's Animal Research Committee. Focal cortical strokes on adult C57BL/6 male mice weighing 20–25 g (2–4 months old, Charles River Laboratories) were produced by photothrombosis at surgery as previously described[4,28,29]. Mice were experimentally naive prior to studies. Briefly, under isoflurane anesthesia, mice were placed in a stereotactic apparatus with the skull exposed through a midline incision, cleared of connective tissue, and dried. A cold light source (KL1500 LCD; Carl Zeiss MicroImaging, Inc.) attached to a 40x objective, giving a 2-mm diameter illumination, was positioned 1.5 mm lateral from the bregma used to produce a 2-mm diameter focal stroke upon light illumination. Rose Bengal is administered (10g/l), with typically 0.2ml per 25g mouse. After 5 min, the brain was illuminated through the intact skull for 15 min. The mice were then sutured along the scalp, removed from the stereotactic frame (Model 900, David Kopf Instruments), and allowed to recover. Body temperature was maintained at 37.0 °C with a heating pad throughout the operation. Control animals received no stroke. Mice are housed in a 12:12 hour light:dark cycle at 4 mice per cage.

Non-human primate model of stroke

Non-human primate tissues are taken from a previously reported stroke neuroprotection study in which stroke animals did not receive study drug[44] (control n = 3, stroke n = 2).

Adult, male rhesus macaques (*M. mulatta*) were single-housed indoors in double cages on a 12:12-hour light/dark cycle, with lights-on from 07003to 1900 hours, and at a constant temperature of 24°C±2°C. Laboratory diet was provided bidaily (Lab Diet 5047, PMI Nutrition International, Richmond, IN, USA) and supplemented with fresh fruits and vegetables. Drinking water was provided ad libitum. The animal care program is compliant with federal and local regulations, regarding the care and use of research animals and is Association for Assessment and Accreditation of Laboratory Animal Care accredited. All experiments were approved by the Institutional Animal Care and Use Committee.

The right MCA (distal to the orbitofrontal branch) and both anterior cerebral arteries were exposed and occluded with vascular clips for 60 min. Animals were given ketamine (~10 mg per kg, intramuscular injection) and then intubated and maintained under general anesthesia using 0.8% to 1.3% isoflurane vaporized in 100% oxygen. A blood sample was taken and a venous line was placed for fluid replacement. An arterial line was established for blood pressure monitoring throughout the surgery and to maintain a mean arterial blood pressure of 60 to 80 mm Hg End-tidal CO_2 and arterial blood gases were continuously monitored to titrate ventilation to achieve a goal CO_2 pressure of 35 to 40 mm Hg. Postoperative analgesia consisted of intramuscular hydromorphone HCl and buprenorphine. Animals were euthanized 2 d after stroke and tissue fixed in formaldehyde.

Human stroke

The cases selected for examination in this study are a retrospective, convenience sample of autopsy cases from a clinicopathologic study of cognitively normal subjects, those with subcortical ischemic vascular dementia (SIVD) or Alzheimer's disease (AD)[45]. Written informed consent for autopsy was obtained from all subjects or legal next-of-kin. From this larger database, cases selected for detailed microscopy included those with definable large artery infarcts determined by expert neuropathologic assessment of H&E stained sections. Sections from 7 of stroke and 4 control cases were evaluated (Supplementary Table 1).

Cultures of primary cortical neurons, iPS-NPCs and RGCs and Quantification of axonal outgrowth

Primary cortical neurons were prepared from postnatal day 4 CD1 mice (Charles River Laboratories)[46]. Briefly, mouse pups were euthanized, brains removed, and the cerebral cortex dissected, stripped of meninges, and dissociated by a combination of calcium and magnesium free HBSS containing 0.2% w/v papain suspension (Worthington Biochemical) digesting for 12 min at 37^{o}C. The triturated cells were passed through a 70 μm strainer and counted. The cells were plated in laminin and poly-D-lysine-coated coverslips (cat. # 354086, BD Biosciences) at a density of 5×10^{4} cells per ml (in 24-well plates) in culture medium (NbActiv4, BrainBits). Experiments were carried out after 24 h of seeding. Primary neurons were incubated with drugs or vehicle in new medium for addition 48 h. For chondroitin sulfate proteoglycans (CSPG) studies, coverslips were coated with CSPG (25 μg/mL; cat. # CC117, Millipore) prior to cell plating. Human induced pluripotent stem cells (iPSCs) (Dr. William Lowry, University of California Los

Angeles[26,47]) were plated on 12 mm polyornithine/laminin coated coverslips at 5×10^4 per well (24-well plates) in NbActiv4 (BrainBits) containing 100 units/ml penicillin, 100 μg/ml streptomycin, fibroblast growth factor 2 (FGF2) (20 ηg/μl) and epidermal growth factor (EGF) (20 ηg/μl) (Invitrogen). iPSCs were cultured for 7 days with every other daily media change. For neural differentiation, media was supplemented with brain-derived neurotrophic factor (BDNF) (20 ng/μl) and (neurotrophin 3) NT3 (20 ηg/μl) (R&D Systems) and changed every other day for 21 days[27]. Experiments were carried out on day 22. This iPS line has been extensively characterized. Expression profiles were compared with NPCs derived under standard conditions from hESCs and hiPSCs grown on murine feeder cells. Clustering and Pearson analysis[49] demonstrate that this iPS-NPCs is highly similar to other iPS-NPCs and ES-NPCS derived under standard conditions (Pearson: 0.926–0.959) and by immunostaining are relatively homogenous[49]. With simple growth factor withdrawal for three weeks, most of these iPS-NPCs develop into neurons expressing Tuj1 or MAP2[50]. BDNF and NT3 treatment were used to promote further neuronal differentiation[27]. This approach generates neurons with markers of maturity by transcript profiling, immunohistochemical staining and action potential generation (Fig. 1, ref 27).

TβRI antagonist SB431542 (Sigma), TβRII siRNA and GDF10 siRNA were applied to cultures during GDF10 incubation for 2 days before fixation and axonal staining. TβRII, Smad2, Smad3 and GDF10 siRNA protein knockdown was evaluated with Western blotting (Supplementary Fig. 3c,d). Axons of primary cortical neurons and iPS-NPCs were stained with anti-SMI-312 monoclonal antibody[51]. 16 images were taken from each coverslips at 40× objective lens using unbiased sampling (Stereoinvestigator, MBF

Biosciences). At least 2 coverslips and 32 images for each condition were analyzed. Axonal length was quantified (NeuriteTracer). Total axonal length per image was calculated for each treatment and normalized for total neuronal cell number in each culture plate (stained for NeuN). Rat RGCs cultures were prepared from dissociated retinas of mature Fisher rats[18]. In brief, rats were anesthetized with a mixture of Ketamine-Xylazine, the superior colliculi were exposed bilaterally, and retinal ganglion cells (RGCs) were retrogradely labeled by injecting Fluorogold (FG, Fluorochrome) into the superior colliculi. After allowing 7 days for retrograde transport of the dye to RGCs, rats were terminally anesthetized and retinas were rapidly dissected, enzymatically dissociated with gentle trituration, and, the dissociated retinal after removing larger tissue fragments, cells were cultured in defined, serum-free medium for 3 days. All conditions were tested in quadruplicate, in two separate experiments. Results were quantified as the percentage of FG-labeled cells, i.e., RGCs, extending an axon ≥ 2 cell diameter (approx. 30 μm) averaged across the 4 wells in each experiment and the two experiments. The observer was blinded to the treatment conditions in each well of the culture plate.

Pharmacological blockade of TGF-β *in-vivo*

Animals received photothrombotic stroke and were treated with two different TGFβ antagonists, SB431542 (R&D Systems) and Losartan (Sigma) at 10mg/kg and 100mg/kg based on published I.P. dosages[19,20]. Each animal (n=3 per group) received daily IP injections for 5 treatment days after stroke. Brains were post-fixed for 4 hours in 4% paraformaldehyde, cryosectioned at 40μm, and immunostained with pSmad2/3 (1:200; Cell Signaling 8828S). 100X photomicrographs were taken in 4 peri-infarct fields per

section, and 2 sections per animal were analyzed. Image analysis to quantify pSmad puncta of 0.45 μm was performed by Imaris Imaging Ver 8.1.2 (Bitplane, Inc).

GDF10 protein, GDF10 siRNA administration and BDA injection

GDF10 protein was delivered from the stroke cavity with a hyaluronan plus heparin sulfate hydrogel (Extracel-HP, Glycosan BioSystems) injected 7 d after stroke (A-P, 0.0 mm; M-L, 1.5 mm; D-V, 1.0 mm). This biopolymer hydrogel releases both small and large molecules over a 3 week period from the infarct core[3,4,29]. Six microliters of hydrogel impregnated with recombinant GDF10 (1.33 mg/ml, n = 8) (cat. no. 1543-BP-025/CF, R&D Systems), or protein control cytochrome C (Cyto C) (1.33 mg/ml, n = 8) (C2506-50MG, Sigma) was implanted into the stroke core. Three GDF10 siRNA duplex (cat. nos. MSS236596, MSS236597, MSS236598; Invitrogen) and negative control samples (12935-200, Invitrogen) were used to determine protein knockdown *in vitro* using day 4 postnatal mouse cortical primary neurons. The combination of MSS236597 and MSS236598 siRNA produced the greatest knockdown in GDF10 protein expression (Supplementary Fig. 3c). This GDF10 siRNA (n = 8) or scrambled control siRNA (n = 8) duplex with RNAiMAX (cat. no. 13778-075, Invitrogen) (6 μl) was introduced at 150 nM directly into the stroke cavity (A/P, 0.0 mm; M/L, 1.5 mm; D/V, 1.0 mm) 7 d after stroke. At day 21 after stroke or 14 d after GDF10 protein, GDF10 siRNA or Cyto C injection, each mouse received an injection of 300 nl of 10% BDA (Sigma) into the forelimb motor cortex (A/P, 1.5 mm; M/L, 1.75 mm; D/V, 0.75 mm)[4]. At 28 d after stroke, mice were perfused with paraformaldehyde and the cortex removed, flattened and sliced to 40 μm tangentially[3,4,28,29].

Quantitative cortical mapping of axonal sprouting

Axonal sprouting was quantified by digitally marking each BDA positive process in the cortex with a digitizing microscope system (Leica Microsystems, Ludl Electronic Products) and analysis program (Stereoinvestigator, MBF Biosciences). A BDA-labeled process was plotted irrespective of its cellular position as an axon shaft, pre-terminal or terminal axon field. This allowed each tangential map of axonal connections to contain an unbiased picture of the entire projection zone and trajectory of projections from forelimb motor cortex in each case. BDA-positive processes were marked in *x*,*y* coordinates relative to the center of the injection site by an observer blind to the treatment conditions. This process generates an *x*,*y* plot of the location of all labeled axons in each brain section. The *x*,*y* axonal plots of each brain from each experimental group were registered to the injection site and co- registered with functionally relevant anatomical regions, produced by the staining of the mouse somatosensory body map in cytochrome oxidase and the retrograde labeling of the corticospinal neurons (Supplementary Fig. 6a) to generate a composite axonal map for each treatment condition. Custom software[3,4] produces quantitative connectional maps that consist of pixels, with the number of axons in each pixel mapped in register with anatomical brain structures. Polar plots were constructed with the *x*,*y* position of each BDA-labeled element plotted in relation to the tracer injection in forelimb motor cortex as the origin. This polar mapping shows both location and direction of axonal label. Surface maps and polar maps analyzed for statistically significant differences in connectional profiles between treatment groups (see below). In a separate quantification method, the number of axons within the ipso-

hemisphere was counted a linear construct from the center of the injection site through the ipsilateral cortical hemisphere.

Stroke infarct volume was calculated by multiplying lesion area by the thickness of each section plus the distance between sections and then added with these measurements from each section through the tangential flattened cortical tissue. BDA injection volume was measured by calculating the average injection core volume for each treatment group. The average BDA injection area in each section, determined by outlining the limit of extracellular tracer deposition, was multiplied by the sum of the thickness of the section and then summed for all sections in the series. Anterior–posterior and medial–lateral BDA injection location was analyzed by measuring the distance from the center of the injection site to the rostral edge of the tissue and the midline of the cortex, respectively. The size and location of each BDA injection and stroke size did not vary significantly across individuals or by treatment condition (Supplementary Fig. 7).

Immunohistochemistry

Fluorescence immunohistochemistry with floating frozen sections was performed as described[3,4]. Primary antibodies are given in Supplementary Table 10. In all experiments, no-primary and no-secondary antibody controls were run in parallel. There was no specific staining with these controls. For the quantification of GFAP, PECAM and IBA1 immunoreactive areas, 3 fields (650μm × 450μm) within peri-infarct cortex were precisely taken from 3 independent tangential sections of each animal using a 20× objective with confocal microscopy (Nikon C2). The parameters for scanning were kept

constant across treatment conditions. Single images were analyzed using ImageJ macro and batch processing (NIH). Average percentage of the fluorescent staining area per image was calculated for each condition. Paraffin-embedded non-human primate and human brain sections (5µm thickness) were de-paraffinized and then stained[52] as with mouse tissue sections. All peri-infarct GDF10 photomicrographs (Supplementary Fig. 2a-e) were acquired at constant confocal parameters (60X, 0.3µm step size). For synapse colocalization studies, 100X confocal stacks were acquired through 10µm of tissue. 3D analysis on Imaris Imaging software (Bitplane, Version 8.1.1) was performed by: 1) creating a surface for BDA positive neurons 2) colocalizing presynaptic VGLUT2 within BDA surface 3) excluding postsynaptic Homer1 in BDA positive cells and 4) colocalizing presynaptic and postsynaptic datasets to <0.80µm.

Behavioral Assessment

Mice (7 per group) were tested once on the grid-walking, cylinder and pasta eating tasks 1 week before surgery to establish baseline performance levels. Animals were tested during the first three hours of their dark cycle. Tests were done at week 1, 3, 5, 7, 11 and 15 after stroke. Treatments were administered as for the axonal sprouting studies: GDF10+stroke, Protein control (Cyto C)+stroke, GDF10 siRNA+stroke and Stroke-only. Assessment on the grid-walking, cylinder and pasta eating tasks were performed as previously described[4,29,333]. Behaviors were scored by observers who were masked to the treatment group of the animals.

FACS

Male C57BL/6 mice age 4 months were anesthetized with isoflurane, decapitated, and cortical tissue removed from underlying white matter. Peri-infarct cortex (for stroke groups) or homologous sensorimotor cortex (for non-stroke groups) was dissected using a double tissue punch method: a ring of cortical tissue 750 μm wide was isolated between two concentric circular tissue punches (3.0 mm and 1.5 mm in diameter) to exclude necrotic stroke core. P4 sensorimotor cortex was isolated using only one 1.5mm tissue punch. Cortical tissue was enzymatically digested and triturated based on a published protocol[46]. Briefly, cortical tissue was equilibrated for 8 min and digested for 30 min at 30°C and 190 rpm in 6 mL papain solution (12 mg per ml). Complete Hibernate buffer (Brainbits) was used to maintain neural metabolites and pH during tissue dissection and digestion. Glutamate antagonists kynurenic acid and AP5 were added to minimize excitotoxicity[53]. Tissue was triturated into 6 mL suspension and loaded onto density gradient column (4 ml of 12.4% OptiPrep in Hibernate), and centrifuged for 15 min at 900 g at 22°C. The bottom 5 ml was collected and washed 2x at 400 g for 5 min before antibody staining. Two cortices were pooled for each of the 12 FACS samples. 6 animals per group (stroke alone, stroke + 7 d GDF10, Adult WT, P4 WT) were coupled into 3 samples each for a total of 12 samples across the 4 experimental groups for FACS analysis.

Prior to flow cytometry, all cell suspensions were stained for neuronal marker NCAM (Mouse; NCAM-1/CD56 Allophycocyanin MAb, 10uL antibody per 10^6 cells, FAB7820A R&D Systems) for 20 minutes at 25 °C, and washed twice with HABG. Samples were maintained on ice during FACS isolation. APC sort gates were set using

positive and negative controls prior to neuron sorting. Neurons were collected via FACS (FACsARIA, Becton Dickinson, UCLA FACS Core) directly into 400 µl lysis buffer for RNA isolation. Total RNA was extracted using RNA-Microprep kit (Zymo-Research) and eluted into 7 µl ddH_2O. RNA quality was verified (RIN>7) on an Agilent Bioanalyzer.

Spinal Cord Injections

Layer V corticospinal motor neurons were labeled by stereotaxic injection of cholera toxin B subunit (CTB), a retrograde neuronal tracer, into the cervical enlargement at C5 of 5 month-old CD1 mice. Surgeries were performed on a stereotaxic apparatus (David Kopf) interfaced with a microinfusion syringe pump (Harvard Instruments). Animals were anesthetized with general isoflurane in oxygen-enriched air. Single vertebra laminectomy at C5 revealed the cord, and 500 nL of CTB tracer (6.67 µg per µl, List Biological Labs) was injected into the right dorsal corticospinal tract (dCST)[54]. CTB infusion progressed at 0.2 mL per min through a glass micropipette connected by special adapters and high pressure tubing to a 10 mL Hamilton syringe. All animals were given analgesic prior to suture wound closure. Ten days after tracer delivery, animals were anesthetized with pentobartital and transcardially perfused with 4% PFA. Brain and spinal cord were isolated and prepared via tangential and coronal cryosectioning, respectively. Tissue preparation and stereological cortical mapping were performed as previously described[4]. Cervical cord was cryosectioned at 40µm and for dCST injection site verification by CTB immunofluorescence (Goat anti-CTB 1:10,000, List Biological Labs).

RNA-seq and Bioinformatics of other neuronal transcriptomes

Total RNA from FACS-isolated cells from each condition (n = 6) was pooled in 2 brains per sample. Total RNA was amplified and converted into double-stranded DNA, which after fragmentation is typically between 200 and 300 bp (Ovation RNA-seq System v2, Nugen, San Carlos, CA) that was further processed with the Ovation UltraLow kit (Nugen). RNA libraries were prepared using a NuGen Ovation Ultra Low Mass kit for paired-end 2 × 69 RNA-sequencing (HiSeq2000, UCLA ICNN core). After library preparation (Encore NGS Library System I, Nugen) amplified double-stranded cDNA was fragmented into 300 bp (Covaris-S2, Woburn, MA). DNA fragments (200 ng) were end-repaired to generate blunt ends with 5'- phosphates and 3'- hydroxyls and adapters ligated. The purified cDNA library products were evaluated using the Agilent Bioanalyzer (Santa Rosa, CA) and diluted to 10 nm for cluster generation in situ on the HiSeq paired-end flow cell using the CBot automated cluster generation system. Three samples at a time, all samples were multiplexed into single pools and run in 9 lanes total of Paired-End 2 × 100 bp flow cells in HiSeq 2000 (Illumina, San Diego, CA).

Six Libraries for RNA-seq were prepared using the NuGEN Ovation UltraLow library preparation protocol (NuGEN Technologies, Inc.) and sequenced using an Illumina HiSeq 2500 sequencer across 10 lanes of 100bp-paired-end sequencing, corresponding to 3 samples per HiSeq 2500 lane. After demultiplexing, we obtained between 50 and 79 million reads per sample. Quality control was performed on base qualities and nucleotide composition of sequences. Alignment to the M. musculus (mm10) refSeq (refFlat)

reference gene annotation was performed using the STAR spliced read aligner[55] with default parameters. Additional QC was performed after the alignment to examine: the level of mismatch rate, mapping rate to the whole genome, repeats, chromosomes, key transcriptomic regions (exons, introns, UTRs, genes), insert sizes, AT/GC dropout, transcript coverage and GC bias. One control sample failed QC and was excluded from analysis. Between 67 and 85% of the reads mapped uniquely to the mouse genome. Total counts of read-fragments aligned to candidate gene regions were derived using HTSeq program (www.huber.embl.de/users/anders/HTSeq/doc/overview.html) and used as a basis for the quantification of gene expression. Only uniquely mapped reads were used for subsequent analyses. Across the samples >25% of the annotated genes have been detected by at least 50 reads. Following alignment and read quantification, we performed quality control using a variety of indices, including sample clustering, consistency of replicates, and average gene coverage.

Differential expression analysis was performed using the EdgeR Bioconductor package[56], and differentially expressed genes were selected based on False Discovery Rate (FDR Benjamini Hochberg-adjusted p values) estimated at < 0.1 (or 10% FDR). Three samples from stroke, stroke+GDF10, P4 and 2 samples from control were compared. Clustering and overlap analyses were performed using Bioconductor packages within the statistical environment R (www.r-project.org/).

Genes that were differentially expressed false discovery rate (FDR) < 10% were submitted to Cluster 3.0 for hierarchical clustering analysis (Euclidian distance, centroid

linkage clustering) and visualized using Java TreeView. Differentially expressed genes were further analyzed by molecular pathway analysis and canonical signaling systems (IPA, Redwood City, CA). Briefly, for IPA analyses the genes regulated in each specific category, filtered to only include genes ≤10% FDR, where compared to all genes known to be involved in a given molecular pathway or canonical signaling system in a large curated database of molecular interactions. Fisher's exact p value was calculated by IPA to determine a statistically different relationship of a data set in the control, stroke+/-GDF10, and P4 cortical transcriptomes to chance representation of these genes. For the upstream analysis there are 4 values that go into the Fisher's exact p-value calculation with Benjamini Hochberg correction for multiple comparisons.

For genome-wide association testing, individual data from .cell, SRA or Excel files was obtained for each experiment (Supplementary Table 9). The gene symbol was located for each probe and average expression computed for duplicated genes. The data were combined with RNA-seq data from this study and variance stabilization transformation normalization was applied.

Statistical analysis

Animal number in *in vivo* quantitative cortical mapping studies utilizes spatial correlation statistics, so sample size was estimated from previous publications with similar mechanistic studies[3,4,28,29]. Sample size in in behavioral studies was assessed by power analysis using a significance level of $\alpha=0.05$ with 80% power to detect differences in ANOVA. This experimental design has been validated by other groups conducting

similar behavioral[4] or tissue outcomes experiments[3,4,28,29]. No animals were excluded from analyses. Mice were randomly allocated to treatment condition and all results were analyzed with the investigator blinded to treatment condition.

For quantitative connectional maps, three statistical analysis paradigms were used. First, scatter plots were analyzed using Hotelling's T^2 test for spatial correlation. For data with a common covariance matrix, such as the map of axonal position in tangential cortical sections, Hotelling's T^2 method tests the hypothesis of multivariate mean equality: that the means for the set outcome variable (axonal location for each individual, averaged by experimental condition) are equivalent across groups. The T statistic is the analog of Student's two-group t-statistic for testing equality of group means for a single outcome variable. P-values were computed without Gaussian assumptions by means of a bootstrap 250 μm was applied around the injection site to account for the uniformity of the injection site itself and immediately adjacent BDA labeling across groups, regardless of sprouting pattern. Second, polar statistics tested for differences in distribution of axonal projection patterns across treatment groups. For each treatment condition, the *x*, *y* coordinate of every BDA-positive process was converted to an equivalent polar coordinate (*r*,) relative to the injection site as center[3,4]. The location of each process was transferred to common polar space and a mean projection vector was computed for each treatment group. Differences in mean projection vectors between groups were analyzed using Watson's nonparametric two-sample U^2 test[3,4]. Third, axon numbers in the linear construct across ipsilateral cortex were analyzed using one-way analysis of variance (ANOVA) with *post hoc* Tukey-Kramer test. In addition, differences between two means

were assessed by unpaired two-tailed Student's *t* test. Differences among multiple means were assessed by one-way ANOVA followed by Tukey-Kramer's *post hoc* tests. Data from behavioral experiments were analyzed by two-way repeated-measures ANOVA followed by Tukey-Kramer's *post hoc* test. All statistical analyses were performed with GraphPad Prism version 6 (GraphPad Software) or StatPlus version 5 (AnalystSoft) except those specifically noted above. Data are shown as mean ± standard error of the mean.

METHODS-ONLY REFERENCES

44. Bahjat FR, Williams-Karnesky RL, Kohama SG, West GA, Doyle KP, Spector MD, Hobbs TR, Stenzel-Poore MP. Proof of concept: pharmacological preconditioning with a Toll-like receptor agonist protects against cerebrovascular injury in a primate model of stroke. J Cereb Blood Flow Metab. 2011; 3:1229-42.
45. Soontornniyomkij V, Lynch MD, Mermash S, Pomakian J, Badkoobehi H, Clare R, Vinters HV. Cerebral microinfarcts associated with severe cerebral beta-amyloid angiopathy. Brain Pathol. 2010 Mar;20(2):459-67.
46. Brewer, G.J. & Torricelli, J.R. Isolation and culture of adult neurons and neurospheres. Nature protocols 2, 1490-1498 (2007).
47. Karumbayaram et al. From skin biopsy to neurons through a pluripotent intermediate under Good Manufacturing Practice protocols. Stem Cells Transl Med. 2012;1:36-43
48. Xu, S.Y., Wu, Y.M., Ji, Z., Gao, X.Y. & Pan, S.Y. A modified technique for culturing primary fetal rat cortical neurons. J Biomed Biotechnol 2012, 803930

49. Patterson et al. Defining the nature of human pluripotent stem cell progeny. Cell Res. 2012;22:178-93

50. Patterson et al. let-7 miRNAs can act through notch to regulate human gliogenesis. Stem Cell Reports. 2014;3:758-73.2012).

51. Andres, R.H. et al. Human neural stem cells enhance structural plasticity and axonal transport in the ischaemic brain. Brain 134, 1777-1789 (2011).

52. Soontornniyomkij V, Lynch MD, Mermash S, Pomakian J, Badkoobehi H, Clare R, Vinters HV. Cerebral microinfarcts associated with severe cerebral beta-amyloid angiopathy. Brain Pathol. 2010 Mar;20(2):459-67.

53. Ozdinler PH, Macklis JD. IGF-I specifically enhances axon outgrowth of corticospinal motor neurons. Nat Neurosci. 2006 Nov;9(11):1371-81.

54. Paxinos, G. & Watson, C. *The Mouse Brain in Stereotaxic Coordinates* 2nd edn. (Academic, San Diego, 2001).

55. Dobin, A., Davis, C.A., Schlesinger, F., Drenkow, J., Zaleski, C., Jha, S., Batut, P., Chaisson, M., Gingeras, T.R. (2013) STAR: ultrafast universal RNA-seq aligner. Bioinformatics. *29*,:15-21.

56. Robinson, M.D., McCarthy, D.J., Smyth, G.K. (2010) edgeR: a Bioconductor package for differential expression analysis of digital gene expression data. Bioinformatics. 26,:139-40.

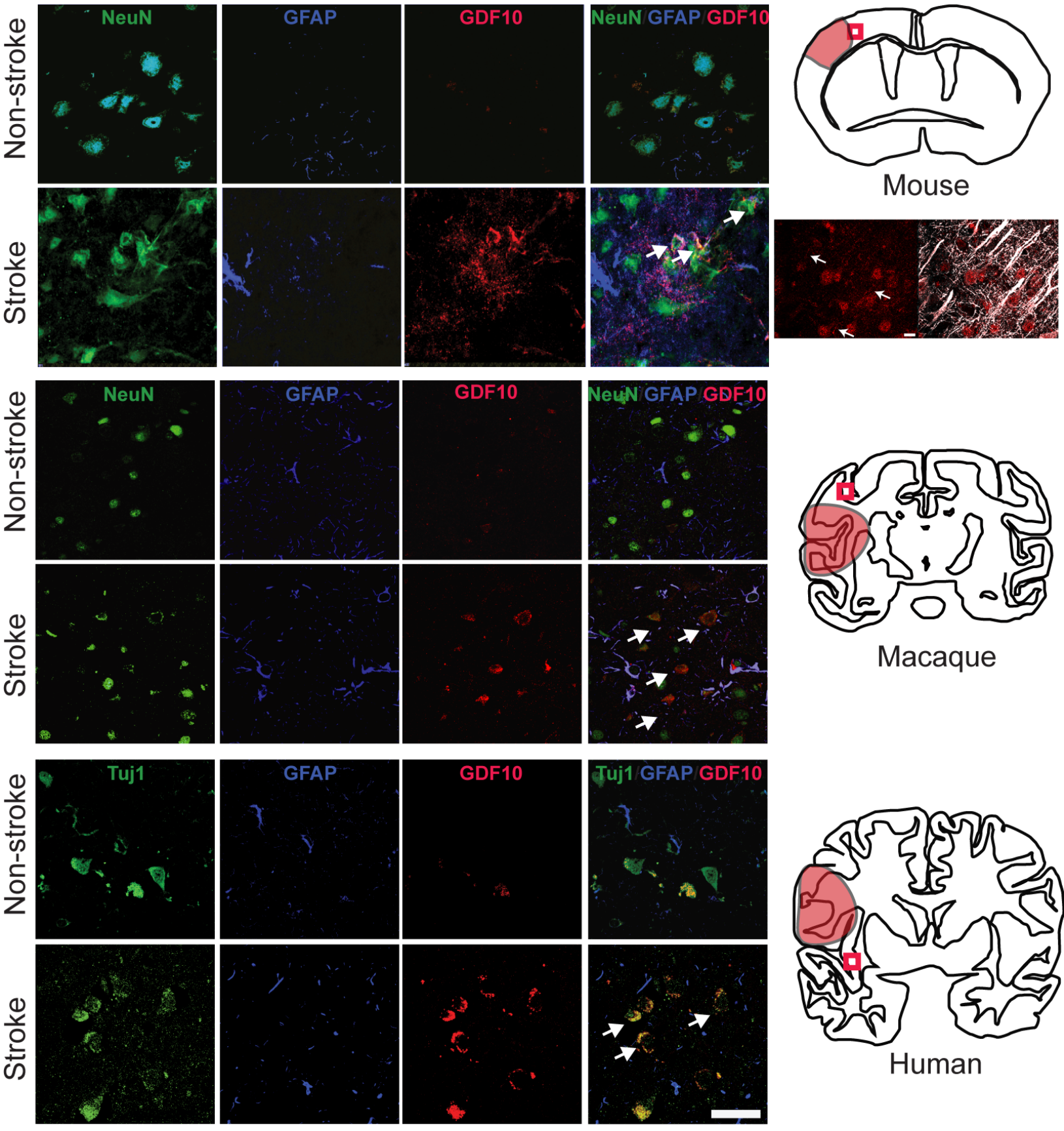
NeuN
GFAP
GDF10
NeuN GFAP GDF10
Non-stroke
Stroke
Mouse
Tuj1
Tuj1 GFAP GDF10
Macaque
Human

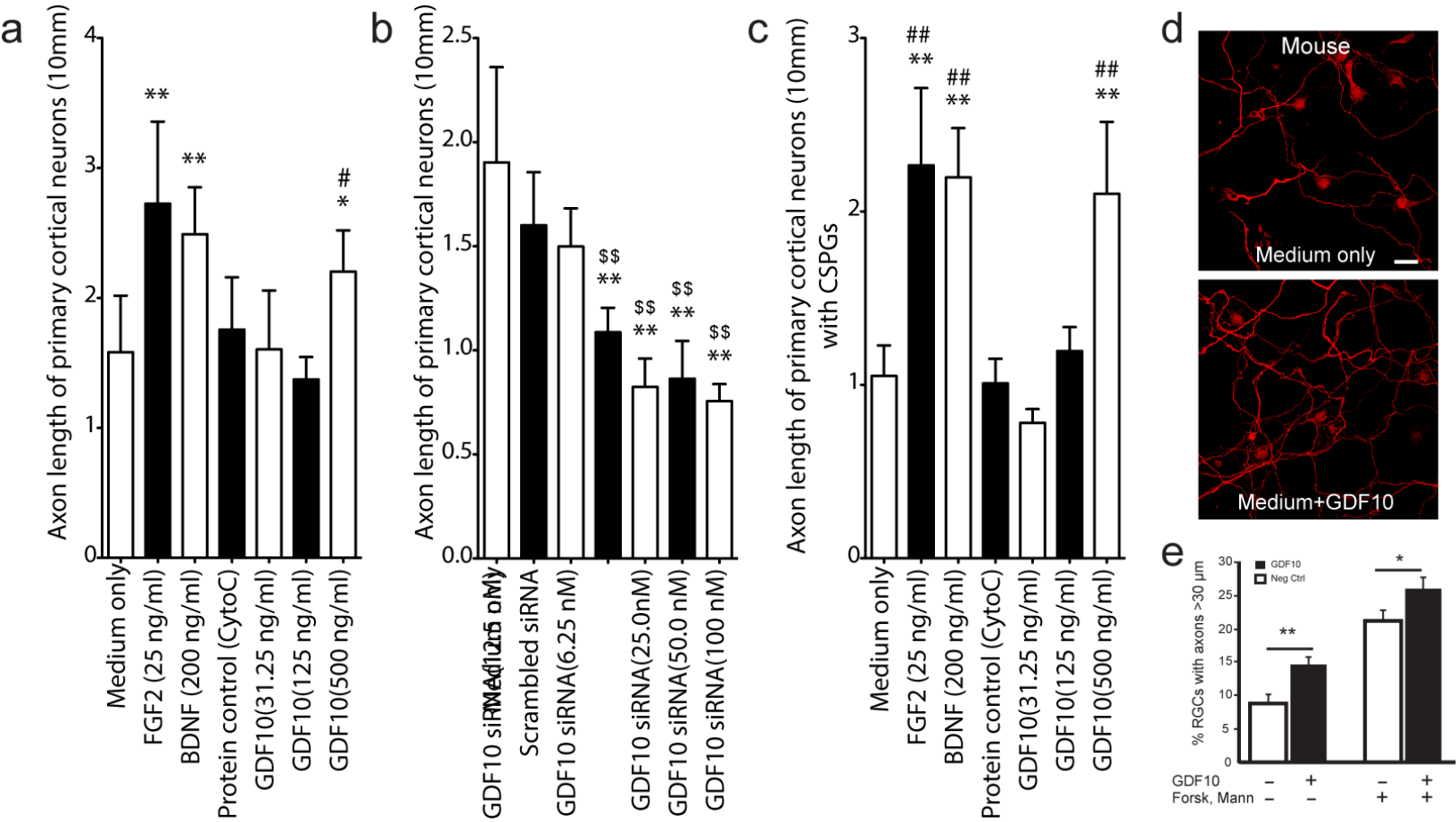
a
Axon length of primary cortical neurons (10mm)
Medium only
FGF2 (25 ng/ml)
BDNF (200 ng/ml)
Protein control (CytoC)
GDF10(31.25 ng/ml)
GDF10(125 ng/ml)
GDF10(500 ng/ml)
b
Axon length of primary cortical neurons (10mm)
Scrambled siRNA
GDF10 siRNA(6.25 nM)
GDF10 siRNA(25.0nM)
GDF10 siRNA(50.0 nM)
GDF10 siRNA(100 nM)
c
Axon length of primary cortical neurons (10mm) with CSPGs
Medium only
FGF2 (25 ng/ml)
BDNF (200 ng/ml)
Protein control (CytoC)
GDF10(31.25 ng/ml)
GDF10(125 ng/ml)
GDF10(500 ng/ml)
d
Mouse
Medium only
Medium+GDF10
e
% RGCs with axons >30 µm
GDF10
Neg Ctrl
GDF10
Forsk, Mann

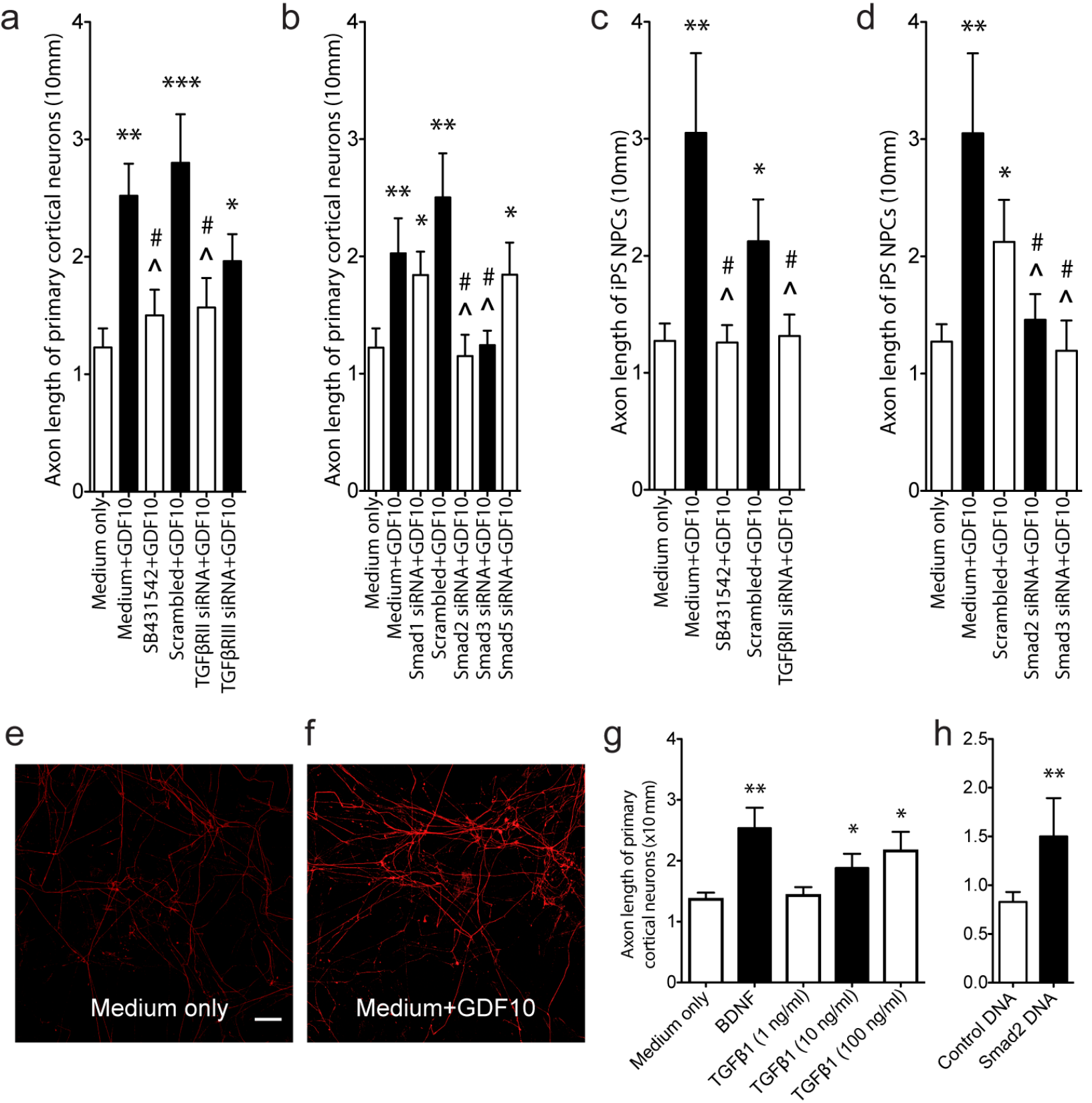
a
b
c
d
Axon length of primary cortical neurons (10mm)
Axon length of iPS NPCs (10mm)
Medium only
Medium+GDF10
SB431542+GDF10
Scrambled+GDF10
TGFβRII siRNA+GDF10
TGFβRIII siRNA+GDF10
Smad1 siRNA+GDF10
Smad2 siRNA+GDF10
Smad3 siRNA+GDF10
Smad5 siRNA+GDF10
e
f
Medium only
Medium+GDF10
g
h
Axon length of primary cortical neurons (x10 mm)
BDNF
TGFβ1 (1 ng/ml)
TGFβ1 (10 ng/ml)
TGFβ1 (100 ng/ml)
Control DNA
Smad2 DNA

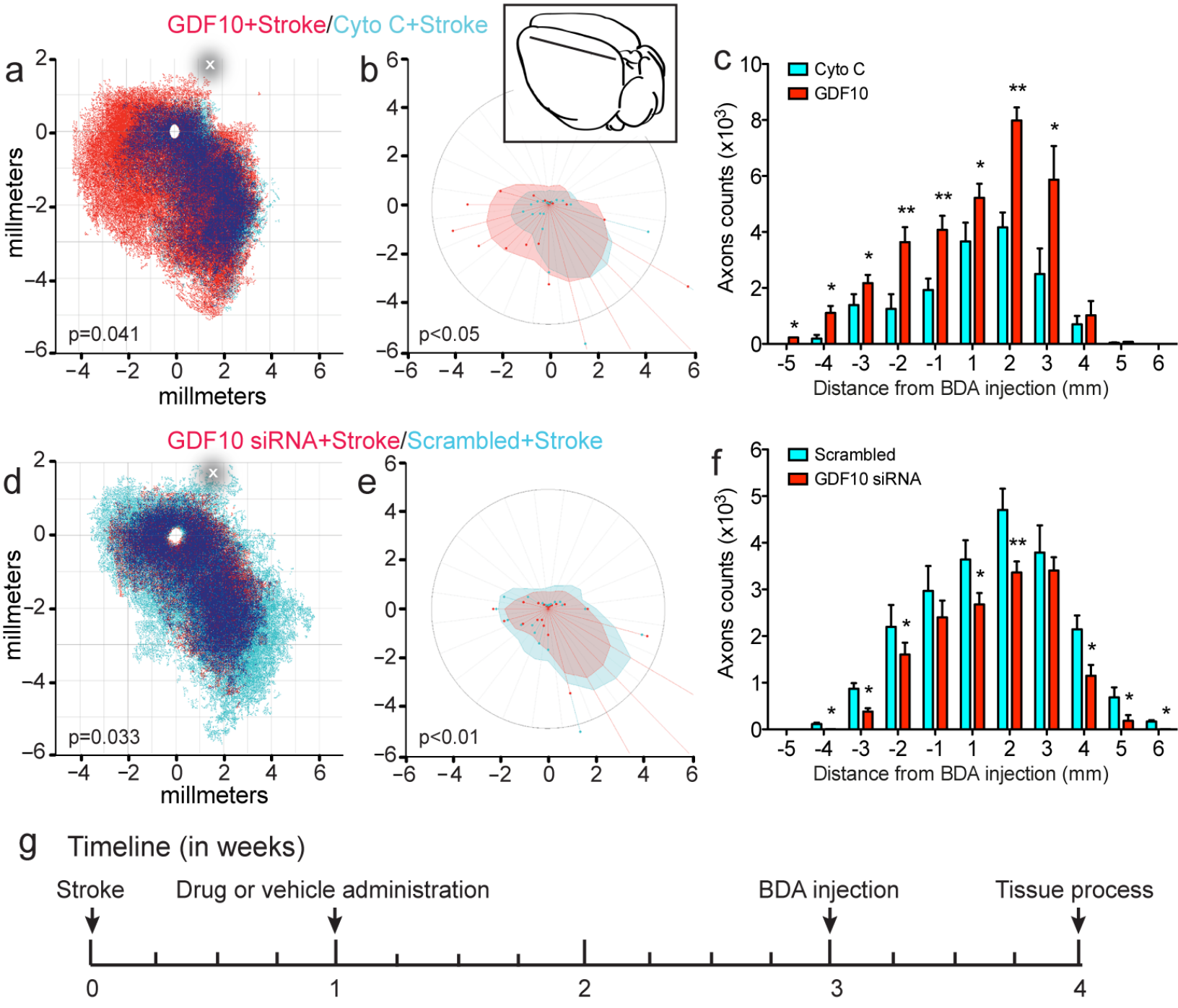
GDF10+Stroke/Cyto C+Stroke
a
b
c
millmeters
millmeters
p=0.041
p<0.05
Cyto C
GDF10
Axons counts (x10³)
Distance from BDA injection (mm)
GDF10 siRNA+Stroke/Scrambled+Stroke
d
e
f
p=0.033
p<0.01
Scrambled
GDF10 siRNA
Axons counts (x10³)
Distance from BDA injection (mm)

g Timeline (in weeks)
Stroke
Drug or vehicle administration
BDA injection
Tissue process
0
1
2
3
4

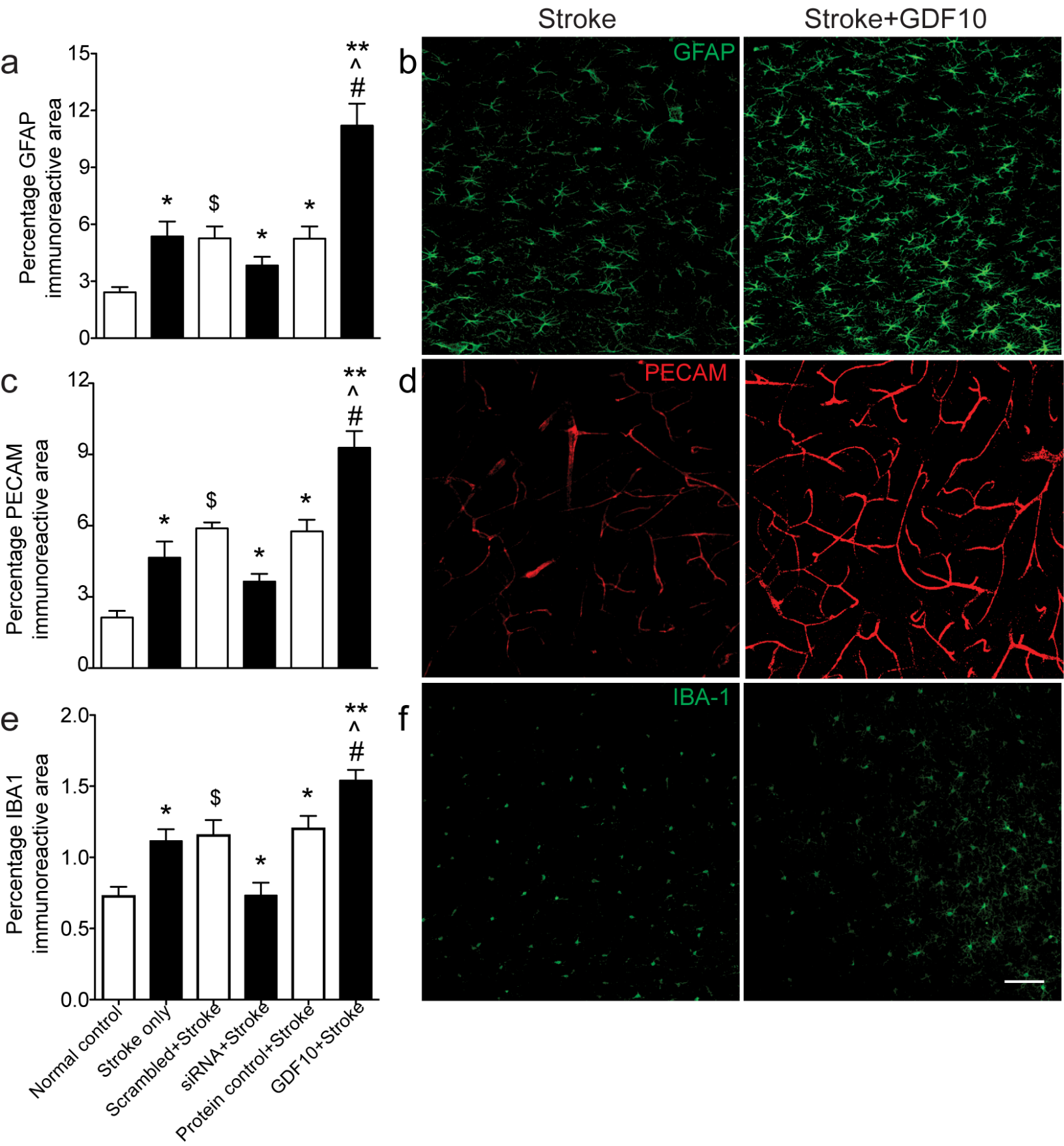
Stroke
Stroke+GDF10
a
Percentage GFAP immunoreactive area
15
12
9
6
3
0
b
GFAP
c
Percentage PECAM immunoreactive area
12
9
6
3
0
d
PECAM
e
Percentage IBA1 immunoreactive area
2.0
1.5
1.0
0.5
0.0
f
IBA-1
Normal control
Stroke only
Scrambled+Stroke
siRNA+Stroke
Protein control+Stroke
GDF10+Stroke

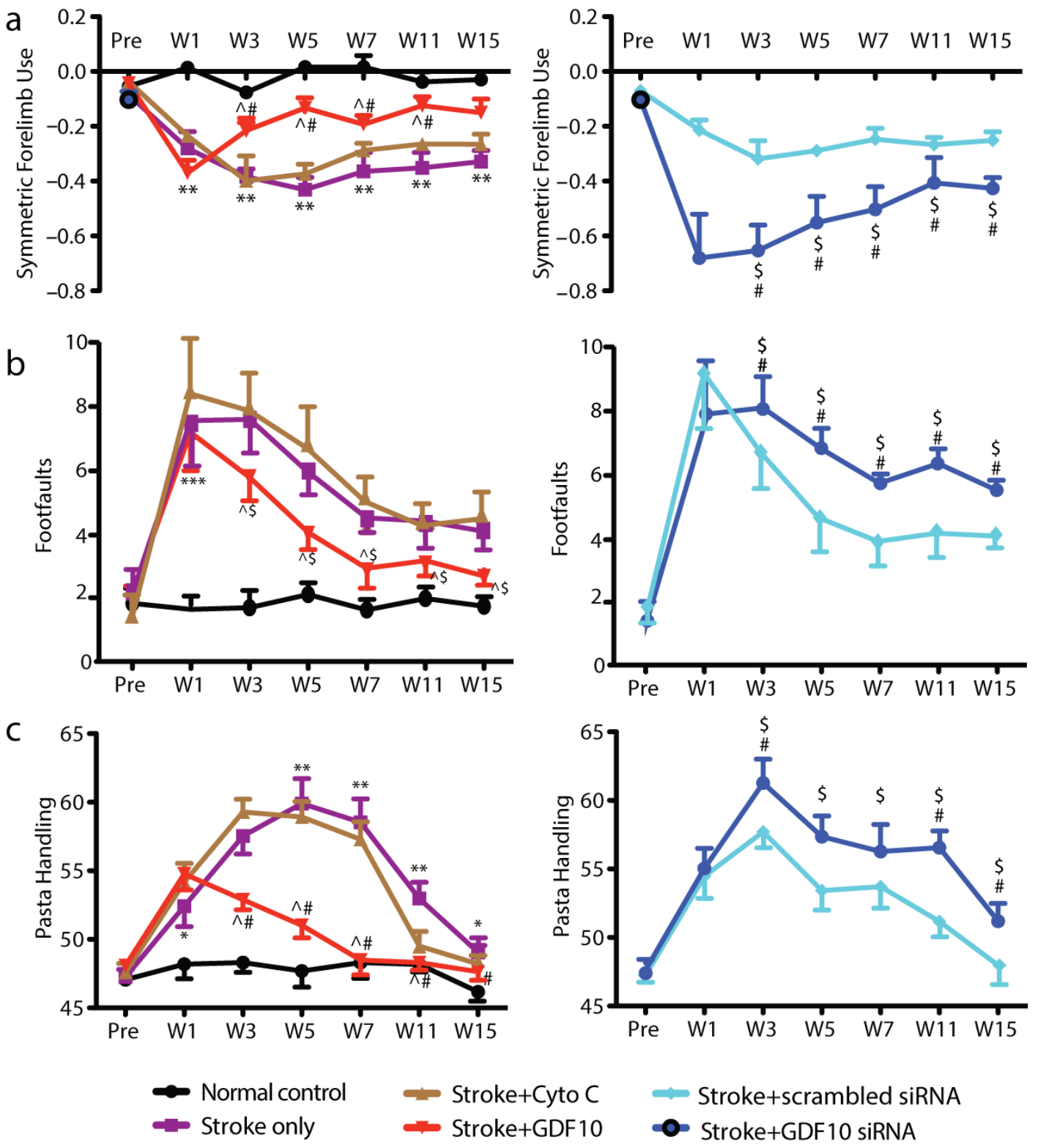
a
Symmetric Forelimb Use
Pre
W1
W3
W5
W7
W11
W15
b
Footfaults
c
Pasta Handling
Normal control
Stroke only
Stroke+Cyto C
Stroke+GDF10
Stroke+scrambled siRNA
Stroke+GDF10 siRNA

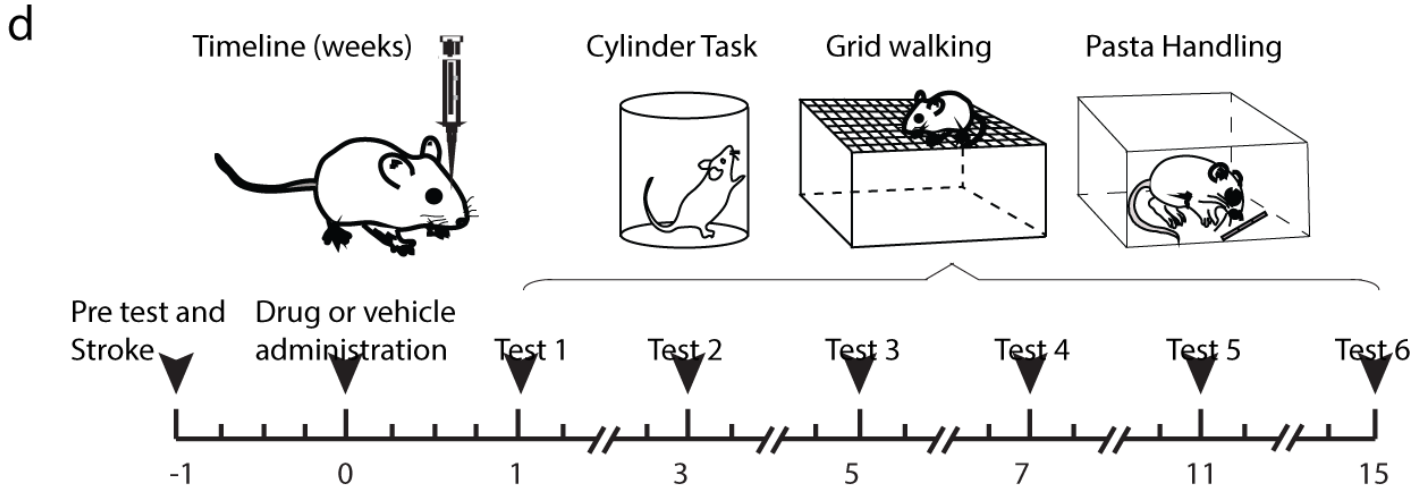
d
Timeline (weeks)
Cylinder Task
Grid walking
Pasta Handling
Pre test and Stroke
Drug or vehicle administration
Test 1
Test 2
Test 3
Test 4
Test 5
Test 6
-1
0
1
3
5
7
11
15

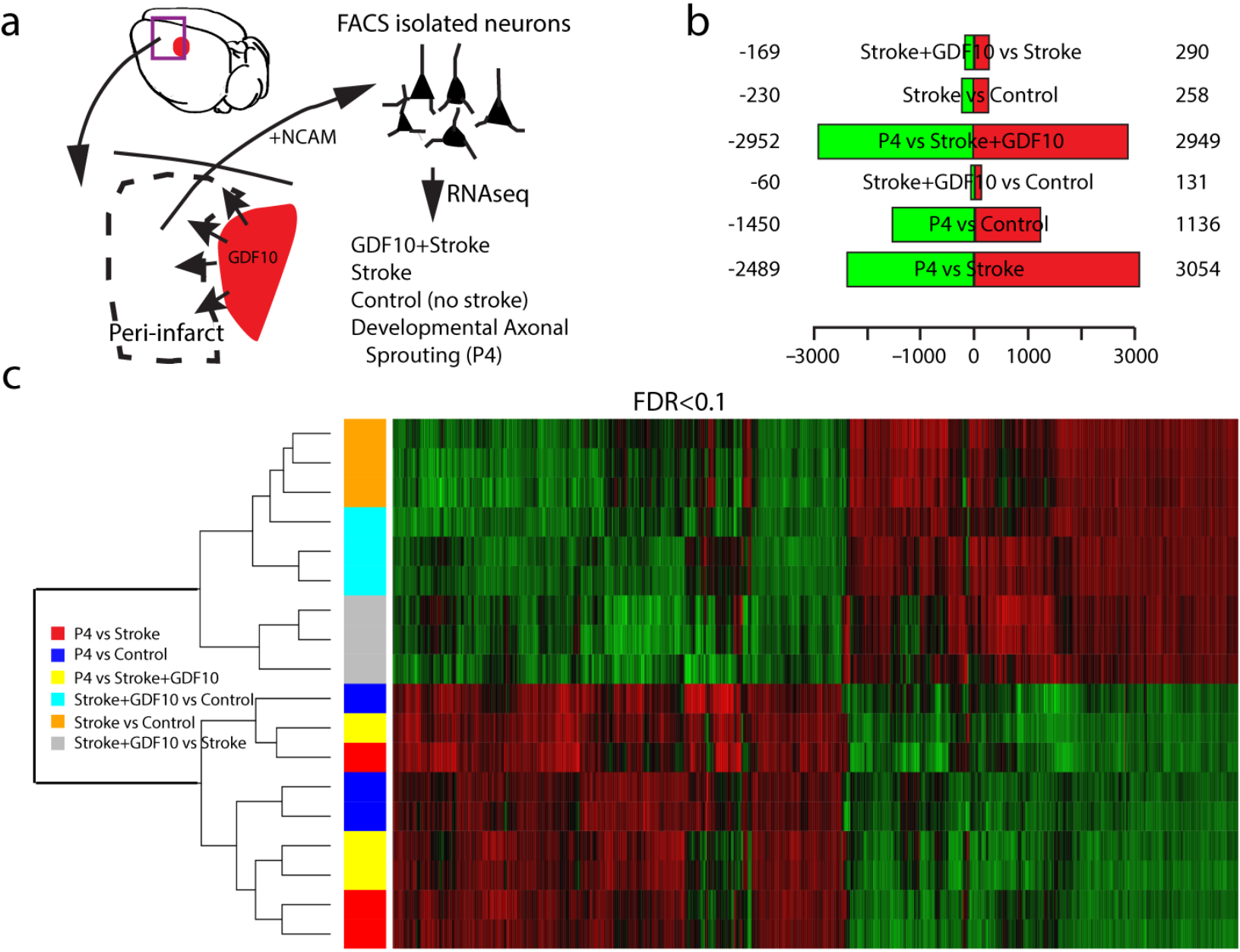
a
FACS isolated neurons
+NCAM
RNAseq
GDF10
Peri-infarct
GDF10+Stroke
Stroke
Control (no stroke)
Developmental Axonal
Sprouting (P4)
b
-169
Stroke+GDF10 vs Stroke
290
-230
Stroke vs Control
258
-2952
P4 vs Stroke+GDF10
2949
-60
Stroke+GDF10 vs Control
131
-1450
P4 vs Control
1136
-2489
P4 vs Stroke
3054
−3000
−1000
0
1000
3000
c
FDR<0.1
P4 vs Stroke
P4 vs Control
P4 vs Stroke+GDF10
Stroke+GDF10 vs Control
Stroke vs Control
Stroke+GDF10 vs Stroke

a

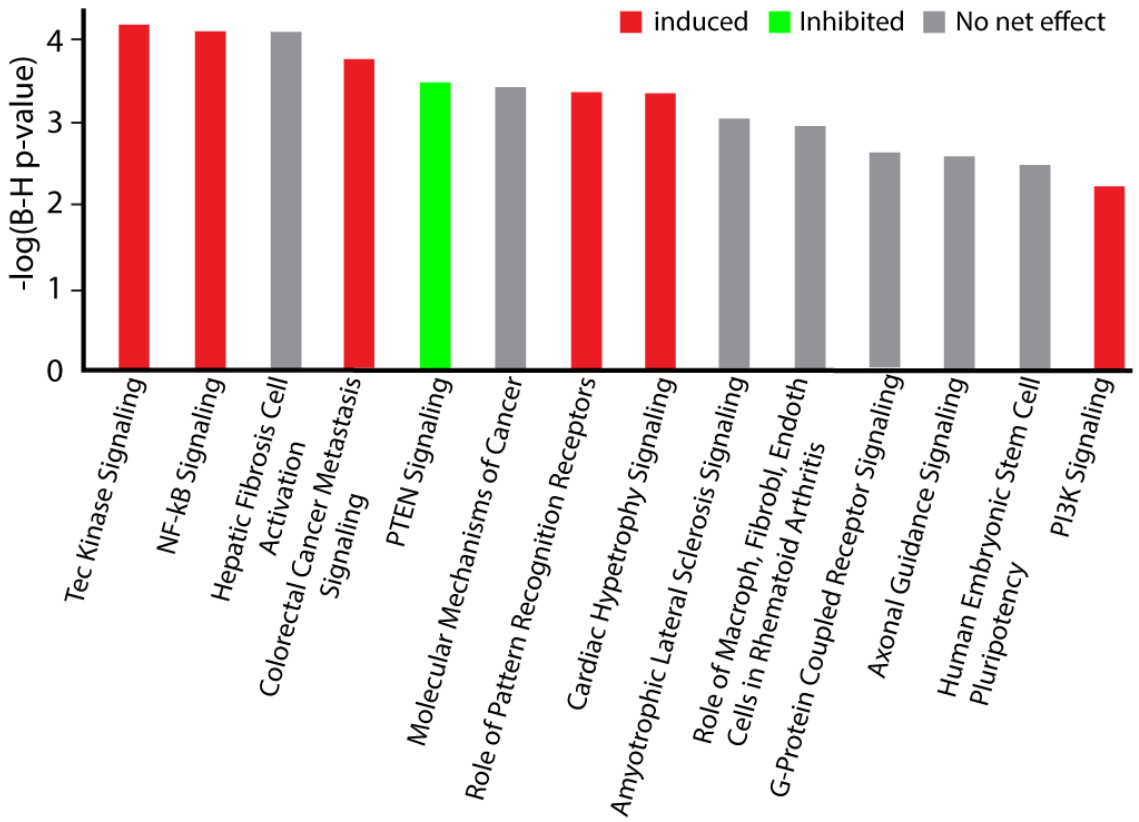
induced
Inhibited
No net effect
-log(B-H p-value)
0
1
2
3
4
Tec Kinase Signaling
NF-kB Signaling
Hepatic Fibrosis Cell Activation
Colorectal Cancer Metastasis Signaling
PTEN Signaling
Molecular Mechanisms of Cancer
Role of Pattern Recognition Receptors
Cardiac Hypetrophy Signaling
Amyotrophic Lateral Sclerosis Signaling
Role of Macroph, Fibrobl, Endoth Cells in Rhematoid Arthritis
G-Protein Coupled Receptor Signaling
Axonal Guidance Signaling
Human Embryonic Stem Cell Pluripotency
PI3K Signaling

b

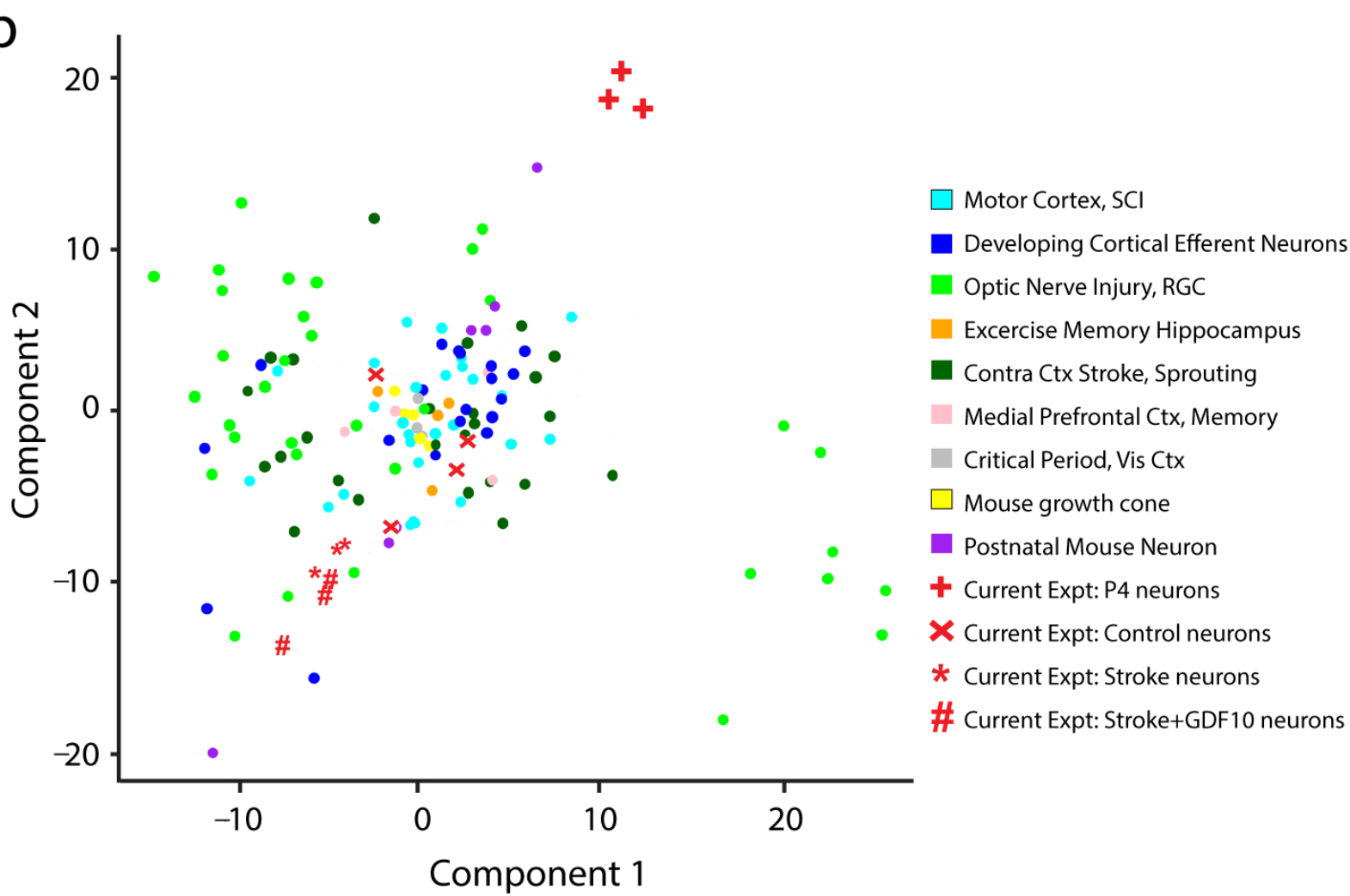
Component 2
20
10
0
−10
−20
−10
0
10
20
Component 1
Motor Cortex, SCI
Developing Cortical Efferent Neurons
Optic Nerve Injury, RGC
Excercise Memory Hippocampus
Contra Ctx Stroke, Sprouting
Medial Prefrontal Ctx, Memory
Critical Period, Vis Ctx
Mouse growth cone
Postnatal Mouse Neuron
Current Expt: P4 neurons
Current Expt: Control neurons
Current Expt: Stroke neurons
Current Expt: Stroke+GDF10 neurons

Supplement. Li et al.

Supplementary Figure Legends

Supplementary Figures

Supplementary Tables

Supplementary Figure 1. TGFβ superfamily. **(a)** TGFβ superfamily members are classified into TGFβ, Activin/inhibin/Nodal group and BMP groups. In the canonical signaling pathway, shown here, TGFβ family members signal through type I and type II receptors for each member to receptor-associated SMAD proteins (R-SMAD), SMAD2 and SMAD3. Activin/inhibin/Nodal proteins signal through distinct type I and II receptors: ACVR1B or ALK-4 acts as a transducer of Activin/inhibin/Nodal signals. These Activin ligands bind to either ACVR2A or ACVR2B and then bind ACVR1B and then activate (phosphorylate) SMAD2/SMAD3. BMP signals are transduced through their distinct type I and type II receptors for each member to R-SMAD proteins SMAD1, SMAD5 and SMAD8. Phosphorylated R-SMADs associate with SMAD4 and are then translocated to the nucleus to activate transcription of target genes. GDF family members signal through both Activin and BMP pathways, except for GDF10, which signals through TGFβ receptors. This summary is simplified and, for example, does not represent the full complexity of signaling that can come through heterotetrameric binding between TGFβ, Activin/inhibin/Nodal and BMP families. **(b)** The genetic relationship of GDF/BMP proteins as established by sequence homology. Figures modified from[12,14].

Supplementary Figure 2. GDF10 is upregulated in peri-infarct cortex. **(a)** GDF10 protein expression in the ipsilateral hemisphere after stroke. This low magnification photomicrograph of the ipsilesional hemisphere shows axonal loss, as indicated by loss of MAP2, in the stroke core. GDF10 is induced in the cortex bordering the stroke core, as seen by the increased intensity of staining (arrows). The stroke core contains an abundance of microglia and macrophages, labeled by CD11b. **(b)** GDF10 expression in the peri-infarct cortex. Image is taken from the region of interest indicated by box in panel **(a)** GDF10 protein expression is upregulated compared to contralateral control in panel 1(c). (**b**) Higher magnification view of peri-infarct cortex shows that GDF10 is present in MAP2+ neuronal dendrites (arrows) in addition to neuronal cell bodies (Fig. 1) and not present in CD11b+ microglia/macrophages. **(c)** GDF10 expression in the non-injured cortex from the contralateral hemisphere. GDF10 has a sparse low level of endogenous expression. This indicates that GDF10 induction is specific to cortex immediately adjacent to the site of stroke injury. In the absence of stroke, CD11b is not induced in the control cortex. **(d)** GDF10 expression in the peri-infarct colocalizes to neurons labeled with MAP2 and excludes microglia and macrophages. GDF10 immunoreactivity is present in MAP2+ neuronal somas and in dendrites (arrows). GDF10 does not colocalize with CD11b+ microglia/ macrophages. **(e)** Secreted GDF10 is also found in the extracellular space in the peri-infarct cortex near surviving processes (MAP2).

Supplementary Figure 3. GDF10 protein levels and siRNA knockdown in vivo. **(a)** GDF10 siRNA, vehicle or scrambled siRNA was delivered into the stroke cavity and peri-infarct tissue processed for Western blot. X axis shows days after stroke and siRNA

delivery. * = p< 0.05, ** = p< 0.01 compared to the scrambled siRNA; # = p<0.05 compared to Stroke only. **(b)** Representative Western blot images from (a). N = 3 for each experiment.

Supplementary Figure 4. Axonal outgrowth of P4 mouse primary cortical neurons on standard and inhibitory substrates. Both myelin and CSPGs inhibit the outgrowth or P4 cortical neurons. *** = p<0.001, multiple comparisons ANOVA, Tukey-Kramer *post-hoc*.

Supplementary Figure 5. siRNA protein knockdown. (**a**) Western blot of GDF10 protein level with two-day treatment of siRNA in P4 neurons. Numbers in the columns indicate the distinct siRNA construct. The gel image at the bottom is a representative blot from each experiment. Each experiment represents 4 samples and 2 technical replicates. (**b**) Western blot results for knockdown of TGFβRI, II and Smads1, 2, 3, 5. Same conventions as in (**a**). ** = p<0.01 compared to the scrambled siRNA.

Supplementary Figure 6. Primary cortical neurons plated *in vitro* express GDF10. (a) Primary cortical neurons stained with GDF10 and MAP2 antibody demonstrates neuronal expression of GDF10 *in vitro*. This substantiates the *in vitro* GDF10 knockdown experiments using siRNAs to study axonal outgrowth, without a need for addition of GDF10 to the system to mimic induction. In contrast to the low endogenous expression of GDF10 in uninjured cortical neurons *in vivo*, GDF10 expression *in vitro* is likely

induced by mechanical stress of dissection and plating of primary neurons. (b) High magnification of neuronal soma expressing GDF10. GDF10 immunoreactivity is also evident along neuronal processes (arrows).

Supplementary Figure 7. pSmad2/3 quantification in peri-infarct cortex after TGFβ antagonism *in vivo*. Stroked animals were treated with two different TGFβ antagonists, SB431542 and Losartan at 10mg/kg and 100mg/kg, respectively, based on published i.p. doses[16,17] for 5 days after stroke (n=3 mice per group). pSmad puncta of 0.45μm were quantified at 100x imaging fields in two sections per animal, and mean puncta values were statistically compared. As seen with *in vitro* axon outgrowth studies in primary cortical neurons from mouse (Fig. 2) and human iPSC-derived neurons (Fig. 3), *in vivo* administration of TGFβ antagonists, SB431542 (*p=0.0056*) and Losartan (*p=0.0244*), each significantly decreases pSmad2/3 signaling within 300μm of the infarct core. *=p<0.05

Supplementary Figure 8. Quantitative connectional mapping and axonal connections in peri-infarct cortex. (**a**) Left panel. Quantitative connectional map of neurons back-labeled from a retrograde tracer injection (cholera toxin b subunit) into cervical level 5 spinal cord (n = 5). This labels all neurons in motor, somatosensory and premotor cortex that send projections to the spinal cord. The location of all neurons is plotted in tangential sections and the x y coordinates are made relative to bregma[49]. Middle panel. Axonal label plotted from BDA injections into forelimb motor cortex in stroke+GDF10 and Cyto C+stroke (protein control). This is the same experiment as in Fig 4a. Right panel: alignment of

corticospinal projections with GDF10/stroke map, to show location of areas of axonal sprouting relative to motor, premotor and somatosensory areas. Note that a substantial region of new connections formed in Stroke+GDF10 is in cortex rostral to the corticospinal populations of neurons. (**b**) The effect of stroke on motor cortex connections. Left panel: quantitative connectional map of connections from tracer injections into forelimb motor cortex in stroke only (red label) and in control, non-stroke (light blue label) mice. The cortical areas with dense overlap of connections in stroke and control are in dark blue. Not the presence of connections only in the stroke condition in posterior cortical areas, that localize to motor cortex and second somatosensory cortex in registering to the corticospinal map and to primary somatosensory cortex by cytochrome oxidase stain (not shown). P value is significant (Hotellings T^2 test). Middle panel: Polar plot of connections in stroke (red) and control (blue). Conventions as in Fig. 4b. Right panel: quantification of neuronal connections in linear array through cortical hemisphere (see Fig. 4c). (n= 7 in both groups) * = p< 0.05, ** = p<0.01, *** = p<0.001.

Supplementary Figure 9. Infarct volume, BDA volume and injection locations. (**a**) Left Y axis: BDA injection volume, right Y axis infarct volume. Columns are for *in vivo* axonal tracing studies. There are no significant differences among groups. (**b**) Location of BDA injections for each group relative to the midline of the cortical hemisphere and to the rostral pole of the brain. There are no significant differences among groups. Error bars are SEM.

Supplementary Figure 10. Quantitative connectional mapping and axonal connections in GDF10 controls compared to normal control. (**a-c**) Cortical connections of forelimb motor cortex in normal control animals only compared to stroke+protein control, cytochrome C delivery from the infarct core via biopolymer hydrogel. (n = 8 for each group). Figure conventions are as in Supplementary Figure 8 and Figure 4. There is a significant difference in the cortical connectional map (a), polar plots (b) and linear measurement of neuronal connections (c) between normal control forelimb motor cortex and stroke+scrambled siRNA. This indicates that the normal mode axonal sprouting that is seen in stroke compared to control brains is also seen in the control conditions for GDF10 delivery. (**d-f**) Cortical connections of forelimb motor area in normal control compared to scrambled siRNA delivered into infarct core. siRNA GDF10 knocks down GDF10 protein levels (Supplementary Fig 5a) and blocks post-stroke axonal sprouting (Fig. 4d-f). To verify that the siRNA is not having effects outside of GDF10 knock down, scrambled sequence siRNA was tested. Figure conventions are as in Supplementary Fig. 8 and Fig. 4. There is a significant difference in cortical connection map (a), polar plots (b) or linear measurement of neuronal connections (c) between control and scrambled siRNA (n = 7-8 for each group). * = $p<0.05$. Note that Cyto C+stroke and scrambled siRNA+stroke produce very similar maps of forelimb motor cortex connections, and are comparable to stroke only (Supplementary Fig. 6b).

Supplementary Figure 11. Quantitative connectional mapping and axonal connections in GDF10 controls compared to stroke-only. (**a-c**) Cortical connections of forelimb motor area in stroke only compared to scrambled siRNA delivered into infarct core. siRNA

GDF10 knocks down GDF10 protein levels (Supplementary Fig 3a) and blocks post-stroke axonal sprouting (Fig. 4d-f). To verify that the siRNA is not having effects outside of GDF10 knock down, scrambled sequence siRNA was tested. Figure conventions are as in Supplementary Fig. 8 and Fig. 4. There is no significant difference in cortical connection map (a), polar plots (b) or linear measurement of neuronal connections (c) between stroke and scrambled siRNA. (**d-f**) Cortical connections of forelimb motor cortex in stroke only compared to stroke+protein control, cytochrome C delivery from the infarct core via biopolymer hydrogel (n = 8 each group). Figure conventions are as in Supplementary Fig 8 and Figure 4. There is no significant difference in cortical connection map (a), polar plots (b) or linear measurement of neuronal connections (c) between stroke and Cyto C. Cohorts (n=8) of mice treated with GDF10 (red) or control protein (Cytochrome C) (light blue).

Supplementary Figure 12. Synaptic protein localization in peri-infarct cortex axons that have undergone axonal sprouting after GDF-10 treatment. (a) Synaptic protein analysis was performed in the same peri-infarct tissues from animals used for BDA axonal sprouting maps in Fig. 4(a) and (b). Presynaptic VGLUT2 and postsynaptic Homer1 antibodies were used for identification of synaptic contacts. Marker colocalization analyses were performed on Imaris Imaging software to uniquely identify the synaptic connections formed by GDF10-induced sprouting cortical neurons after stroke (mapped in Fig. 4). **(b)** Video through a 10.5μm thick section of peri-infarct cortex taken at 100x. BDA surface is shown in light blue. VGLUT2 presynaptic marker is shown by green spots, and Homer1 postsynaptic marker in red spots.

Supplementary Figure 13. Pipeline for incorporating microarray and RNAseq data sets for neurodevelopmental and CNS injury experiments. Raw data from different platforms are processed to have gene symbols which were subsequently used to merge the datasets. Merged datasets were normalized, then batch effect was adjusted. In one case, the datasets have very few common genes on different array platforms and these datasets were combined (unionized) instead of taking intersections.

Supplementary Figure 14. The numbers of neurons used for each *in vitro* experiment to generate the data on axonal outgrowth effect of GDF10 and other experimental manipulations in Figures 2 and 3. There is no significant difference in neuronal sampling number across experiments.

Supplementary Figure 15. Comparison of forelimb motor system connections in CytoC+stroke vs. GDF10siRNA+ stroke. Conventions as in Supplementary Figures 10 and 11.

a

TGFβ Family	TGFβ	Activin/inhibin/Nodal	BMP
Ligands	TGFβ1, TGFβ2, TGFβ3, GDF10	Activin A, activin B, inhibin A, inihibin B, Nodal, GDF8, GDF11	BMP2, BMP4, BMP5, BMP6, BMP7, BMP8a, BMP8b, BMP9, BMP10, GDF7, GDF8 (myostatin), GDF9
Type I receptors	TGFβRI (ALK5) ACVRL1 (ALK1)	ACVR1B (ALK4), ACVR1C (ALK7)	ACVRL1 (ALk1) ACVR1 (ALK2) BMPR1A (ALK3) BMPR1B (ALK6)
Type II receptors	TGFβRII	ACTRIIA, ACTRIIB	BMPR2, ACTRIIA, ACTRIIB
Type III receptors	TGFβRIII, endoglin, CRIPTO3	CRIPTO1, CRIPTO3, TGFβRIII	RGMA, RGMB, RGMC, endoglin
Receptor SMAD	SMAD2, SMAD3	SMAD2, SMAD3	SMAD1, SMAD5, SMAD8
Co-SMAD	SMAD4	SMAD4	SMAD4
Inhibitory SMAD	SMAD7	SMAD7	SMAD6,7

b

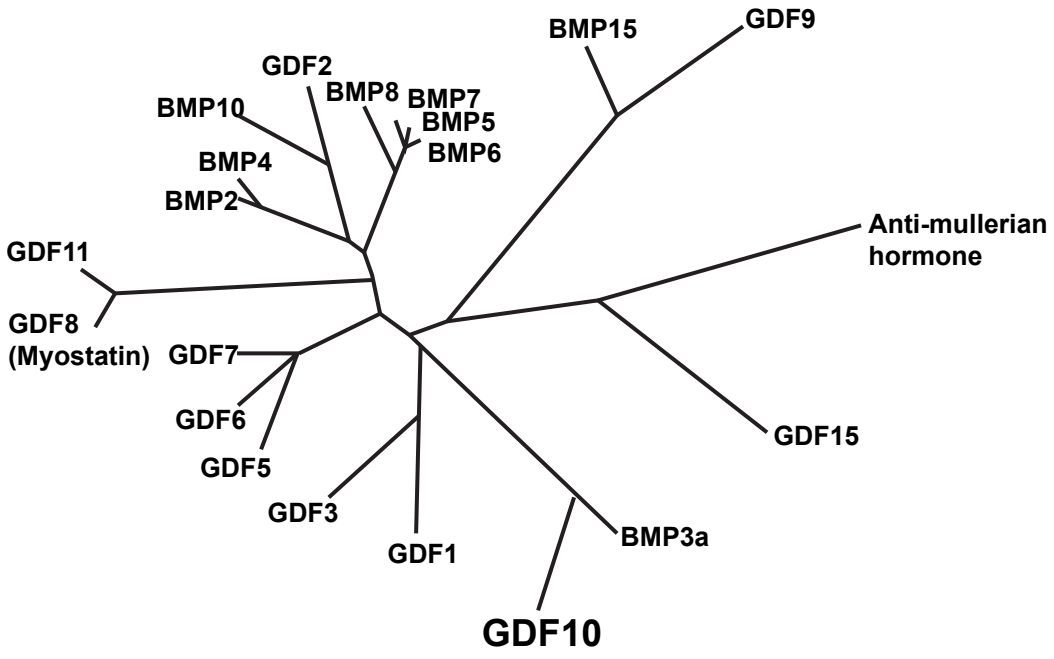

Suppl Fig 1. GDF10 relationship with TGFβR Superfamily

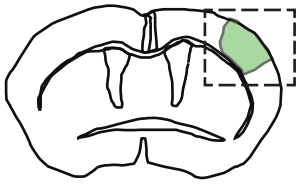

a) Stroke infarct and ipsilesional cortex (hemispheric overview)

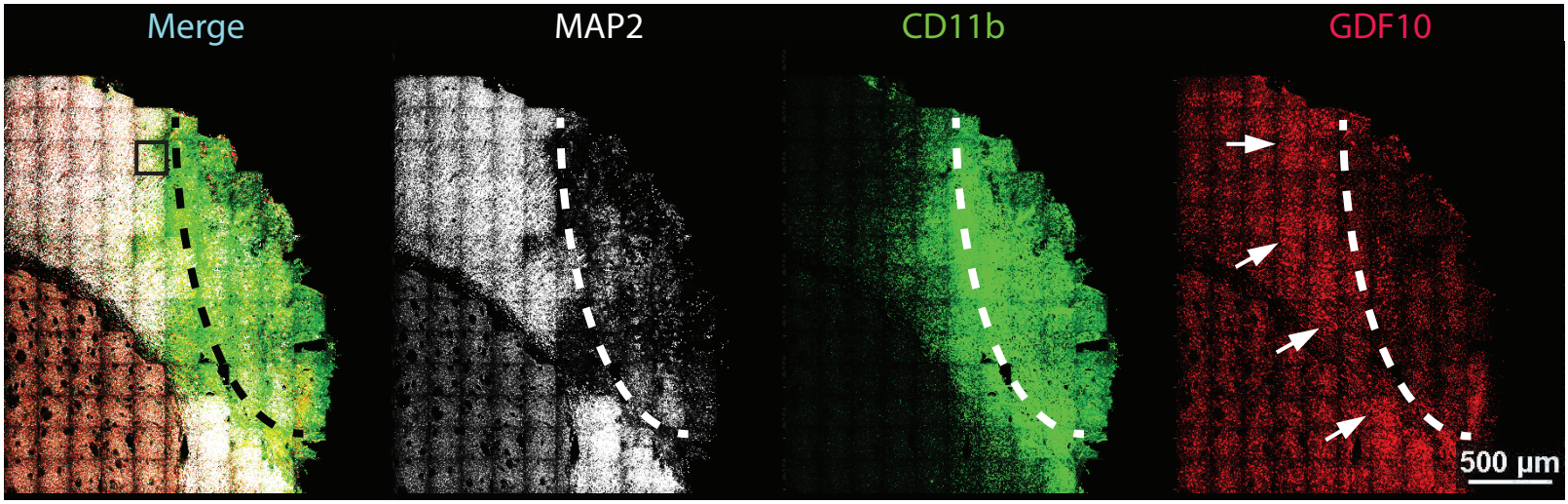

b) Peri-infarct Cortex (60X)

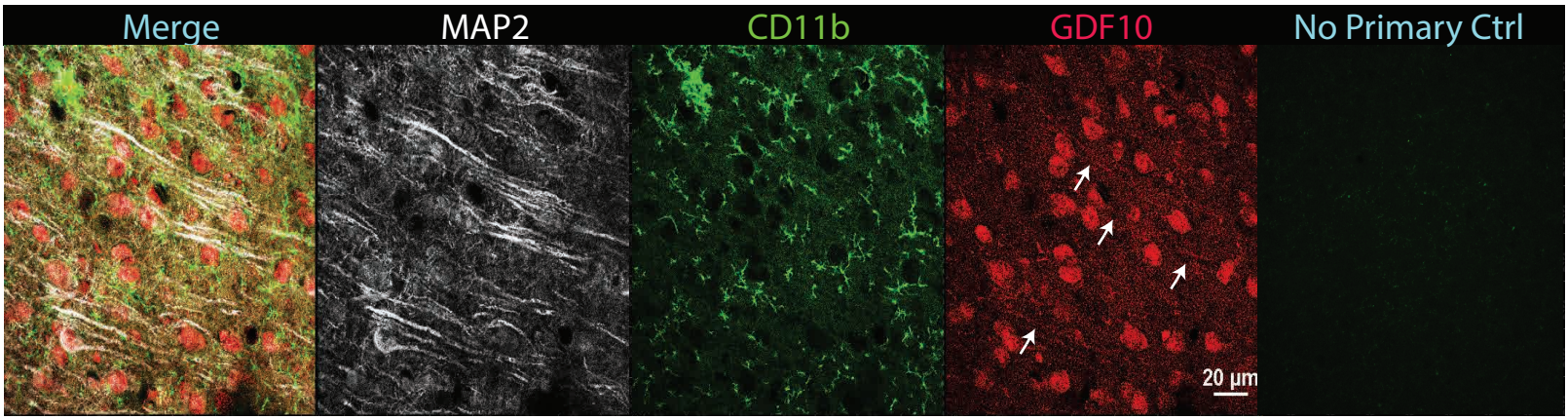

c) Contralateral Cortex Control (60X)

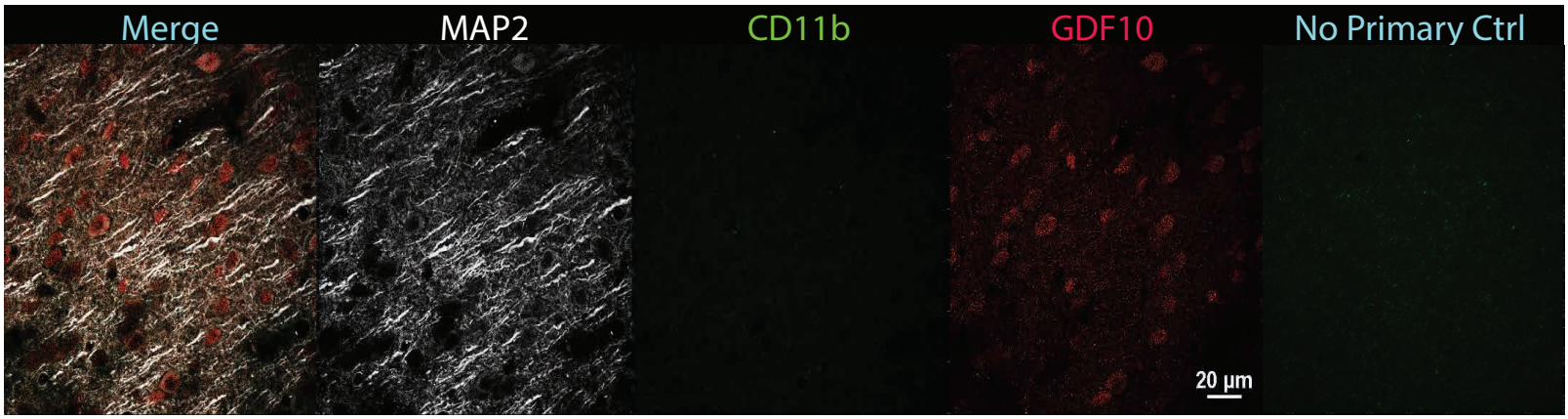

Suppl Fig 2, page 1. GDF10 protein distribution in peri-infarct tissue

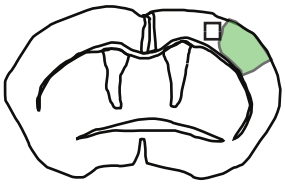

d) GDF10 upregulated in peri-infarct neurons and excludes microglial/macrophages

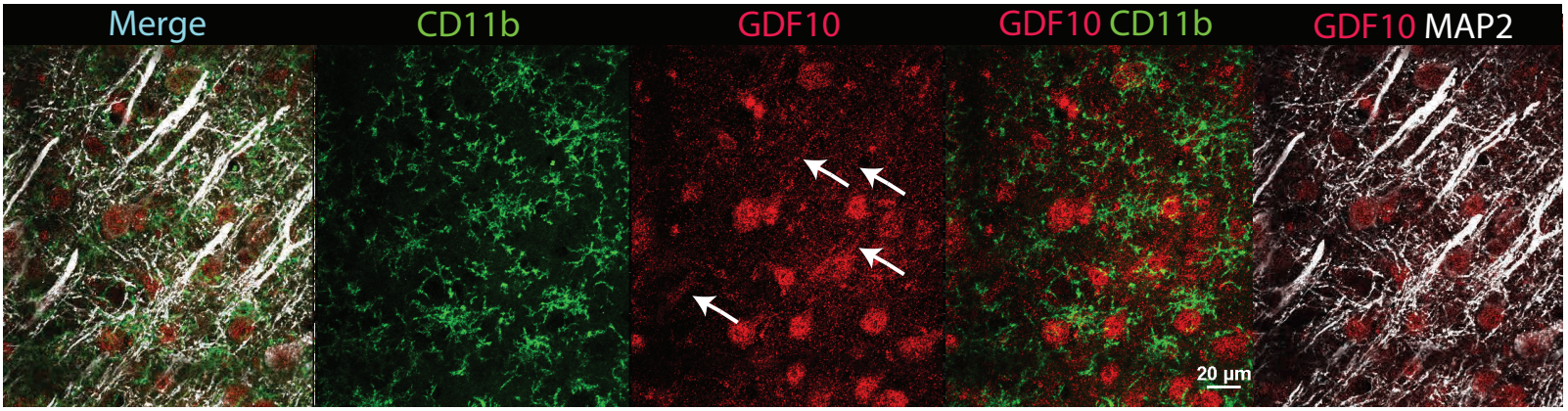

e) Extracellular GDF10 adjacent to infarct area near surviving neurites

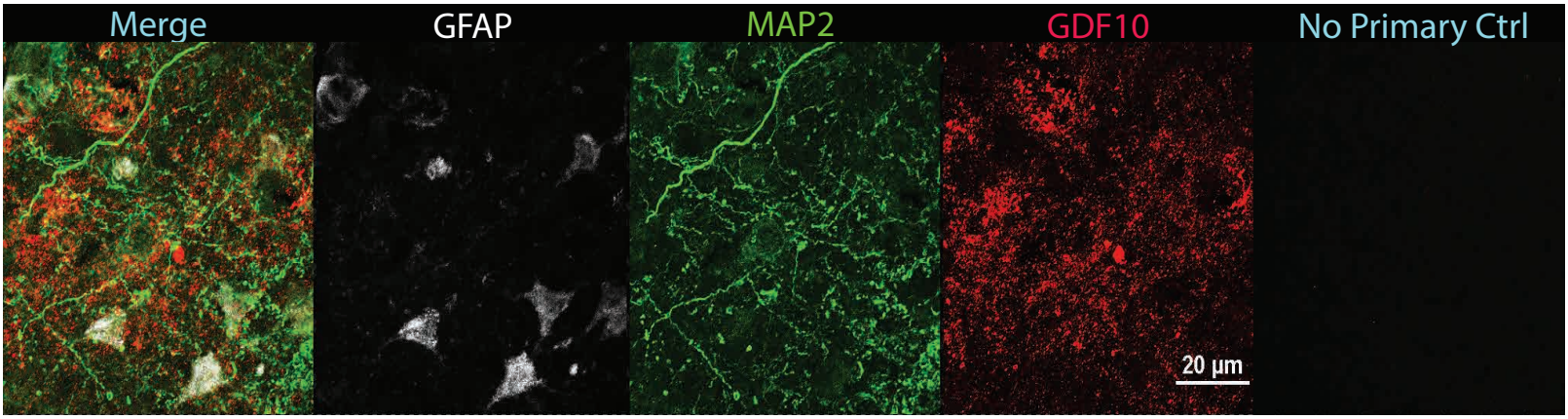

Suppl Fig 2 . page 2. GDF10 protein distribution in peri-infarct tissue

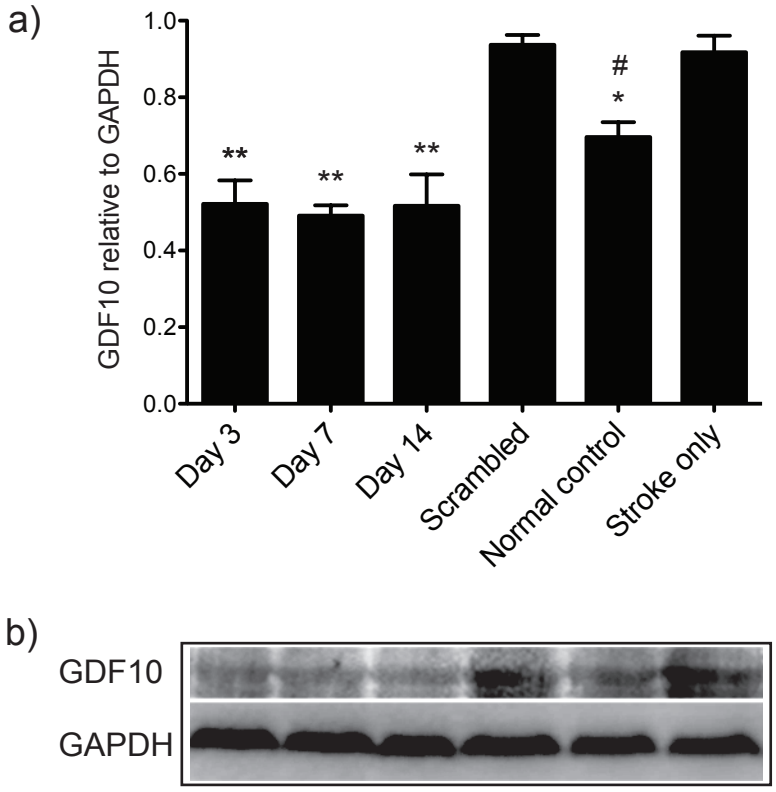

Suppl Fig 3. Effect of GDF10 siRNA knockdown protein in vivo

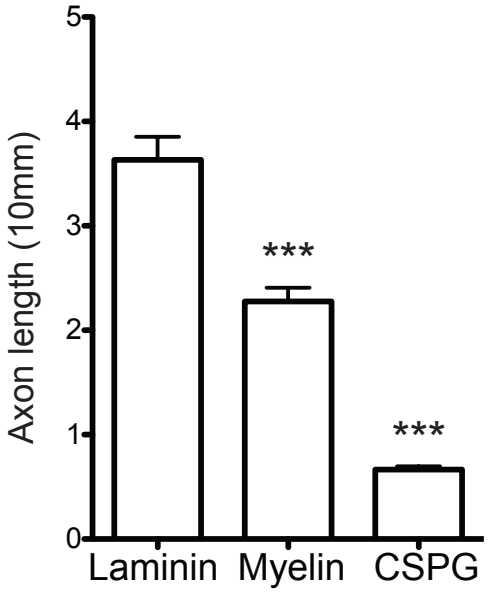

Suppl Fig 4. Axonal outgrowth of primary cortical neurons on standard and inhibitory substrates

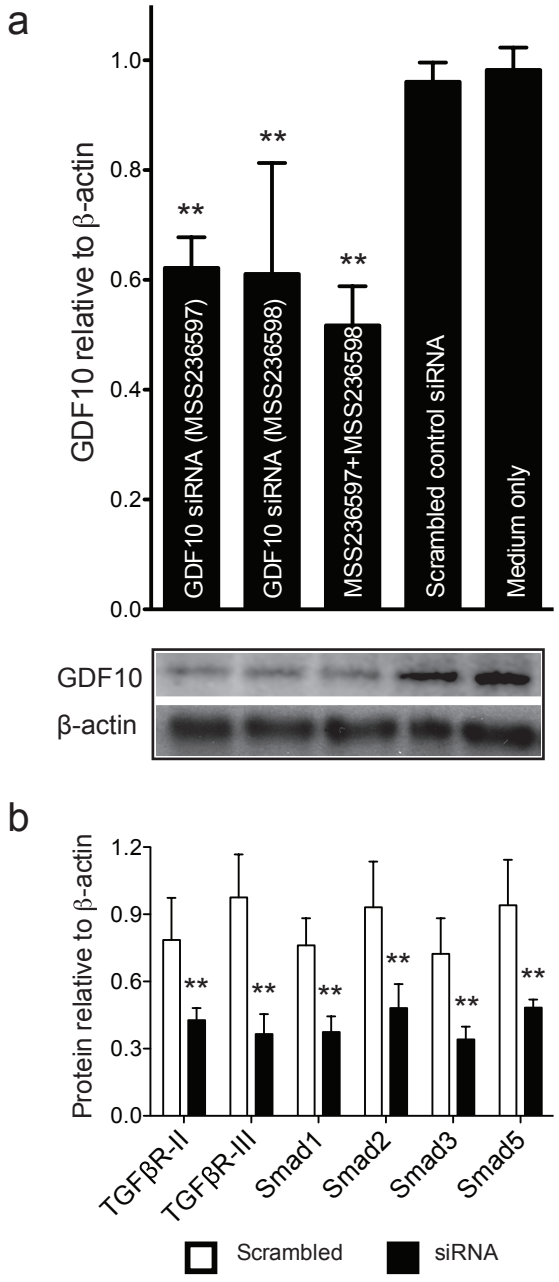

Suppl Fig 5. Effect of GDF10, TGFβR and Smad siRNA knockdown protein in vitro

a) Primary Cortical Neurons express GDF10

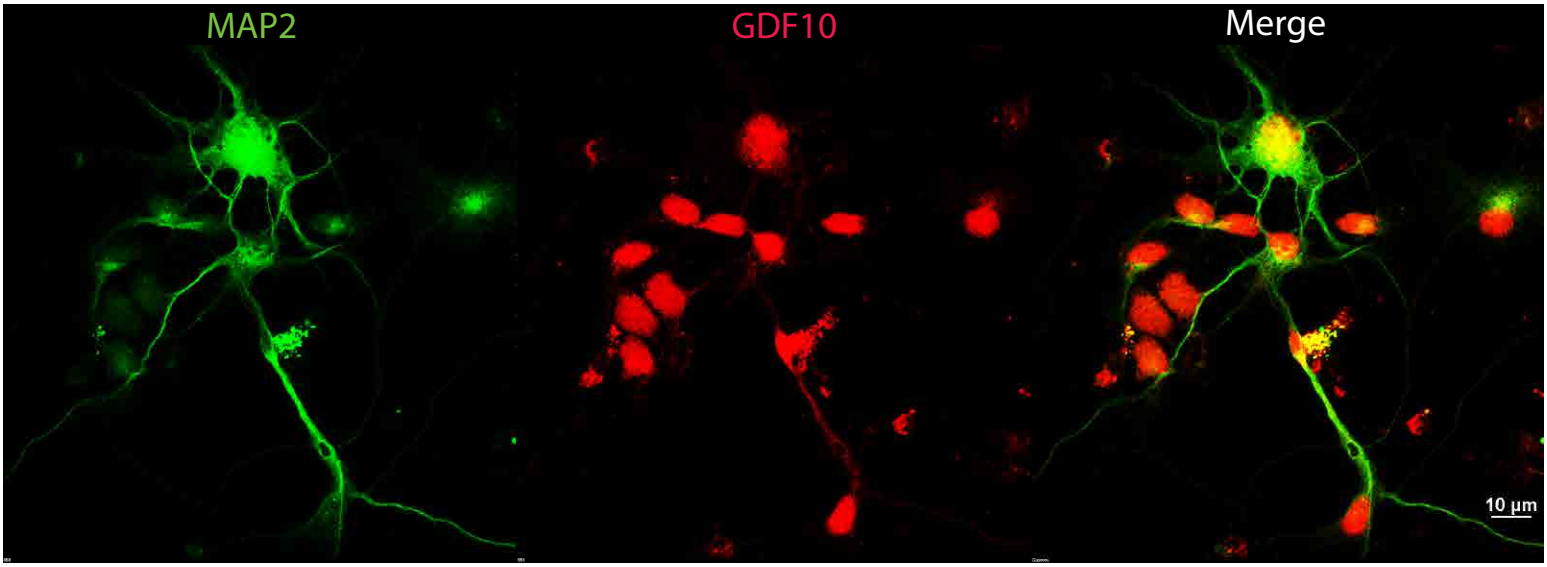

b) High magnification of neuronal GDF10

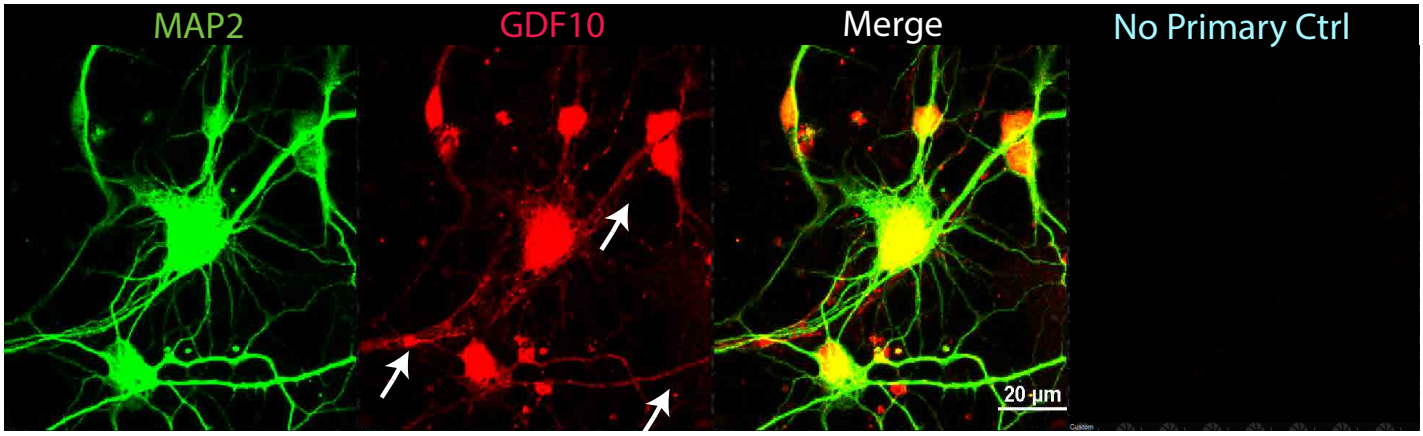

Suppl Fig 6. Primary cortical neurons plated in-vitro express GDF10

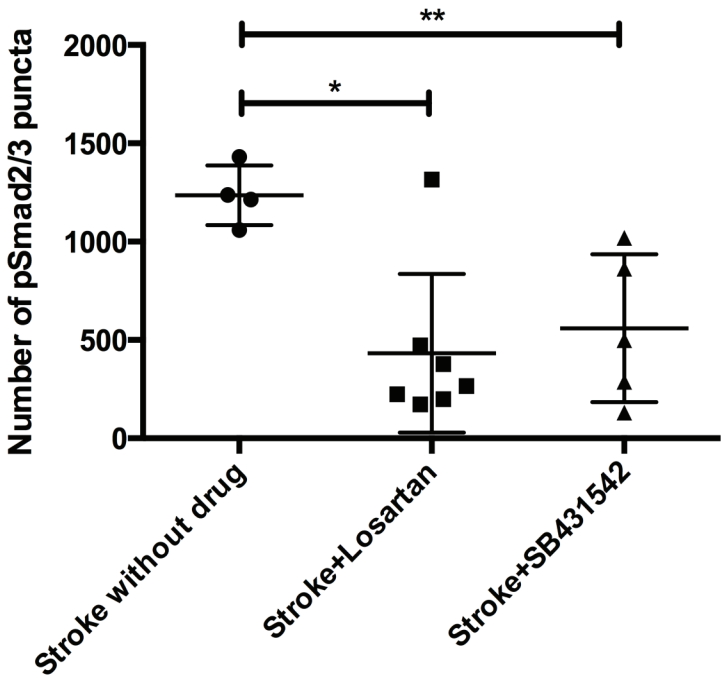

Stroke vs Stroke+Losartan: p=0.0056

Stroke vs Stroke+SB431542: p=0.0244

Suppl Fig 7. TGF-β antagonism blocks pSmad2/3 signaling inperi-infarct cortex

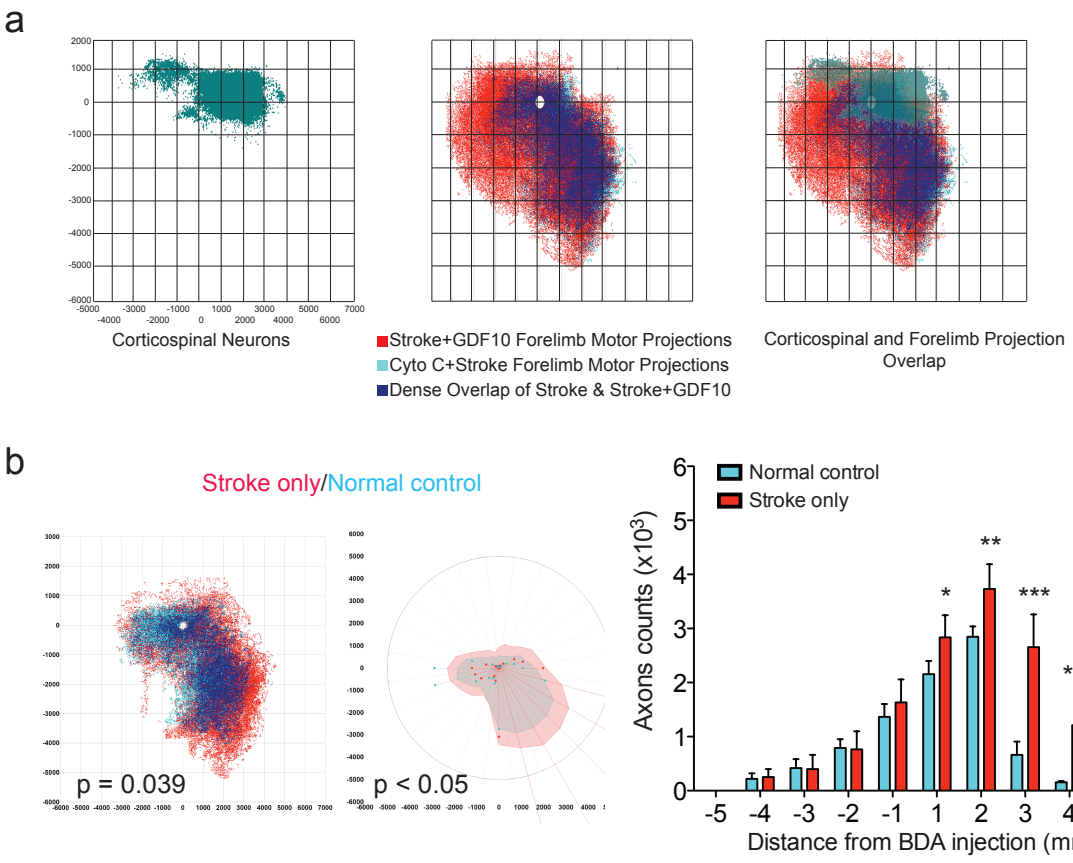

Suppl Fig 8. Quantitative connectional mapping and axonal connections in peri-infarct cortex

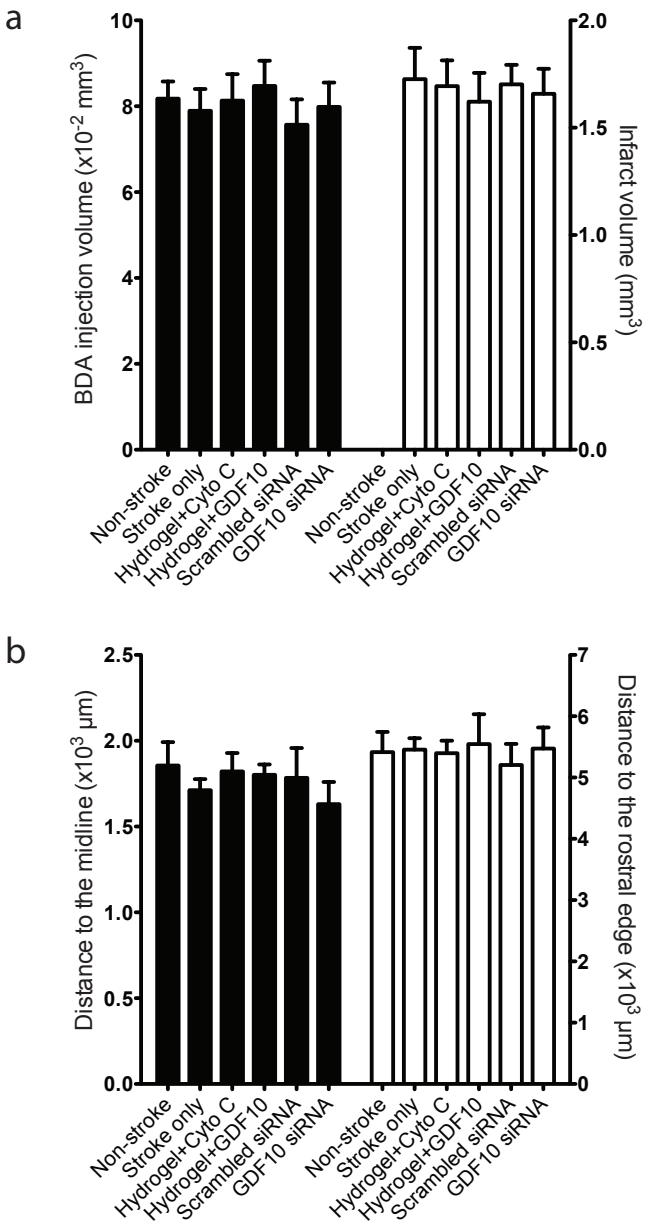

Suppl Fig 9. Infarct volume, BDA volume and injection locations

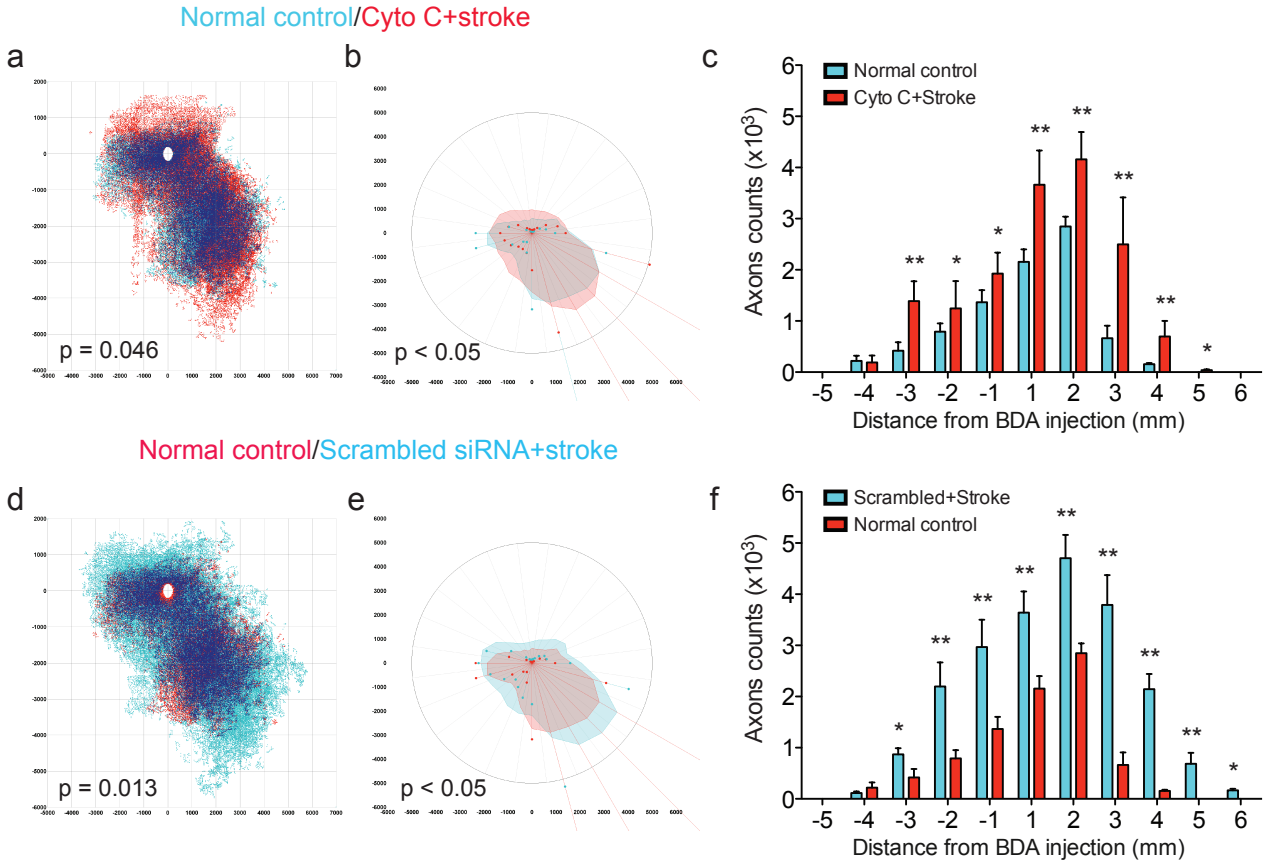

Suppl Fig 10. Quantitative connectional mapping and axonal connections in GDF10 controls compared to normal control

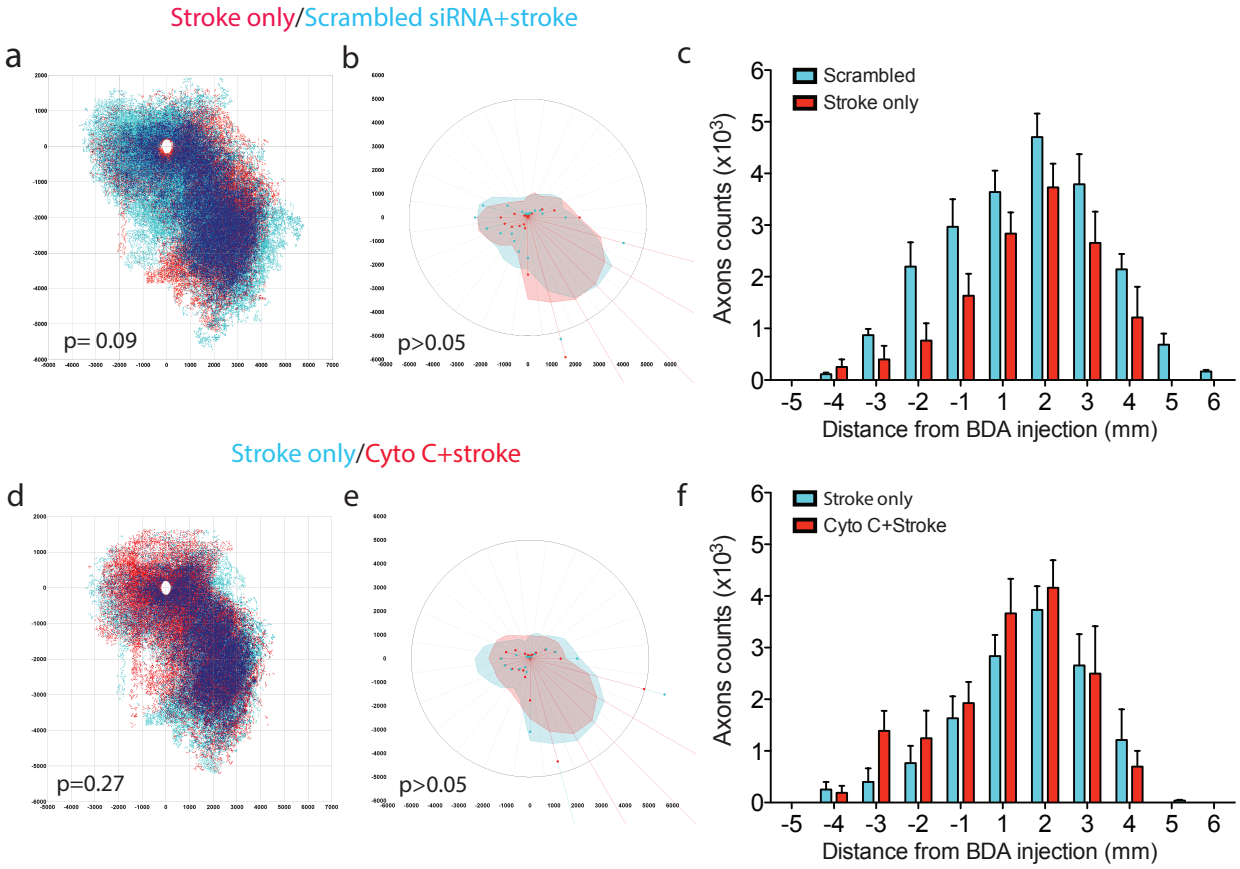

Suppl Fig 11. Quantitative connectional mapping and axonal connections in GDF10 controls compared to stroke-only

a

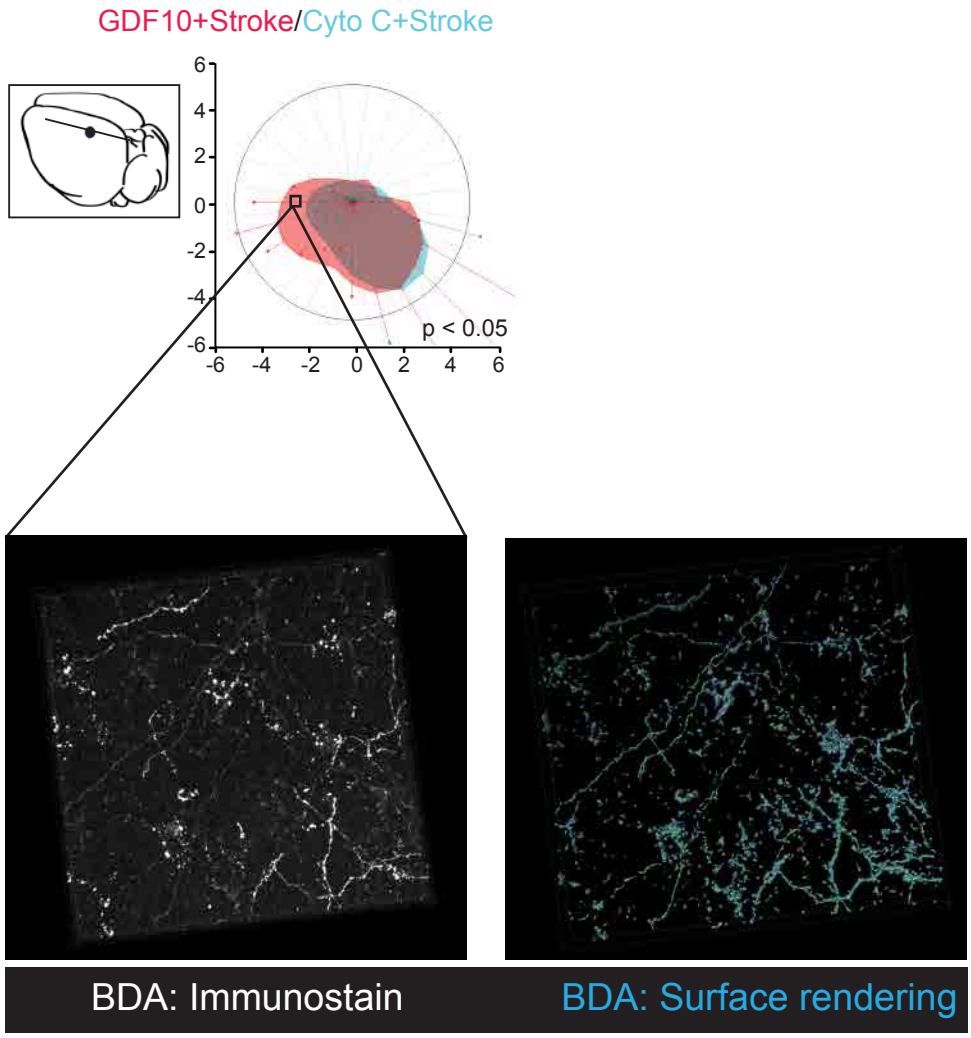

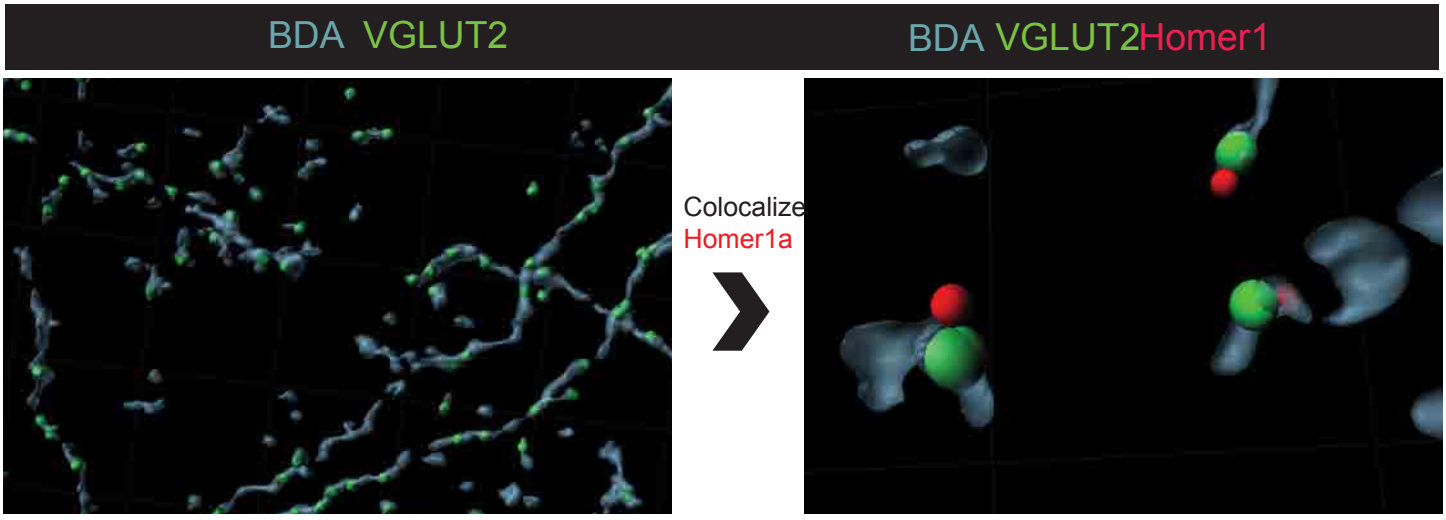

b Video: Synaptic proteins identified in axons that have undergone axonal sprouting in peri-infarct cortex after GDF10 treatment

Suppl Fig 12. Synaptic protein analysis using VGLUT2 and Homer1 colocalization in peri-infarct sprouting neurons

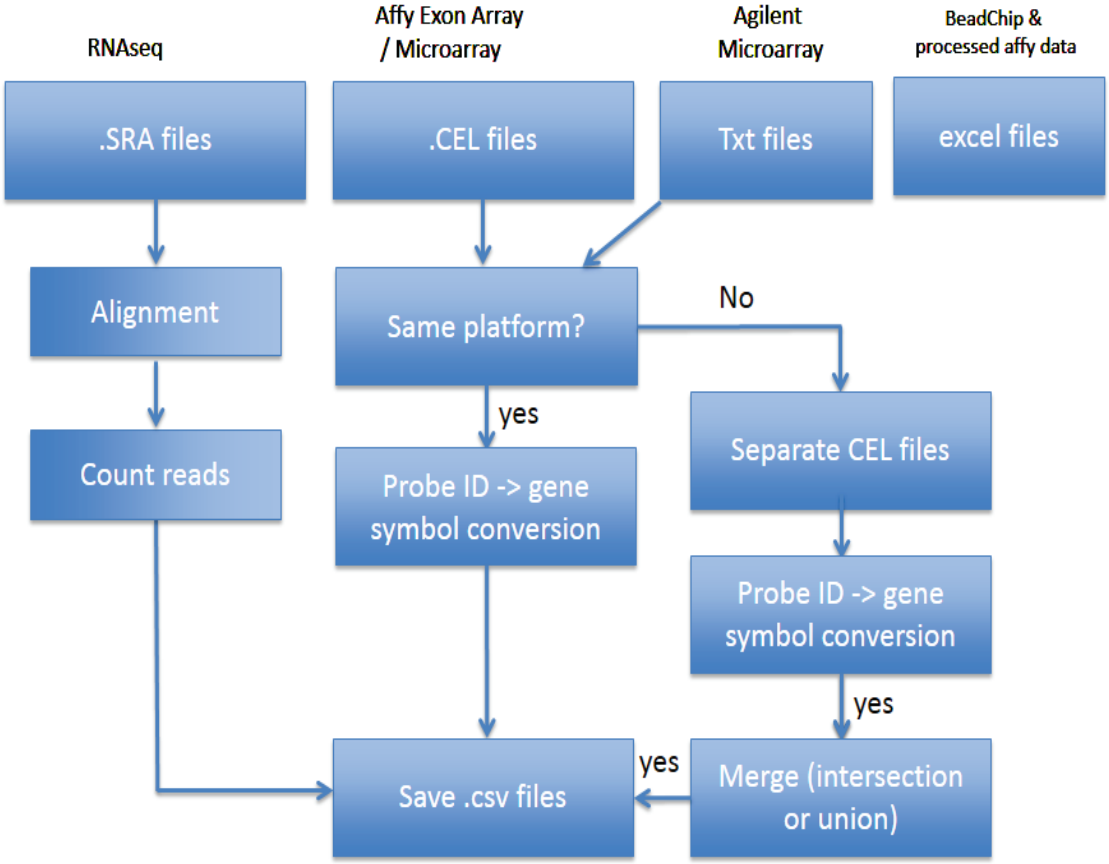

Suppl Fig 13. Pipeline for incorporating microarray and RNAseq data sets for neurodevelopmental and CNS injury experiments

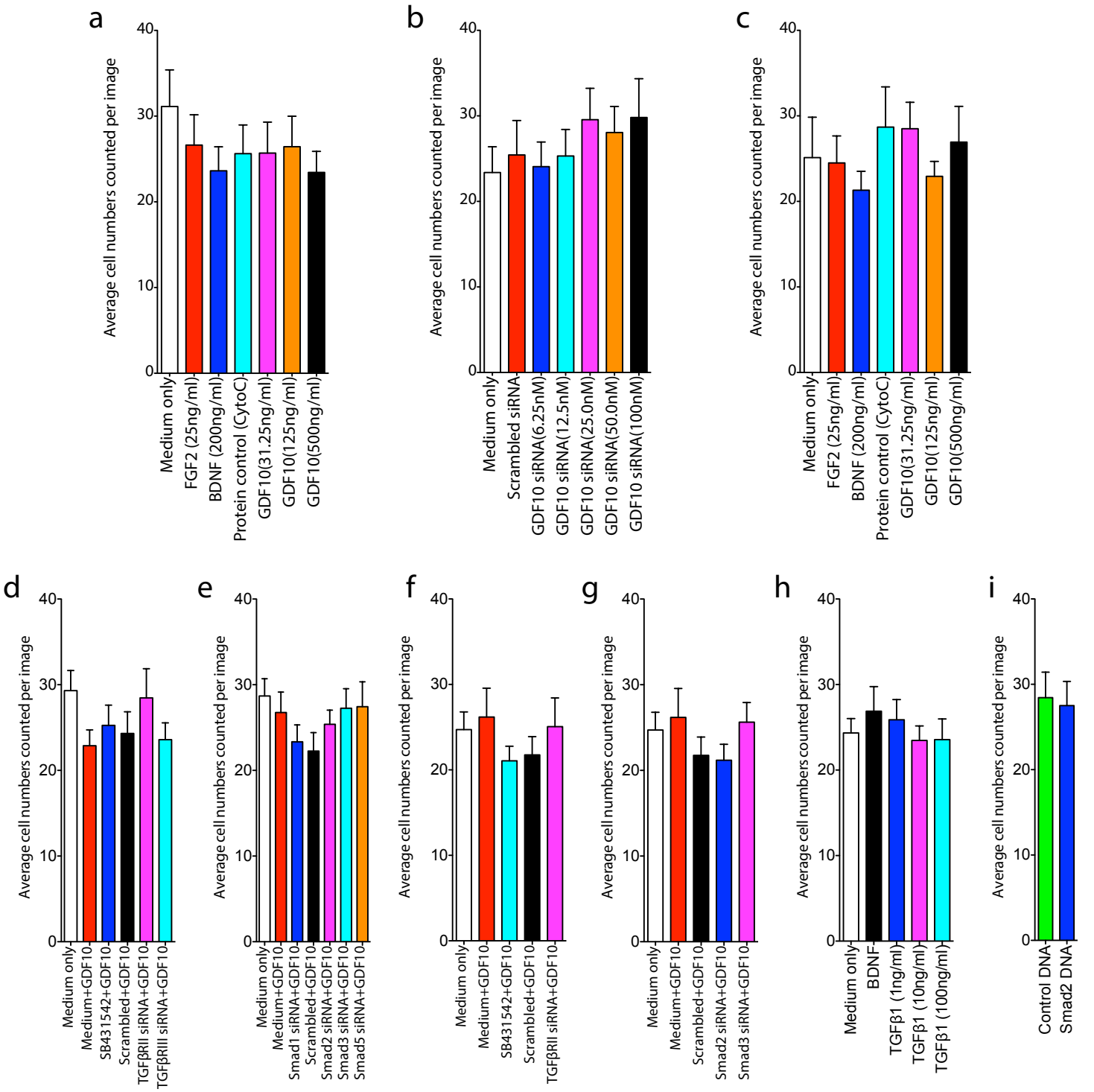

Supplementary Fig 14 . Cell numbers counted per image for axonal length quantification in all conditions.

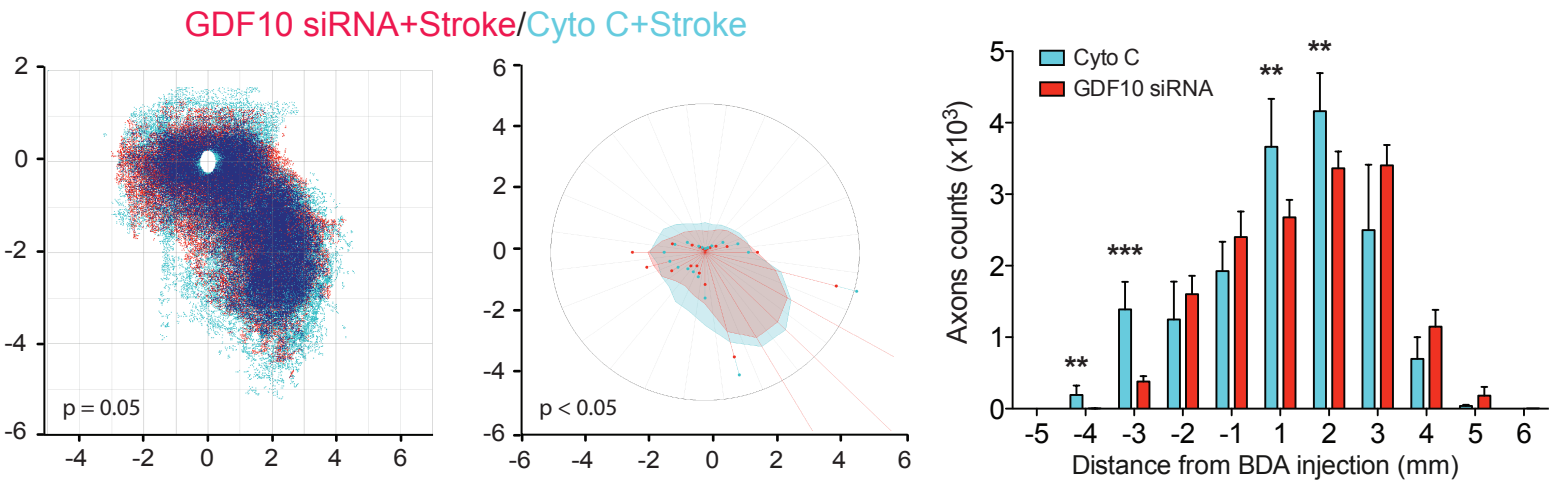

Supplementary Fig 15. GDF10 siRNA reduced axonal connections in peri-infarct cortex after stroke.

Supplementary Table 1

Human Cases

Condition	Age	Sex	Cause of Death
Control	93	M	Hypovolemic shock
Control	85	M	Septic shock
Control	68	M	Septic shock
Control	63	F	Pneumonia
Stroke	81	M	Cardipulmonary arrest
Stroke	65	M	Stroke
Stroke	54	M	Liver failure/pneumonia
Stroke	81	F	Pancreatic carcinoma
Stroke	88	F	Cardipulmonary arrest
Stroke	92	F	Cardipulmonary arrest
Stroke	96	F	Cardipulmonary arrest

Supplementary Table 2

Canonical Pathways Mult Comp Stroke+GDF10 vs Stroke

Canonical Pathways	-log(B-H p-value)	Ratio	z-score	Molecules
Tec Kinase Signaling	4.22E00	1.01E-01	0.277	RND2,TNFRSF21,GNG4,FYN,GNA14,TEC,PIK3R3,TLR4,PIK3CG,LYN,PIK3CD,STAT2,STAT1,FASLG,ITK,ITGA4
NF-κB Signaling	4.08E00	9.25E-02	2.500	MAP3K14,IL1A,TGFBR1,TNFAIP3,TNFRSF11A,TLR2,IL1R2,PIK3R3,TLR4,PIK3CG,TLR1,TLR7,MAP3K8,PIK3CD,FGFRL1,PDGFRB
Hepatic Fibrosis / Hepatic Stel	4.08E00	8.63E-02		COL5A2,IL1A,TGFBR1,COL9A3,CXCR3,COL20A1,IL1R2,CXCL3,TLR4,IGF1,TNFSF8,CD14,FIGF,COL11A1,STAT1,FASLG,PDGFRB
Colorectal Cancer Metastasis	3.78E00	7.66E-02	1.500	RND2,GNG4,TGFBR1,CASP3,PTGER3,MYC,TLR2,PIK3R3,TLR4,PIK3CG,TLR1,TLR7,FIGF,PIK3CD,STAT1,ADCY8,PTGER4,TCF7L2
Role of Osteoblasts, Osteocla	3.7E00	7.8E-02		MAP3K14,Naip1 (includes others),IL1A,SFRP2,TNFRSF11A,BMP5,IL1R2,PIK3R3,PPP3R2,IGF1,PIK3CG,PIK3CD,SFRP1,SOST,BMP6,BIRC3,TCF7L2
PTEN Signaling	3.47E00	1.02E-01	-2.309	PIK3R3,TGFBR1,CASP3,PIK3CG,INPPL1,PIK3CD,FGFRL1,CNKSR3,TNFRSF11A,FASLG,PDGFRB,ITGA4
Molecular Mechanisms of Can	3.43E00	6.03E-02		RND2,FYN,Naip1 (includes others),TGFBR1,CASP3,ARHGEF7,CDK6,GNA14,BMP5,MYC,PIK3R3,PIK3CG,IRS1,ARHGEF6,PIK3CD,ADCY8,BMP6,NOTCH1,BIRC3,PTCH2,FASLG,ITGA
Role of Pattern Recognition R	3.26E00	9.45E-02	1.667	TLR2,PIK3R3,TLR4,CLEC7A,IL1A,PIK3CG,DDX58,TLR1,TLR7,PIK3CD,RIPK2
Cardiac Hypertrophy Signaling	3.2E00	7.17E-02	1.807	RND2,GNG4,MAP3K14,TGFBR1,GNA14,PPP3R2,PLCD1,PIK3R3,IGF1,IRS1,PIK3CG,MEF2C,MAP3K8,PIK3CD,ADCY8,ADRB2
Amyotrophic Lateral Sclerosis	2.92E00	1.02E-01		PIK3R3,CAPN6,Naip1 (includes
Role of Macrophages, Fibrobla	2.83E00	6.06E-02		PIK3R3,IL1R2,TLR2,PLCD1,PPP3R2,MYC,TLR4,MAP3K14,IL1A,SFRP2,PIK3CG,TLR1,TLR7,FIGF,PIK3CD,SFRP1,SOST,TCF7L2
G-Protein Coupled Receptor S	2.6E00	6.25E-02		GPR17,FYN,RGS2,PTGER3,PDE9A,GNA14,PIK3R3,P2RY13,PIK3CG,P2RY12,MAP3K8,PIK3CD,HTR1A,ADCY8,PTGER4,ADRB2
Axonal Guidance Signaling	2.6E00	5.08E-02		GNG4,FYN,ARHGEF7,EFNA3,GNA14,BMP5,TUBB2B,PPP3R2,PLCD1,PIK3R3,MICAL1,SDCBP,TUBA1A,IGF1,PIK3CG,ARHGEF6,FIGF,PIK3CD,BMP6,PTC
Human Embryonic Stem Cell I	2.6E00	8.21E-02		PIK3R3,NANOG,TGFBR1,PIK3CG,PIK3CD,FGFRL1,BMP6,LEFTY2,BMP5,TC
Glucocorticoid Receptor Signa	2.6E00	6.13E-02		MAP3K14,TGFBR1,POU2F2,SGK1,Hspa1b,HSPA1A/HSPA1B,CD163,TSC22D3,IL1R2,PIK3R3,PPP3R2,CXCL3,PIK3CG,PIK3CD,STAT1,ADRB2
Toll-like Receptor Signaling	2.55E00	1.1E-01	1.890	TLR2,TLR4,MAP3K14,IL1A,TLR1,TLR7,TNFAIP3,CD14
TREM1 Signaling	2.54E00	1.08E-01	2.828	TLR2,TLR4,CXCL3,Naip1 (includes others),MPO,TLR1,TLR7,CD83
Myc Mediated Apoptosis Signa	2.44E00	1.21E-01		PIK3R3,MYC,IGF1,CASP3,PIK3CG,PIK3CD,FASLG
Reelin Signaling in Neurons	2.4E00	1.01E-01		PIK3R3,FYN,PIK3CG,ARHGEF6,ITGA6,LYN,PIK3CD,ITGA4
Role of NFAT in Regulation of	2.4E00	7.02E-02	1.667	PIK3R3,GNG4,PPP3R2,FYN,ITPR2,PIK3CG,HLA-

GM-CSF Signaling	2.33E00	1.13E-01	0.816	PIK3R3,PPP3R2,PIK3CG,LYN,PIK3CD,STAT1,BCL2A1
B Cell Receptor Signaling	2.32E00	6.82E-02		PTPRC,PIK3R3,PPP3R2,MAP3K14,POU2F2,PIK3CG,LYN,INPPL1,MAP3K8,MEF2C,PIK3CD,BCL2A1
PI3K Signaling in B Lymphocy	2.31E00	7.81E-02	1.000	PLCD1,PTPRC,PPP3R2,TLR4,FYN,ITPR2,IRS1,PIK3CG,LYN,PIK3CD
Dendritic Cell Maturation	2.29E00	6.7E-02		PLCD1,TLR2,PIK3R3,TLR4,MAP3K14,IL1A,PIK3CG,HLA-
FAK Signaling	2.23E00	9.2E-02		PIK3R3,FYN,CAPN6,ARHGEF7,PIK3CG,ARHGEF6,PIK3CD,ITGA4
Role of Tissue Factor in Canc	2.23E00	8.18E-02		PIK3R3,FYN,CASP3,PIK3CG,ITGA6,LYN,PLAUR,PIK3CD,GNA14
Altered T Cell and B Cell Signa	2.23E00	9.09E-02		TLR2,TLR4,MAP3K14,IL1A,TLR1,HLA-DQA1,TLR7,FASLG
RANK Signaling in Osteoclast	2.23E00	9.09E-02		PIK3R3,PPP3R2,MAP3K14,PIK3CG,MAP3K8,PIK3CD,TNFRSF11A,BIRC3
ILK Signaling	2.23E00	6.45E-02	0.632	RND2,PIK3R3,MYC,PARVB,CASP3,LIMS2,IRS1,PIK3CG,ARHGEF6,FIGF,PIK
PAK Signaling	2.23E00	8.99E-02	1.134	PIK3R3,CASP3,ARHGEF7,PIK3CG,ARHGEF6,PIK3CD,PDGFRB,ITGA4
Death Receptor Signaling	2.16E00	8.7E-02	-1.414	TNFRSF21,MAP3K14,Naip1 (includes
IL-9 Signaling	2.16E00	1.47E-01	-0.447	PIK3R3,IRS1,PIK3CG,PIK3CD,STAT1
eNOS Signaling	2.13E00	7.09E-02	2.121	PIK3R3,CASP3,ITPR2,PIK3CG,Hspa1b,HSPA1A/HSPA1B,FIGF,PIK3CD,ADC
CD28 Signaling in T Helper Ce	2.11E00	7.63E-02	0.707	PTPRC,PIK3R3,PPP3R2,FYN,ITPR2,PIK3CG,HLA-DQA1,PIK3CD,ITK
Prolactin Signaling	2.11E00	9.59E-02	-1.134	PIK3R3,MYC,FYN,IRS1,PIK3CG,PIK3CD,STAT1
T Cell Receptor Signaling	2.06E00	8.25E-02		TEC,PTPRC,PIK3R3,PPP3R2,FYN,PIK3CG,PIK3CD,ITK
Glioblastoma Multiforme Signa	2.06E00	6.85E-02	-0.333	RND2,PLCD1,PIK3R3,MYC,IGF1,ITPR2,PIK3CG,CDK6,PIK3CD,PDGFRB
PDGF Signaling	2.01E00	9.09E-02	-0.378	PIK3R3,MYC,PIK3CG,INPPL1,PIK3CD,STAT1,PDGFRB
Docosahexaenoic Acid (DHA)	1.97E00	1.28E-01		PIK3R3,CASP3,PIK3CG,PIK3CD,BCL2A1
PPARα/RXRα Activation	1.97E00	6.15E-02	-0.707	PLCD1,IL1R2,MAP3K14,GPD1,TGFBR1,IRS1,LPL,MEF2C,GNA14,ADCY8,AB
Role of NFAT in Cardiac Hype	1.97E00	6.15E-02		PLCD1,PIK3R3,GNG4,PPP3R2,TGFBR1,IGF1,ITPR2,PIK3CG,MEF2C,PIK3CD
Production of Nitric Oxide and	1.96E00	6.11E-02	1.265	RND2,TLR2,PIK3R3,TLR4,MAP3K14,MPO,PIK3CG,NCF2,MAP3K8,PIK3CD,S
iCOS-iCOSL Signaling in T He	1.84E00	7.41E-02	1.633	PTPRC,PIK3R3,PPP3R2,ITPR2,PIK3CG,HLA-DQA1,PIK3CD,ITK
Germ Cell-Sertoli Cell Junctio	1.84E00	6.25E-02		RND2,PIK3R3,MAP3K14,TGFBR1,TUBA1A,PIK3CG,ITGA6,MAP3K8,PIK3CD,
Sphingosine-1-phosphate Sig	1.83E00	7.34E-02	-0.378	RND2,PLCD1,PIK3R3,CASP3,PIK3CG,PIK3CD,ADCY8,PDGFRB
IL-12 Signaling and Productio	1.82E00	6.67E-02		PPARG,TLR2,PIK3R3,TLR4,PIK3CG,MAF,MAP3K8,PIK3CD,STAT1
UVA-Induced MAPK Signaling	1.76E00	7.95E-02	-0.447	PLCD1,PIK3R3,CASP3,PIK3CG,PARP12,PIK3CD,STAT1
Apoptosis Signaling	1.75E00	7.87E-02	-2.449	MAP3K14,CAPN6,Naip1 (includes others),CASP3,BCL2A1,BIRC3,FASLG
MSP-RON Signaling Pathway	1.74E00	1.09E-01		TLR2,PIK3R3,TLR4,PIK3CG,PIK3CD
TNFR2 Signaling	1.69E00	1.38E-01		MAP3K14,Naip1 (includes others),TNFAIP3,BIRC3
p38 MAPK Signaling	1.69E00	6.84E-02	0.707	IL1R2,MYC,IL1A,TIFA,TGFBR1,MEF2C,STAT1,FASLG
Growth Hormone Signaling	1.69E00	8.7E-02	-0.447	PIK3R3,IGF1,IRS1,PIK3CG,PIK3CD,STAT1
Ephrin A Signaling	1.69E00	1.04E-01		PIK3R3,FYN,PIK3CG,EFNA3,PIK3CD
PKCθ Signaling in T Lymphoc	1.69E00	6.78E-02	1.414	PIK3R3,PPP3R2,FYN,MAP3K14,PIK3CG,HLA-DQA1,MAP3K8,PIK3CD
P2Y Purigenic Receptor Signa	1.68E00	6.72E-02	-0.378	PLCD1,PIK3R3,GNG4,MYC,PIK3CG,P2RY12,PIK3CD,ADCY8
TNFR1 Signaling	1.68E00	1.02E-01	-1.000	MAP3K14,Naip1 (includes others),CASP3,TNFAIP3,BIRC3

Gαq Signaling	1.67E00	6.12E-02	0.000	RND2,PIK3R3,GNG4,PPP3R2,RGS2,ITPR2,PIK3CG,PIK3CD,GNA14
Mouse Embryonic Stem Cell F	1.67E00	7.37E-02	0.000	PIK3R3,MYC,NANOG,T,PIK3CG,PIK3CD,TCF7L2
LPS-stimulated MAPK Signali	1.63E00	8.22E-02	1.633	PIK3R3,TLR4,MAP3K14,PIK3CG,CD14,PIK3CD
NF-κB Activation by Viruses	1.63E00	8.22E-02	1.633	PIK3R3,MAP3K14,PIK3CG,ITGA6,PIK3CD,ITGA4
Phospholipase C Signaling	1.62E00	5.02E-02	0.707	RND2,GNG4,PPP3R2,FYN,ITPR2,ARHGEF7,ARHGEF6,LYN,MEF2C,ADCY8,I
Leptin Signaling in Obesity	1.61E00	8.11E-02		PLCD1,NPY,PIK3R3,PIK3CG,PIK3CD,ADCY8
CXCR4 Signaling	1.61E00	5.92E-02	-0.378	RND2,PIK3R3,GNG4,ITPR2,PIK3CG,LYN,PIK3CD,GNA14,ADCY8
Neuropathic Pain Signaling In	1.59E00	7E-02	0.378	PLCD1,TACR1,PIK3R3,ITPR2,PIK3CG,TAC1,PIK3CD
IL-4 Signaling	1.58E00	7.89E-02		PIK3R3,IRS1,PIK3CG,HLA-DQA1,INPPL1,PIK3CD
Gap Junction Signaling	1.58E00	5.81E-02		PLCD1,PIK3R3,PPP3R2,TUBA1A,ITPR2,PIK3CG,PIK3CD,ADCY8,TUBB2B
Lymphotoxin β Receptor Signa	1.58E00	9.26E-02	0.447	PIK3R3,MAP3K14,CASP3,PIK3CG,PIK3CD
TWEAK Signaling	1.58E00	1.18E-01	-1.000	MAP3K14,Naip1 (includes others),CASP3,BIRC3
Inhibition of Angiogenesis by T	1.58E00	1.18E-01		FYN,TGFBR1,CASP3,THBS1
Paxillin Signaling	1.58E00	6.86E-02	0.816	PIK3R3,ARHGEF7,PIK3CG,ARHGEF6,ITGA6,PIK3CD,ITGA4
Thrombopoietin Signaling	1.56E00	9.09E-02	-0.447	PIK3R3,MYC,PIK3CG,PIK3CD,STAT1
LPS/IL-1 Mediated Inhibition o	1.55E00	5.05E-02	0.447	IL1R2,CHST2,TLR4,IL1A,FMO2,ALDH1L2,CHST3,CD14,FABP5,PAPSS2,ABC
Rac Signaling	1.55E00	6.73E-02	0.378	PIK3R3,CYFIP2,PIK3CG,NCF2,SH3RF1,PIK3CD,ITGA4
cAMP-mediated signaling	1.55E00	5.02E-02	1.265	PPP3R2,GPR17,P2RY13,RGS2,PDE9A,PTGER3,P2RY12,HTR1A,ADCY8,PT
EGF Signaling	1.55E00	8.93E-02	-0.447	PIK3R3,ITPR2,PIK3CG,PIK3CD,STAT1
Glycerol Degradation I	1.55E00	3.33E-01		GPD1,Gyk
Thrombin Signaling	1.55E00	5.24E-02	-0.707	RND2,PLCD1,PIK3R3,GNG4,ITPR2,PIK3CG,ARHGEF6,PIK3CD,GNA14,ADCY
Breast Cancer Regulation by S	1.55E00	5.24E-02		PIK3R3,GNG4,TUBA1A,ITPR2,ARHGEF7,PIK3CG,ARHGEF6,PIK3CD,ADCY8,
Glioma Invasiveness Signaling	1.55E00	8.77E-02	0.447	RND2,PIK3R3,PIK3CG,PLAUR,PIK3CD
Pancreatic Adenocarcinoma S	1.55E00	6.6E-02	0.000	PIK3R3,TGFBR1,PIK3CG,FIGF,PIK3CD,STAT1,NOTCH1
fMLP Signaling in Neutrophils	1.51E00	6.48E-02	0.816	PIK3R3,GNG4,PPP3R2,ITPR2,PIK3CG,NCF2,PIK3CD
Induction of Apoptosis by HIV1	1.46E00	8.33E-02	-1.342	MAP3K14,Naip1 (includes others),CASP3,BIRC3,FASLG
Role of NANOG in Mammalian	1.46E00	6.31E-02	0.447	PIK3R3,NANOG,T,PIK3CG,PIK3CD,BMP6,BMP5
Huntington's Disease Signaling	1.45E00	4.78E-02		PIK3R3,GNG4,CAPN6,IGF1,CASP3,SGK1,PIK3CG,Hspa1b,HSPA1A/HSPA1B,
Estrogen-Dependent Breast C	1.43E00	8.06E-02	1.000	PIK3R3,IGF1,PIK3CG,HSD17B7,PIK3CD
Endothelin-1 Signaling	1.43E00	5.26E-02	-0.333	PLCD1,PIK3R3,MYC,CASP3,ITPR2,PIK3CG,PIK3CD,GNA14,ADCY8
CREB Signaling in Neurons	1.43E00	5.26E-02	-0.378	PLCD1,PIK3R3,GNG4,ITPR2,PIK3CG,GRIK3,PIK3CD,GNA14,ADCY8
Integrin Signaling	1.43E00	4.95E-02	0.000	RND2,PIK3R3,FYN,PARVB,CAPN6,ARHGEF7,PIK3CG,ITGA6,PIK3CD,ITGA4
Signaling by Rho Family GTPa	1.42E00	4.7E-02	0.333	RND2,PIK3R3,GNG4,SEPT3,ARHGEF7,PIK3CG,NCF2,ARHGEF6,PIK3CD,GN
Role of JAK1 and JAK3 in γc C	1.42E00	7.94E-02		PIK3R3,IRS1,PIK3CG,PIK3CD,STAT1
FcγRIIB Signaling in B Lymph	1.41E00	9.76E-02	1.000	PIK3R3,PIK3CG,LYN,PIK3CD
Ephrin Receptor Signaling	1.41E00	5.17E-02		GNG4,FYN,MAP3K14,SDCBP,PIK3CG,EFNA3,FIGF,GNA14,ITGA4
Virus Entry via Endocytic Path	1.41E00	6.74E-02		PIK3R3,FYN,PIK3CG,ITGA6,PIK3CD,ITGA4

IL-6 Signaling	1.41E00	6.03E-02	1.633	IL1R2,PIK3R3,MAP3K14,IL1A,PIK3CG,CD14,PIK3CD
CD40 Signaling	1.39E00	7.69E-02	1.000	PIK3R3,MAP3K14,PIK3CG,TNFAIP3,PIK3CD
Non-Small Cell Lung Cancer S	1.39E00	7.69E-02	0.000	PIK3R3,ITPR2,PIK3CG,CDK6,PIK3CD
Communication between Innat	1.38E00	6.59E-02		TLR2,TLR4,IL1A,TLR1,TLR7,CD83
IL-15 Signaling	1.37E00	7.58E-02		PIK3R3,PIK3CG,PIK3CD,AXL,FASLG
Gαi Signaling	1.36E00	5.83E-02	0.816	GNG4,GPR17,P2RY13,PTGER3,P2RY12,HTR1A,ADCY8
Chronic Myeloid Leukemia Sig	1.35E00	6.45E-02		PIK3R3,MYC,TGFBR1,PIK3CG,CDK6,PIK3CD
LXR/RXR Activation	1.35E00	5.79E-02	-2.236	IL1R2,TLR4,SCD,IL1A,LPL,CD14,ABCA1
GDNF Family Ligand-Recepto	1.33E00	7.35E-02	0.000	PIK3R3,ITPR2,IRS1,PIK3CG,PIK3CD
Aldosterone Signaling in Epith	1.33E00	5.26E-02		PLCD1,PIK3R3,DNAJB4,ITPR2,SGK1,PIK3CG,HSPA1A/HSPA1B,PIK3CD
PI3K/AKT Signaling	1.33E00	5.69E-02	2.646	PIK3R3,NANOG,PIK3CG,INPPL1,MAP3K8,PIK3CD,ITGA4
Glioma Signaling	1.33E00	6.32E-02	1.633	PIK3R3,IGF1,PIK3CG,CDK6,PIK3CD,PDGFRB
Agrin Interactions at Neuromu	1.33E00	7.25E-02		LAMC1,ARHGEF7,ARHGEF6,ITGA6,ITGA4
Actin Cytoskeleton Signaling	1.31E00	4.61E-02		PIK3R3,CYFIP2,ARHGEF7,PIK3CG,ARHGEF6,ARHGAP35,CD14,TRIO,PIK3C
IGF-1 Signaling	1.3E00	6.19E-02	1.000	PIK3R3,IGF1,IRS1,PIK3CG,PIK3CD,IGFBP7
IL-3 Signaling	1.3E00	7.04E-02	0.447	PIK3R3,PPP3R2,PIK3CG,PIK3CD,STAT1
Small Cell Lung Cancer Signa	1.3E00	7.04E-02		PIK3R3,MYC,PIK3CG,CDK6,PIK3CD
PEDF Signaling	1.3E00	7.04E-02	0.447	PPARG,PIK3R3,PIK3CG,PIK3CD,FASLG
Caveolar-mediated Endocytos	1.28E00	6.94E-02		FYN,ITGA6,CD48,DYRK3,ITGA4
JAK/Stat Signaling	1.28E00	6.94E-02	-0.447	PIK3R3,PIK3CG,STAT2,PIK3CD,STAT1
Embryonic Stem Cell Different	1.26E00	2E-01		NANOG,T
STAT3 Pathway	1.26E00	6.85E-02		MYC,TGFBR1,FGFRL1,TNFRSF11A,PDGFRB
FLT3 Signaling in Hematopoie	1.24E00	6.76E-02		PIK3R3,PIK3CG,STAT2,PIK3CD,STAT1
HER-2 Signaling in Breast Ca	1.21E00	6.58E-02		PIK3R3,PIK3CG,CDK6,PIK3CD,AREG
VEGF Family Ligand-Recepto	1.21E00	6.58E-02	1.000	PIK3R3,PIK3CG,FIGF,PIK3CD,NRP1
Insulin Receptor Signaling	1.2E00	5.22E-02		PIK3R3,FYN,SGK1,IRS1,PIK3CG,INPPL1,PIK3CD
Leukocyte Extravasation Signa	1.2E00	4.57E-02	2.121	TEC,PIK3R3,PIK3CG,NCF2,ITGA6,ARHGAP35,PIK3CD,ITGA4,ITK
Melatonin Degradation III	1.2E00	1E00		MPO
Acute Myeloid Leukemia Signa	1.2E00	6.49E-02	-0.447	PIK3R3,MYC,PIK3CG,PIK3CD,TCF7L2
HGF Signaling	1.2E00	5.71E-02	1.633	PIK3R3,MAP3K14,PIK3CG,MAP3K8,PIK3CD,ITGA4
Relaxin Signaling	1.2E00	5.19E-02		PIK3R3,GNG4,PDE9A,PIK3CG,PIK3CD,GNA14,ADCY8
CNTF Signaling	1.2E00	7.69E-02	0.000	PIK3R3,PIK3CG,PIK3CD,STAT1
Endometrial Cancer Signaling	1.2E00	7.69E-02		PIK3R3,MYC,PIK3CG,PIK3CD
Wnt/β-catenin Signaling	1.18E00	4.76E-02	0.707	SOX4,MYC,SFRP2,TGFBR1,SOX6,SFRP1,SOX11,TCF7L2
NGF Signaling	1.18E00	5.61E-02	0.816	PIK3R3,MAP3K14,PIK3CG,TRIO,MAP3K8,PIK3CD
Role of p14/p19ARF in Tumor	1.18E00	1E-01		PIK3R3,PIK3CG,PIK3CD
Xenobiotic Metabolism Signali	1.17E00	4.07E-02		PIK3R3,CHST2,MAP3K14,IL1A,FMO2,ALDH1L2,PIK3CG,MAF,CHST3,MAP3K

Role of IL-17A in Arthritis	1.16E00	7.41E-02		PIK3R3,CXCL3,PIK3CG,PIK3CD
Fc Epsilon RI Signaling	1.16E00	5.5E-02	0.816	PIK3R3,FYN,PIK3CG,LYN,INPPL1,PIK3CD
Renin-Angiotensin Signaling	1.16E00	5.5E-02	0.816	PIK3R3,ITPR2,PIK3CG,PIK3CD,ADCY8,STAT1
Natural Killer Cell Signaling	1.15E00	5.45E-02		PIK3R3,FYN,LAIR1,PIK3CG,INPPL1,PIK3CD
RhoGDI Signaling	1.14E00	4.62E-02	0.816	RND2,GNG4,ARHGEF7,ARHGEF6,ARHGAP35,GNA14,ARHGDIB,ITGA4
Oleate Biosynthesis II (Animal	1.12E00	1.54E-01		SCD,PTPRT
ErbB2-ErbB3 Signaling	1.1E00	7.02E-02		PIK3R3,MYC,PIK3CG,PIK3CD
MIF-mediated Glucocorticoid I	1.1E00	9.09E-02		TLR4,CD14,CD74
Leukotriene Biosynthesis	1.06E00	1.43E-01		GGT5,ALOX5
14-3-3-mediated Signaling	1.06E00	5.13E-02		PLCD1,PIK3R3,TUBA1A,PIK3CG,PIK3CD,TUBB2B
Type II Diabetes Mellitus Signa	1.06E00	5.13E-02		PPARG,PIK3R3,MAP3K14,IRS1,PIK3CG,PIK3CD
Coagulation System	1.05E00	8.57E-02		PLAUR,TFPI,THBD
IL-8 Signaling	1.04E00	4.37E-02	1.134	RND2,PIK3R3,GNG4,MPO,PIK3CG,NCF2,FIGF,PIK3CD
p70S6K Signaling	1.04E00	5.04E-02	0.000	PLCD1,PIK3R3,IRS1,PIK3CG,LYN,PIK3CD
Regulation of the Epithelial-Me	1.04E00	4.35E-02		PIK3R3,TGFBR1,PIK3CG,PIK3CD,FGFRL1,NOTCH1,TCF7L2,PDGFRB
Interferon Signaling	1.03E00	8.33E-02		IFIT3,STAT2,STAT1
HMGB1 Signaling	1.03E00	5E-02	0.447	RND2,PIK3R3,TLR4,IL1A,PIK3CG,PIK3CD
IL-1 Signaling	1.01E00	5.49E-02	2.000	GNG4,MAP3K14,IL1A,GNA14,ADCY8
ERK/MAPK Signaling	1.01E00	4.28E-02	-0.707	PPARG,PIK3R3,MYC,FYN,PIK3CG,PIK3CD,STAT1,ITGA4
Antiproliferative Role of Somat	1.01E00	6.35E-02		PIK3R3,GNG4,PIK3CG,PIK3CD
ERK5 Signaling	1.01E00	6.35E-02	1.000	MYC,SGK1,MAP3K8,MEF2C
Factors Promoting Cardiogene	1.01E00	5.43E-02		TGFBR1,MEF2C,BMP6,BMP5,TCF7L2
Sulfate Activation for Sulfonati	1.01E00	5E-01		PAPSS2
Extrinsic Prothrombin Activatic	1E00	1.25E-01		TFPI,THBD
Dermatan Sulfate Degradation	1E00	1.25E-01		HEXB,FGFRL1
IL-17A Signaling in Airway Cel	1E00	6.25E-02		PIK3R3,CXCL3,PIK3CG,PIK3CD
Fcγ Receptor-mediated Phago	1E00	5.38E-02	0.447	PIK3R3,FYN,PIK3CG,LYN,FYB
PPAR Signaling	9.87E-01	5.32E-02	-1.342	PPARG,IL1R2,MAP3K14,IL1A,PDGFRB
Thyroid Cancer Signaling	9.49E-01	7.5E-02		PPARG,MYC,TCF7L2
Macropinocytosis Signaling	9.3E-01	5.88E-02		PIK3R3,PIK3CG,CD14,PIK3CD
MIF Regulation of Innate Immu	9.28E-01	7.32E-02		TLR4,CD14,CD74
Nitric Oxide Signaling in the C	9.19E-01	5.05E-02	0.447	PIK3R3,ITPR2,PIK3CG,FIGF,PIK3CD
IL-10 Signaling	9.19E-01	5.8E-02		IL1R2,MAP3K14,IL1A,CD14
Melanoma Signaling	9.1E-01	7.14E-02		PIK3R3,PIK3CG,PIK3CD
IL-17 Signaling	8.73E-01	5.56E-02		PIK3R3,MAP3K14,PIK3CG,PIK3CD
Basal Cell Carcinoma Signalin	8.73E-01	5.56E-02		BMP6,BMP5,PTCH2,TCF7L2
Glycerol-3-phosphate Shuttle	8.73E-01	3.33E-01		GPD1

iNOS Signaling	8.71E-01	6.82E-02		TLR4,CD14,STAT1
Cardiomyocyte Differentiation	8.64E-01	1E-01		MEF2C,BMP5
Gαs Signaling	7.98E-01	4.59E-02	1.000	GNG4,RGS2,ADCY8,PTGER4,ADRB2
Calcium Signaling	7.98E-01	3.93E-02	0.000	PPP3R2,ITPR2,TNNC1,CHRNA7,TRPC4,MEF2C,ASPH
Polyamine Regulation in Color	7.98E-01	9.09E-02		PPARG,MYC
Graft-versus-Host Disease Sig	7.94E-01	6.25E-02		IL1A,HLA-DQA1,FASLG
Type I Diabetes Mellitus Signa	7.93E-01	4.55E-02	-1.000	MAP3K14,CASP3,HLA-DQA1,STAT1,FASLG
Corticotropin Releasing Hormo	7.82E-01	4.5E-02		ITPR2,MEF2C,ADCY8,PTCH2,FASLG
Proline Biosynthesis I	7.76E-01	2.5E-01		PYCR1
Tumoricidal Function of Hepat	7.47E-01	8.33E-02		CASP3,FASLG
Role of JAK1, JAK2 and TYK2	7.47E-01	8.33E-02		STAT2,STAT1
Clathrin-mediated Endocytosis	7.47E-01	3.78E-02		PIK3R3,PPP3R2,CD2AP,IGF1,PIK3CG,FIGF,PIK3CD
CD27 Signaling in Lymphocyte	7.3E-01	5.77E-02		MAP3K14,CASP3,MAP3K8
CCR3 Signaling in Eosinophils	7.25E-01	4.27E-02		PIK3R3,GNG4,ITPR2,PIK3CG,PIK3CD
Gα12/13 Signaling	7.25E-01	4.27E-02	1.342	TEC,PIK3R3,PIK3CG,MEF2C,PIK3CD
Melanocyte Development and	7.25E-01	4.76E-02	1.000	PIK3R3,PIK3CG,PIK3CD,ADCY8
Semaphorin Signaling in Neur	7.25E-01	5.66E-02		RND2,FYN,NRP1
UVB-Induced MAPK Signaling	7.25E-01	5.66E-02		PIK3R3,PIK3CG,PIK3CD
IL-2 Signaling	7.25E-01	5.66E-02		PIK3R3,PIK3CG,PIK3CD
FGF Signaling	7.17E-01	4.71E-02	0.000	PIK3R3,PIK3CG,PIK3CD,FGFRL1
Protein Kinase A Signaling	7.17E-01	3.12E-02		PLCD1,PTPRC,GNG4,PPP3R2,TGFBR1,PDE9A,ITPR2,PTPN14,ADCY8,PTP
Synaptic Long Term Potentiati	7.17E-01	4.2E-02		PLCD1,PPP3R2,ITPR2,GNA14,ADCY8
Unfolded protein response	7.16E-01	5.56E-02		PPARG,Hspa1b,HSPA1A/HSPA1B
ErbB Signaling	7.13E-01	4.65E-02		PIK3R3,PIK3CG,PIK3CD,AREG
Superpathway of Inositol Phos	7.13E-01	3.65E-02		PLCD1,PTPRC,PIK3R3,TNS3,PIK3CG,INPPL1,PIK3CD
Neuregulin Signaling	6.93E-01	4.55E-02		PIK3R3,MYC,AREG,ITGA4
CTLA4 Signaling in Cytotoxic	6.93E-01	4.55E-02		PIK3R3,FYN,PIK3CG,PIK3CD
G Beta Gamma Signaling	6.93E-01	4.55E-02		GNG4,PIK3CG,ARHGEF6,GNA14
Crosstalk between Dendritic C	6.82E-01	4.49E-02		TLR4,TLR7,CD83,FASLG
Nur77 Signaling in T Lymphoc	6.81E-01	5.26E-02		PPP3R2,CASP3,HLA-DQA1
Regulation of Cellular Mechan	6.81E-01	5.26E-02		CAPN6,CDK6,ITGA4
Hepatic Cholestasis	6.79E-01	3.7E-02		IL1R2,TLR4,MAP3K14,IL1A,CD14,ADCY8
VEGF Signaling	6.79E-01	4.4E-02	1.000	PIK3R3,PIK3CG,FIGF,PIK3CD
Proline Biosynthesis II (from A	6.79E-01	1.67E-01		PYCR1
Arginine Degradation VI (Argir	6.79E-01	1.67E-01		PYCR1
Pentose Phosphate Pathway (	6.79E-01	1.67E-01		TKTL2
Glycine Cleavage Complex	6.79E-01	1.67E-01		T

Zymosterol Biosynthesis	6.79E-01	1.67E-01		HSD17B7
Pregnenolone Biosynthesis	6.79E-01	1.67E-01		MICAL1
NAD Biosynthesis III	6.79E-01	1.67E-01		NMNAT2
ErbB4 Signaling	6.53E-01	5E-02		PIK3R3,PIK3CG,PIK3CD
GNRH Signaling	6.52E-01	3.88E-02	1.342	MAP3K14,ITPR2,MAP3K8,GNA14,ADCY8
SAPK/JNK Signaling	6.49E-01	4.26E-02	1.000	PIK3R3,IRS1,PIK3CG,PIK3CD
Salvage Pathways of Pyrimidir	6.39E-01	4.21E-02		CMPK2,SGK1,CDK6,MAP3K8
Ovarian Cancer Signaling	6.38E-01	3.82E-02		PIK3R3,PIK3CG,FIGF,PIK3CD,TCF7L2
Acute Phase Response Signa	6.33E-01	3.55E-02	1.633	PIK3R3,MAP3K14,IL1A,PIK3CG,SERPINA3,PIK3CD
NAD Biosynthesis from 2-amir	6.33E-01	1.43E-01		NMNAT2
NAD Salvage Pathway III	6.33E-01	1.43E-01		NMNAT2
Eicosanoid Signaling	6.24E-01	4.76E-02		PTGER3,ALOX5,PTGER4
Cytotoxic T Lymphocyte-media	6.24E-01	6.25E-02		CASP3,FASLG
AMPK Signaling	6.21E-01	3.73E-02	0.447	PIK3R3,IRS1,PIK3CG,PIK3CD,ADRB2
p53 Signaling	6.21E-01	4.08E-02	0.000	PIK3R3,THBS1,PIK3CG,PIK3CD
Activation of IRF by Cytosolic	6.21E-01	4.69E-02		DDX58,STAT2,STAT1
Calcium-induced T Lymphocyt	6.21E-01	4.69E-02		PPP3R2,ITPR2,HLA-DQA1
Pyridoxal 5'-phosphate Salvag	6.21E-01	4.69E-02		SGK1,CDK6,MAP3K8
Telomerase Signaling	6.16E-01	4.04E-02	0.000	PIK3R3,MYC,PIK3CG,PIK3CD
Complement System	6.16E-01	6.06E-02		CFH,C3AR1
Airway Pathology in Chronic O	6.09E-01	1.25E-01		CXCL3
HIF1α Signaling	6.09E-01	3.96E-02		PIK3R3,PIK3CG,FIGF,PIK3CD
Cholecystokinin/Gastrin-media	6.09E-01	3.96E-02	0.000	RND2,IL1A,ITPR2,MEF2C
Angiopoietin Signaling	6.09E-01	4.55E-02		PIK3R3,PIK3CG,PIK3CD
Role of PI3K/AKT Signaling in	6.09E-01	4.55E-02		PIK3R3,PIK3CG,PIK3CD
Granulocyte Adhesion and Dia	6.09E-01	3.41E-02		IL1R2,CXCL3,IL1A,ITGA6,Cxcl3,ITGA4
B Cell Development	6.09E-01	5.88E-02		PTPRC,HLA-DQA1
Erythropoietin Signaling	6E-01	4.48E-02		PIK3R3,PIK3CG,PIK3CD
Neurotrophin/TRK Signaling	6E-01	4.48E-02		PIK3R3,PIK3CG,PIK3CD
Aryl Hydrocarbon Receptor Si	5.96E-01	3.57E-02	0.000	MYC,IL1A,ALDH1L2,CDK6,FASLG
Role of JAK2 in Hormone-like	5.96E-01	5.71E-02		IRS1,STAT1
Synaptic Long Term Depressi	5.9E-01	3.55E-02	0.447	PLCD1,IGF1,ITPR2,LYN,GNA14
Systemic Lupus Erythematosu	5.85E-01	3.18E-02		PTPRC,PIK3R3,IL1A,PIK3CG,TLR7,LYN,PIK3CD
Pathogenesis of Multiple Scler	5.78E-01	1.11E-01		CXCR3
Histidine Degradation VI	5.78E-01	1.11E-01		MICAL1
Estrogen Biosynthesis	5.69E-01	5.41E-02		CYP4F8,HSD17B7
Antigen Presentation Pathway	5.69E-01	5.41E-02		HLA-DQA1,CD74

Regulation of eIF4 and p70S6	5.68E-01	3.45E-02	0.447	PIK3R3,IRS1,PIK3CG,PIK3CD,ITGA4
T Helper Cell Differentiation	5.68E-01	4.23E-02		TGFBR1,HLA-DQA1,STAT1
Renal Cell Carcinoma Signalir	5.68E-01	4.23E-02		PIK3R3,PIK3CG,PIK3CD
Epithelial Adherens Junction S	5.64E-01	3.42E-02		TGFBR1,TUBA1A,NOTCH1,TCF7L2,TUBB2B
mTOR Signaling	5.53E-01	3.21E-02		RND2,PIK3R3,IRS1,PIK3CG,FIGF,PIK3CD
Role of PKR in Interferon Indu	5.3E-01	5E-02		CASP3,STAT1
Neuroprotective Role of THOF	5.3E-01	5E-02		TAC1,SERPINA3
Pentose Phosphate Pathway	5.17E-01	9.09E-02		TKTL2
Hereditary Breast Cancer Sigr	5.06E-01	3.48E-02		PIK3R3,PIK3CG,CDK6,PIK3CD
3-phosphoinositide Biosynthes	5.05E-01	3.23E-02		PTPRC,PIK3R3,TNS3,PIK3CG,PIK3CD
Dermatan Sulfate Biosynthesis	5.05E-01	4.76E-02		CHST2,CHST3
Regulation of IL-2 Expression	4.93E-01	3.8E-02		PPP3R2,FYN,TGFBR1
Ubiquinol-10 Biosynthesis (Eu	4.93E-01	8.33E-02		MICAL1
Ceramide Signaling	4.84E-01	3.75E-02		PIK3R3,PIK3CG,PIK3CD
Serotonin Receptor Signaling	4.82E-01	4.55E-02		HTR1A,ADCY8
Dopamine-DARPP32 Feedbac	4.79E-01	3.11E-02	0.447	KCNJ12,PLCD1,PPP3R2,ITPR2,ADCY8
Chondroitin Sulfate Biosynthes	4.79E-01	4.44E-02		CHST2,CHST3
Prostate Cancer Signaling	4.79E-01	3.66E-02		PIK3R3,PIK3CG,PIK3CD
Role of IL-17A in Psoriasis	4.79E-01	7.69E-02		CXCL3
Cholesterol Biosynthesis I	4.79E-01	7.69E-02		HSD17B7
Bile Acid Biosynthesis, Neutra	4.79E-01	7.69E-02		AKR1D1
Cholesterol Biosynthesis II (via	4.79E-01	7.69E-02		HSD17B7
Cholesterol Biosynthesis III (vi	4.79E-01	7.69E-02		HSD17B7
Atherosclerosis Signaling	4.65E-01	3.25E-02		IL1A,LPL,ALOX5,ITGA4
nNOS Signaling in Neurons	4.57E-01	4.26E-02		PPP3R2,CAPN6
γ-glutamyl Cycle	4.56E-01	7.14E-02		GGT5
TR/RXR Activation	4.56E-01	3.53E-02		PIK3R3,PIK3CG,PIK3CD
Cdc42 Signaling	4.52E-01	2.99E-02		H2-M5,ARHGEF6,HLA-DQA1,ITGA4,ITK
Allograft Rejection Signaling	4.52E-01	3.49E-02		H2-M5,HLA-DQA1,FASLG
Bladder Cancer Signaling	4.52E-01	3.49E-02		MYC,THBS1,FIGF
α-Adrenergic Signaling	4.45E-01	3.45E-02		GNG4,ITPR2,ADCY8
Autoimmune Thyroid Disease	4.45E-01	4.08E-02		HLA-DQA1,FASLG
Heparan Sulfate Biosynthesis	4.45E-01	4.08E-02		CHST2,CHST3
NAD biosynthesis II (from tryp	4.45E-01	6.67E-02		NMNAT2
Chondroitin Sulfate Degradatic	4.45E-01	6.67E-02		HEXB
Granzyme B Signaling	4.24E-01	6.25E-02		CASP3
Parkinson's Signaling	4.24E-01	6.25E-02		CASP3

Chondroitin Sulfate Biosynthes	4.05E-01	3.77E-02	CHST2,CHST3
Sertoli Cell-Sertoli Cell Junctio	3.99E-01	2.81E-02	MAP3K14,TUBA1A,MAP3K8,TUBB2B,ITGA4
NRF2-mediated Oxidative Stre	3.89E-01	2.78E-02	PIK3R3,DNAJB4,PIK3CG,MAF,PIK3CD
Dermatan Sulfate Biosynthesis	3.89E-01	3.64E-02	CHST2,CHST3
D-myo-inositol (1,4,5)-trisphos	3.89E-01	5.56E-02	INPPL1
Role of Cytokines in Mediating	3.83E-01	3.57E-02	IL1A,IL24
Actin Nucleation by ARP-WAS	3.83E-01	3.57E-02	RND2,ITGA4
Heparan Sulfate Biosynthesis	3.83E-01	3.57E-02	CHST2,CHST3
1D-myo-inositol Hexakisphosp	3.78E-01	5.26E-02	INPPL1
D-myo-inositol (1,3,4)-trisphos	3.78E-01	5.26E-02	INPPL1
Glutamate Receptor Signaling	3.78E-01	3.51E-02	GRIK3,SLC1A1
CDK5 Signaling	3.73E-01	3.03E-02	LAMC1,ITGA6,ADCY8
Superpathway of Melatonin De	3.71E-01	3.45E-02	CYP4F8,MPO
3-phosphoinositide Degradatic	3.66E-01	2.78E-02	PTPRC,TNS3,INPP4B,INPPL1
Agranulocyte Adhesion and Di	3.66E-01	2.66E-02	CXCL3,IL1A,ITGA6,Cxcl3,ITGA4
Nicotine Degradation II	3.66E-01	3.39E-02	CYP4F8,FMO2
Endoplasmic Reticulum Stress	3.53E-01	4.76E-02	CASP3
Pyrimidine Deoxyribonucleotid	3.38E-01	4.55E-02	CMPK2
Role of BRCA1 in DNA Damag	3.29E-01	3.12E-02	BRIP1,STAT1
Retinoic acid Mediated Apoptc	3.29E-01	3.12E-02	CASP3,PARP12
Cell Cycle: G1/S Checkpoint R	3.29E-01	3.12E-02	MYC,CDK6
Differential Regulation of Cyto	3.29E-01	4.35E-02	IL1A
IL-22 Signaling	3.2E-01	4.17E-02	STAT1
Estrogen-mediated S-phase E	3.2E-01	4.17E-02	MYC
Triacylglycerol Degradation	3.2E-01	4.17E-02	LPL
Superpathway of D-myo-inosit	3.2E-01	4.17E-02	INPPL1
PXR/RXR Activation	3.12E-01	2.99E-02	SCD,PAPSS2
Role of JAK family kinases in I	3.11E-01	4E-02	STAT1
Bupropion Degradation	3.11E-01	4E-02	CYP4F8
Remodeling of Epithelial Adhe	3.09E-01	2.94E-02	TUBA1A,TUBB2B
CCR5 Signaling in Macrophag	3.05E-01	2.9E-02	GNG4,FASLG
Antiproliferative Role of TOB i	3.05E-01	3.85E-02	TGFBR1
NAD Salvage Pathway II	3.05E-01	3.85E-02	NMNAT2
Acetone Degradation I (to Met	3.05E-01	3.85E-02	CYP4F8
IL-15 Production	2.98E-01	3.7E-02	STAT1
Cell Cycle Control of Chromos	2.98E-01	3.7E-02	CDK6
D-myo-inositol (1,4,5)-Trispho	2.98E-01	3.7E-02	PLCD1

Pyrimidine Ribonucleotides Int	2.98E-01	3.7E-02	CMPK2
Superpathway of Cholesterol E	2.88E-01	3.57E-02	HSD17B7
Ephrin B Signaling	2.87E-01	2.74E-02	GNG4,GNA14
Intrinsic Prothrombin Activatio	2.8E-01	3.45E-02	THBD
Pyrimidine Ribonucleotides De	2.8E-01	3.45E-02	CMPK2
RhoA Signaling	2.77E-01	2.46E-02	IGF1,SEPT3,ARHGAP35
Sonic Hedgehog Signaling	2.74E-01	3.33E-02	PTCH2
BMP signaling pathway	2.74E-01	2.63E-02	BMP6,BMP5
Adipogenesis pathway	2.71E-01	2.42E-02	PPARG,LPL,FGFRL1
4-1BB Signaling in T Lymphoc	2.66E-01	3.23E-02	MAP3K14
VDR/RXR Activation	2.65E-01	2.56E-02	CD14,THBD
FXR/RXR Activation	2.6E-01	2.36E-02	PPARG,IL1A,LPL
RAR Activation	2.58E-01	2.27E-02	PIK3R3,PIK3CG,PIK3CD,ADCY8
Cellular Effects of Sildenafil (V	2.55E-01	2.33E-02	PLCD1,ITPR2,ADCY8
G Protein Signaling Mediated I	2.55E-01	3.03E-02	GNG4
Retinol Biosynthesis	2.55E-01	3.03E-02	LPL
Oncostatin M Signaling	2.47E-01	2.94E-02	STAT1
Cardiac β-adrenergic Signalin	2.43E-01	2.26E-02	GNG4,PDE9A,ADCY8
IL-17A Signaling in Fibroblasts	2.43E-01	2.86E-02	NFKBIZ
tRNA Splicing	2.43E-01	2.86E-02	PDE9A
HIPPO signaling	2.34E-01	2.33E-02	TEAD4,CRB1
April Mediated Signaling	2.23E-01	2.63E-02	MAP3K14
Notch Signaling	2.23E-01	2.63E-02	NOTCH1
OX40 Signaling Pathway	2.22E-01	2.25E-02	H2-M5,HLA-DQA1
Netrin Signaling	2.18E-01	2.56E-02	PPP3R2
Regulation of Actin-based Mot	2.16E-01	2.2E-02	RND2,ITGA4
D-myo-inositol-5-phosphate M	2.16E-01	2.1E-02	PLCD1,PTPRC,TNS3
B Cell Activating Factor Signal	2.16E-01	2.5E-02	MAP3K14
Transcriptional Regulatory Net	2.16E-01	2.5E-02	NANOG
Role of IL-17F in Allergic Inflar	1.91E-01	2.27E-02	IGF1
Role of RIG1-like Receptors ir	1.88E-01	2.22E-02	DDX58
Role of Hypercytokinemia/hyp	1.88E-01	2.22E-02	IL1A
Role of Oct4 in Mammalian Er	1.83E-01	2.17E-02	NANOG

Notes:
The significance values for the canonical pathways is calculated by
Fisher's exact test right-tailed, corrected for mutliple comparisons with the Benjamini-Hochberg method (B-H).

The significance indicates the probability of association of molecules from Stroke+GDF10 vs stroke (FDR<0.1) with the canonical pathway by random chance alone.

The z-score reflects whether a pathway has significantly more "activated" predictions than "inhibited" predictions (z>0) or vice versa (z<0). and the value in the positive or negative direction reflects the strenght of that prediction.

Supplementary Table 3

PI3K Pathway Mult Comp Stroke+GDF10 vs Stroke

Symbol	Entrez Gene Name	Gene Symbol	Log Ratio
FYN	FYN proto-oncogene, Src family tyrosine kinase	NM_008054	-1.542
IRS1	insulin receptor substrate 1	NM_010570	-1.568
ITPR2	inositol 1,4,5-trisphosphate receptor, type 2	NM_019923	-1.454
LYN	LYN proto-oncogene, Src family tyrosine kinase	NM_010747	1.748
PIK3CD	phosphatidylinositol-4,5-bisphosphate 3-kinase, catalytic subunit delta	NM_008840	2.424
PIK3CG	phosphatidylinositol-4,5-bisphosphate 3-kinase, catalytic subunit gamma	NM_020272	2.233
PLCD1	phospholipase C, delta 1	NM_019676	-3.573
PPP3R2	protein phosphatase 3, regulatory subunit B, beta	NM_001004025	4.616
PTPRC	protein tyrosine phosphatase, receptor type, C	NM_011210	2.646
TLR4	toll-like receptor 4	NM_021297	2.689

Supplementary Table 4

PTEN Pathway Mult Comp Stroke+GDF10 vs Stroke

Symbol	Entrez Gene Name	Gene Symbol	Log Ratio
CASP3	caspase 3, apoptosis-related cysteine peptidase	NM_009810	-1.615
CNKSR3	CNKSR family member 3	NM_172546	-2.073
FASLG	Fas ligand (TNF superfamily, member 6)	NM_010177	-5.479
FGFRL1	fibroblast growth factor receptor-like 1	NM_054071	-2.019
INPPL1	inositol polyphosphate phosphatase-like 1	NM_010567	-1.706
ITGA4	integrin, alpha 4 (antigen CD49D, alpha 4 subunit of VLA-4 receptor)	NM_010576	2.235
PDGFRB	platelet-derived growth factor receptor, beta polypeptide	NM_008809	4.023
PIK3CD	phosphatidylinositol-4,5-bisphosphate 3-kinase, catalytic subunit delta	NM_008840	2.424
PIK3CG	phosphatidylinositol-4,5-bisphosphate 3-kinase, catalytic subunit gamma	NM_020272	2.233
PIK3R3	phosphoinositide-3-kinase, regulatory subunit 3 (gamma)	NM_181585	-1.753
TGFBR1	transforming growth factor, beta receptor 1	NM_009370	1.737
TNFRSF1	tumor necrosis factor receptor superfamily, member 11a, NFKB activator	NM_009399	3.488

Supplementary Table 5
PI3K Pathway Mult Comp Stroke+GDF10 vs Stroke

Symbol	Entrez Gene Name	Gene symbol	Log Ratio
AKT3	v-akt murine thymoma viral oncogene homolog 3	NM_011785	-3.355
BCL2	B-cell CLL/lymphoma 2	NM_177410	-1.449
BCL2L1	BCL2-like 1	NM_009743	1.624
CCND1	cyclin D1	NM_007631	2.305
CDKN1A	cyclin-dependent kinase inhibitor 1A (p21, Cip1)	NM_007669	1.299
CTNNB1	catenin (cadherin-associated protein), beta 1, 88kDa	NM_007614	-1.038
EIF4E	eukaryotic translation initiation factor 4E	NM_007917	-0.968
FOXO1	forkhead box O1	NM_019739	0.934
FOXO3	forkhead box O3	NM_019740	0.958
GAB1	GRB2-associated binding protein 1	NM_021356	4.938
GAB2	GRB2-associated binding protein 2	NM_010248	-1.307
GDF15	growth differentiation factor 15	NM_011819	6.197
GSK3A	glycogen synthase kinase 3 alpha	NM_00103166	-1.040
GSK3B	glycogen synthase kinase 3 beta	NM_019827	-1.033
HSP90AA	heat shock protein 90kDa alpha (cytosolic), class A member 1	NM_010480	-1.011
INPP5D	inositol polyphosphate-5-phosphatase, 145kDa	NM_010566	4.287
INPP5F	inositol polyphosphate-5-phosphatase F	NM_178641	-1.045
INPPL1	inositol polyphosphate phosphatase-like 1	NM_010567	2.060
ITGA3	integrin, alpha 3 (antigen CD49C, alpha 3 subunit of VLA-3 receptor)	NM_013565	-1.911
ITGA4	integrin, alpha 4 (antigen CD49D, alpha 4 subunit of VLA-4 receptor)	NM_010576	1.597
ITGA5	integrin, alpha 5 (fibronectin receptor, alpha polypeptide)	NM_010577	3.037
ITGB1	integrin, beta 1 (fibronectin receptor, beta polypeptide, antigen CD29 include	NM_010578	1.525
JAK1	Janus kinase 1	NM_146145	-0.747
KRAS	Kirsten rat sarcoma viral oncogene homolog	NM_021284	-1.358
LIMS1	LIM and senescent cell antigen-like domains 1	NM_201242	2.110
MAP2K1	mitogen-activated protein kinase kinase 1	NM_008927	1.209
MAP3K8	mitogen-activated protein kinase kinase kinase 8	NM_007746	3.790
MAPK1	mitogen-activated protein kinase 1	NM_011949	-0.953
MAPK3	mitogen-activated protein kinase 3	NM_011952	1.214
MDM2	MDM2 proto-oncogene, E3 ubiquitin protein ligase	NM_010786	1.770
MTOR	mechanistic target of rapamycin (serine/threonine kinase)	NM_020009	-1.063
NFKB1	nuclear factor of kappa light polypeptide gene enhancer in B-cells 1	NM_008689	1.644
NFKBIA	nuclear factor of kappa light polypeptide gene enhancer in B-cells inhibitor, a	NM_010907	3.749
OCRL	oculocerebrorenal syndrome of Lowe	NM_177215	-1.308
PIK3CG	phosphatidylinositol-4,5-bisphosphate 3-kinase, catalytic subunit gamma	NM_020272	2.828
PIK3R3	phosphoinositide-3-kinase, regulatory subunit 3 (gamma)	NM_181585	1.769
PPP2R1A	protein phosphatase 2, regulatory subunit A, alpha	NM_016891	-1.581
PPP2R2B	protein phosphatase 2, regulatory subunit B, beta	NM_028392	-3.589
PPP2R2C	protein phosphatase 2, regulatory subunit B, gamma	NM_172994	-0.884
PPP2R3A	protein phosphatase 2, regulatory subunit B'', alpha	NM_172144	1.464
PPP2R5A	protein phosphatase 2, regulatory subunit B', alpha	NM_144880	1.728
PPP2R5D	protein phosphatase 2, regulatory subunit B', delta	NM_009358	-1.213
PPP2R5E	protein phosphatase 2, regulatory subunit B', epsilon isoform	NM_012024	-1.214
PTEN	phosphatase and tensin homolog	NM_008960	-1.078
PTGS2	prostaglandin-endoperoxide synthase 2 (prostaglandin G/H synthase and cy	NM_011198	3.319
RELA	v-rel avian reticuloendotheliosis viral oncogene homolog A	NM_009045	2.387
RHEB	Ras homolog enriched in brain	NM_053075	-0.933
RRAS	related RAS viral (r-ras) oncogene homolog	NM_009101	3.766
RRAS2	related RAS viral (r-ras) oncogene homolog 2	NM_025846	-1.557

SHC1	SHC (Src homology 2 domain containing) transforming protein 1	NM_011368	2.886
SOS2	son of sevenless homolog 2 (Drosophila)	NM_00113555	1.638
SYNJ1	synaptojanin 1	NM_00116448	-0.788
SYNJ2	synaptojanin 2	NM_011523	3.899
THEM4	thioesterase superfamily member 4	NM_029431	-1.421
YWHAB	tyrosine 3-monooxygenase/tryptophan 5-monooxygenase activation protein,	NM_018753	-1.524
YWHAE	tyrosine 3-monooxygenase/tryptophan 5-monooxygenase activation protein,	NM_009536	-0.736
YWHAG	tyrosine 3-monooxygenase/tryptophan 5-monooxygenase activation protein,	NM_018871	-2.144
YWHAH	tyrosine 3-monooxygenase/tryptophan 5-monooxygenase activation protein,	NM_011738	-1.554
YWHAZ	tyrosine 3-monooxygenase/tryptophan 5-monooxygenase activation protein,	NM_011740	-1.294

Supplementary Table 6
PTEN Pathway Mult Comp Stroke+GDF10 vs P4

Symbol	Entrez Gene Name	Gene symbol	Log Ratio
AKT3	v-akt murine thymoma viral oncogene homolog 3	NM_011785	-3.355
BCAR1	breast cancer anti-estrogen resistance 1	NM_009954	1.410
BCL2	B-cell CLL/lymphoma 2	NM_177410	-1.449
BCL2L1	BCL2-like 1	NM_009743	1.624
BCL2L11	BCL2-like 11 (apoptosis facilitator)	NM_207681	1.827
BMPR1B	bone morphogenetic protein receptor, type IB	NM_007560	-1.746
CASP3	caspase 3, apoptosis-related cysteine peptidase	NM_009810	-3.036
CCND1	cyclin D1	NM_007631	2.305
CDKN1A	cyclin-dependent kinase inhibitor 1A (p21, Cip1)	NM_007669	1.299
CNKSR3	CNKSR family member 3	NM_172546	2.970
CSNK2A2	casein kinase 2, alpha prime polypeptide	NM_009974	-0.986
DDR1	discoidin domain receptor tyrosine kinase 1	NM_172962	3.288
EGFR	epidermal growth factor receptor	NM_207655	-3.280
FGFR2	fibroblast growth factor receptor 2	NM_201601	5.923
FGFRL1	fibroblast growth factor receptor-like 1	NM_054071	3.200
FOXG1	forkhead box G1	NM_008241	-4.016
FOXO1	forkhead box O1	NM_019739	0.934
FOXO3	forkhead box O3	NM_019740	0.958
FOXO4	forkhead box O4	NM_018789	3.788
FOXO6	forkhead box O6	NM_194060	-3.380
GSK3A	glycogen synthase kinase 3 alpha	NM_0010316(	-1.040
GSK3B	glycogen synthase kinase 3 beta	NM_019827	-1.033
IGF1R	insulin-like growth factor 1 receptor	NM_010513	-0.996
INPP5D	inositol polyphosphate-5-phosphatase, 145kDa	NM_010566	4.287
INPP5F	inositol polyphosphate-5-phosphatase F	NM_178641	-1.045
INPPL1	inositol polyphosphate phosphatase-like 1	NM_010567	2.060
ITGA3	integrin, alpha 3 (antigen CD49C, alpha 3 subunit of	NM_013565	-1.911
ITGA4	integrin, alpha 4 (antigen CD49D, alpha 4 subunit of	NM_010576	1.597
ITGA5	integrin, alpha 5 (fibronectin receptor, alpha polypept	NM_010577	3.037
ITGB1	integrin, beta 1 (fibronectin receptor, beta polypeptid	NM_010578	1.525
KRAS	Kirsten rat sarcoma viral oncogene homolog	NM_021284	-1.358
MAGI3	membrane associated guanylate kinase, WW and PI	NM_133853	-2.447
MAP2K1	mitogen-activated protein kinase kinase 1	NM_008927	1.209
MAPK1	mitogen-activated protein kinase 1	NM_011949	-0.953
MAPK3	mitogen-activated protein kinase 3	NM_011952	1.214
MAST2	microtubule associated serine/threonine kinase 2	NM_008641	-2.121
NFKB1	nuclear factor of kappa light polypeptide gene enhan	NM_008689	1.644
NTRK2	neurotrophic tyrosine kinase, receptor, type 2	NM_008745	-1.233
NTRK3	neurotrophic tyrosine kinase, receptor, type 3	NM_182809	-2.055
OCRL	oculocerebrorenal syndrome of Lowe	NM_177215	-1.308
PDGFRA	platelet-derived growth factor receptor, alpha polypep	NM_011058	1.897
PIK3CG	phosphatidylinositol-4,5-bisphosphate 3-kinase, cata	NM_020272	2.828
PIK3R3	phosphoinositide-3-kinase, regulatory subunit 3 (gam	NM_181585	1.769
PIK3R5	phosphoinositide-3-kinase, regulatory subunit 5	NM_177320	4.327
PREX2	phosphatidylinositol-3,4,5-trisphosphate-dependent R	NM_029525	1.200
PTEN	phosphatase and tensin homolog	NM_008960	-1.078
RAC1	ras-related C3 botulinum toxin substrate 1 (rho family	NM_009007	1.056
RAC2	ras-related C3 botulinum toxin substrate 2 (rho family	NM_009008	3.499
RAC3	ras-related C3 botulinum toxin substrate 3 (rho family	NM_133223	-5.199

RELA	v-rel avian reticuloendotheliosis viral oncogene homc	NM_009045	2.387
RRAS	related RAS viral (r-ras) oncogene homolog	NM_009101	3.766
RRAS2	related RAS viral (r-ras) oncogene homolog 2	NM_025846	-1.557
SHC1	SHC (Src homology 2 domain containing) transformi	NM_011368	2.886
SOS2	son of sevenless homolog 2 (Drosophila)	NM_0011355	1.638
SYNJ1	synaptojanin 1	NM_0011644	-0.788
SYNJ2	synaptojanin 2	NM_011523	3.899
TGFBR2	transforming growth factor, beta receptor II (70/80kD	NM_029575	6.086
TGFBR3	transforming growth factor, beta receptor III	NM_011578	1.795
TNFRSF1	tumor necrosis factor receptor superfamily, member	NM_009399	1.978
YWHAH	tyrosine 3-monooxygenase/tryptophan 5-monooxyge	NM_011738	-1.554

Supplementary Table 7

Axonal Guidance Molecules Differentially Regulated in Stroke+GDF10 vs Stroke

Symbol	Entrez Gene Name	Gene Symbol	Log Ratio
ARHGEF6	Rac/Cdc42 guanine nucleotide exchange factor (GEF) 6	NM_152801	1.996
ARHGEF7	Rho guanine nucleotide exchange factor (GEF) 7	NM_017402	-1.369
BMP5	bone morphogenetic protein 5	NM_007555	8.086
BMP6	bone morphogenetic protein 6	NM_007556	4.009
EFNA3	ephrin-A3	NM_010108	-3.280
FIGF	c-fos induced growth factor (vascular endothelial growth factor D)	NM_010216	4.538
FYN	FYN proto-oncogene, Src family tyrosine kinase	NM_008054	-1.542
GNA14	guanine nucleotide binding protein (G protein), alpha 14	NM_008137	5.834
GNG4	guanine nucleotide binding protein (G protein), gamma 4	NM_010317	-2.855
IGF1	insulin-like growth factor 1 (somatomedin C)	NM_184052	3.191
ITGA4	integrin, alpha 4 (antigen CD49D, alpha 4 subunit of VLA-4 receptor)	NM_010576	2.235
MICAL1	microtubule associated monooxygenase, calponin and LIM domain co	NM_138315	-2.110
NRP1	neuropilin 1	NM_008737	1.878
PIK3CD	phosphatidylinositol-4,5-bisphosphate 3-kinase, catalytic subunit delta	NM_008840	2.424
PIK3CG	phosphatidylinositol-4,5-bisphosphate 3-kinase, catalytic subunit gam	NM_020272	2.233
PIK3R3	phosphoinositide-3-kinase, regulatory subunit 3 (gamma)	NM_181585	-1.753
PLCD1	phospholipase C, delta 1	NM_019676	-3.573
PPP3R2	protein phosphatase 3, regulatory subunit B, beta	NM_001004025	4.616
PTCH2	patched 2	NM_008958	6.952
SDCBP	syndecan binding protein (syntenin)	NM_016807	1.265
SOCS3	suppressor of cytokine signaling 3	NM_007707	-1.662
TUBA1A	tubulin, alpha 1a	NM_011653	-1.910
TUBB2B	tubulin, beta 2B class IIb	NM_023716	-1.874

Supplementary Table 8

Genes Differentially Regulated in Stroke+GDF10 vs Stroke at FDR<0.1

Gene	refSeq	Description	logFC_Stroke_GDF10_vs_Stroke	FDR_Stroke_GDF10_vs_Stroke
Foxd2	NM_008593	forkhead box D2	10.30644189	0.047777933
Olfr491	NM_146736	olfactory receptor 491	10.07927263	0.06234243
Gm18409	NR_038018	NA	9.893043729	0.029656196
Hoxa11os	NR_015348.1	NA	9.680689819	0.043583959
Gm8439	NM_001101603	predicted gene 8439	9.661677694	0.062358662
Olfr78	NM_130866	olfactory receptor 78	9.607540161	0.013983452
Gm13023	NM_001007077	predicted gene 13023	9.554883339	0.031140506
Sost	NM_024449	sclerostin	9.537966002	0.044428841
Tcl1b5	NM_013776	T-cell leukemia/lymphoma 1B, 5	9.470756771	0.049649098
Gm1653	NR_040591	NA	9.435560603	0.001950082
Ccer1	NM_152638.2.	Coiled-Coil Glutamate-Rich Protein 1	9.373546971	0.046332795
4933402N	NM_173409	RIKEN cDNA 4933402N03 gene	9.302927757	0.103290198
Olfr248	NM_146714	NA	9.285255186	0.06532461
Olfr538	NM_001011867	olfactory receptor 538	9.276452515	0.058751737
Slc2a7	NM_001085529	solute carrier family 2 (facilitated glucose transporter), member 7	9.274561418	0.104237538
Akr1d1	NM_145364	aldo-keto reductase family 1, member D1	9.260192621	0.044844933
Gpr113	NM_001014394	G protein-coupled receptor 113	9.256662134	0.057243188
Il24	NM_053095	interleukin 24	9.156890455	0.065167572
2310069B(	NA	NA	9.143382276	0.061392734
Olfr1274-p	NP_666375	NA	9.120073328	0.092290804
Prss34	NM_178372	protease, serine, 34	9.094173004	0.101707419
Flg2	NM_001013804	filaggrin family member 2	9.090310911	0.068681755
2410141K(	NA	NA	8.985517345	0.103243216
Olfr152	NM_146646	olfactory receptor 152	8.944913402	0.056294996
Dnase2b	NM_019957	deoxyribonuclease II beta	8.928171154	0.036994744
Hoxa9	NM_010456	homeobox A9	8.915969978	0.090379122
T	NM_009309	brachyury	8.904764933	0.103290198
Olfr1002	NM_146573	olfactory receptor 1002	8.876780023	0.062358662
Tead4	NM_011567	TEA domain family member 4	8.873274305	0.046246529

Olfr279	NM_001001807.1	NA	8.844494417	0.071844195
Clec3a	NM_001007223	C-type lectin domain family 3, member a	8.823154864	0.077383796
Olfr26	NM_146783	olfactory receptor 26	8.607980852	0.040919454
Lcn10	NM_178036	lipocalin 10	8.607095563	0.096536291
8430423G	NA	NA	8.604312449	0.084512025
Rnf183	NM_153504	ring finger protein 183	8.499148302	0.095457719
Kcnv2	NM_183179	potassium channel, subfamily V, member 2	8.483117242	0.063961373
Cxcr3	NM_009910	chemokine (C-X-C motif) receptor 3	8.481067225	0.037603524
Gimap4	NM_175048	GTPase, IMAP family member 4	8.425877199	0.052787992
Gm10280	NR_033584	NA	8.409918417	0.108808862
1700041M	NA	NA	8.391635666	0.099826211
H2-M5	NM_001115075	histocompatibility 2, M region locus 5	8.367831494	0.015172992
Gm101	NM_001115074	predicted gene 101	8.330171091	0.049649098
Krt84	NM_008474	keratin 84	8.242740639	0.004337294
Nanog	NM_028016	Nanog homeobox	8.134636501	0.090161184
Tnfsf8	NM_009403	tumor necrosis factor (ligand) superfamily, member 8	8.096518159	0.090161184
Bpifb5	NA	NA	8.087478507	0.084325697
Bmp5	NM_007555	bone morphogenetic protein 5	8.086063346	0.044647191
Vtcn1	NM_178594	V-set domain containing T cell activation inhibitor 1	8.076480729	0.046339199
Xlr4c	NM_183094	X-linked lymphocyte-regulated 4C	8.046287196	0.085329719
A530016L2	NM_177039	RIKEN cDNA A530016L24 gene	8.045030102	0.101344262
Spic	NM_011461	Spi-C transcription factor (Spi-1/PU.1 related)	8.04195506	0.045363028
Olfr267	NM_146920	olfactory receptor 267	8.039661974	0.064189922
Btla	NM_177584	B and T lymphocyte associated	8.009644726	0.080923771
Ccr6	NM_009835	chemokine (C-C motif) receptor 6	7.959835629	0.10712552
Olfr1084	NM_207135	olfactory receptor 1084	7.924775939	0.084512025
Tekt3	NM_027660	tektin 3	7.924489194	0.103342177
Mstn	NM_010834	myostatin	7.904026365	0.013983452
Il1r2	NM_010555	interleukin 1 receptor, type II	7.872741205	0.105946651
Scn11a	NM_011887	sodium channel, voltage-gated, type XI, alpha	7.763430432	0.043583959

Pi15	NM_053191	peptidase inhibitor 15	7.700842868	0.030467285
Cxcl3	NM_203320	chemokine (C-X-C motif) ligand 3	7.700666465	0.108083818
Arhgap36	NA	NA	7.680097825	0.090161184
Slc4a1	NM_011403	solute carrier family 4 (anion exchanger), member 1	7.62593527	0.037603524
Areg	NM_009704	amphiregulin	7.568387751	0.103290198
LOC10003	NA	NA	7.526169811	0.067409087
Ltk	NM_206942	leukocyte tyrosine kinase	7.43171394	0.028317112
Dnaaf3	NM_178837.4	NA	7.402371564	0.046339199
Mpo	NM_010824	myeloperoxidase	7.39060256	0.103290198
4930558J1	NA	NA	7.379563666	0.093872544
Gm20743	NR_040303	NA	7.346056463	0.044042082
Olfr1082	NM_207674	olfactory receptor 1082	7.201852823	0.103422753
Stk31	NM_029916	serine threonine kinase 31	7.18455802	0.060881523
Accsl	NM_001033452	1-aminocyclopropane-1-carboxylate synthase homolog (Arabidopsis)(non-functional)-like	7.109872731	0.059883828
Ms4a4b	NM_021718	membrane-spanning 4-domains, subfamily A, member 4B	7.091536537	0.043583959
Lypd8	NM_001085474.1	NA	7.061130358	0.103342177
Ybx2	NM_016875	Y box protein 2	7.023196695	0.010989006
Olfr495	NM_146364	olfactory receptor 495	6.981869413	0.093247532
Ptch2	NM_008958	patched homolog 2	6.952490072	0.061689489
Itk	NM_010583	IL2-inducible T-cell kinase	6.945223754	0.065805091
6720483E2	NA	NA	6.942045473	0.074343946
Ccdc129	NM_001081665	coiled-coil domain containing 129	6.930586542	0.001950082
Ldoc1	NM_001018087	leucine zipper, down-regulated in cancer 1	6.818761905	0.093247532
Emilin3	NM_182840	elastin microfibril interfacer 3	6.748319674	0.10725794
Patl2	NM_026251	protein associated with topoisomerase II homolog 2 (yeast)	6.666188604	0.044652762
Vit	NM_028813	vitrin	6.660283355	0.09973943
E430016F1	NR_015542	RIKEN cDNA E430016F16 gene	6.559380531	0.054515623
A730020M	NA	NA	6.525493247	0.049649098

Gm11346	NR_024599	X-linked lymphocyte-regulated 5 pseudogene	6.410849236	0.092423491
Agr2	NM_011783	anterior gradient 2 (Xenopus laevis)	6.402511019	0.076956638
Cd300lb	NM_199221	CD300 antigen like family member B	6.356539175	0.076275813
Hhla1	NM_001145096	HERV-H LTR-associating 1	6.26616856	0.083635465
Pdlim3	NM_016798	PDZ and LIM domain 3	6.245563907	0.057332192
Msx3	NM_010836	homeobox, msh-like 3	6.157860782	0.073632838
Gm15816	NA	NA	6.152429628	0.066579738
6330407A	NR_028126	RIKEN cDNA 6330407A03 gene	6.06364092	0.084826493
A130077B	NA	NA	6.036054262	0.000329283
Abca15	NM_177213	ATP-binding cassette, sub-family A (ABC1), member 15	5.918819175	0.060406725
Gna14	NM_008137	guanine nucleotide binding protein, alpha 14	5.833850906	0.039460915
Dsg1a	NM_010079	desmoglein 1 alpha	5.778944815	0.051248528
AU022793	NA	NA	5.649077074	0.039294848
Fmo2	NM_018881	flavin containing monooxygenase 2	5.60944922	0.055868414
Crb1	NM_133239	crumbs homolog 1 (Drosophila)	5.604209788	0.060949454
Ccdc88b	NM_001081291	coiled-coil domain containing 88B	5.492300523	0.003176829
4930444F(	NA	NA	5.356533875	0.065877738
Lpl	NM_008509	lipoprotein lipase	5.347853257	1.92E-06
Tacr1	NM_009313	tachykinin receptor 1	5.307136008	0.051389161
Atp6v0d2	NM_175406	ATPase, H+ transporting, lysosomal V0 subunit D2	5.261584667	0.041844204
Dnaic1	NM_175138	dynein, axonemal, intermediate chain 1	5.178984109	0.039294848
Fermt1	NM_198029	fermitin family homolog 1 (Drosophila)	5.122742044	0.092423491
Ggt5	NM_011820	gamma-glutamyltransferase 5	5.004484753	0.045124864
Ebf2	NM_010095	early B-cell factor 2	4.963044536	0.036994744
Emx1	NM_010131	empty spiracles homolog 1 (Drosophila)	4.9535696	0.043583959
Tnfrsf23	NM_024290	tumor necrosis factor receptor superfamily, member 23	4.939771914	0.046339199
A530058N	NR_028423	RIKEN cDNA A530058N18 gene	4.934694454	0.084325697
Unc13d	NP_954712.1	NA	4.892924891	0.091582765
Nostrin	NM_181547	nitric oxide synthase trafficker	4.877436341	0.057332192
Mei4	NM_175213.3	NA	4.839914641	0.084512025

Ranbp3l	NM_198024	RAN binding protein 3-like	4.823265515	0.013861277
Aim1l	NM_001162970	absent in melanoma 1-like	4.674010941	0.029486386
Scn4a	NM_133199	sodium channel, voltage-gated, type IV, alpha	4.662605533	0.092408269
Ppp3r2	NM_001004025	protein phosphatase 3, regulatory subunit B, alpha isoform (calcineurin B, type II)	4.61599177	0.010989006
H2-Aa	NM_010378	histocompatibility 2, class II antigen A, alpha	4.602360895	0.077383796
Glipr1	NM_028608	GLI pathogenesis-related 1 (glioma)	4.551902771	0.059527446
Figf (VEGF	NM_010216	c-fos induced growth factor	4.53813027	0.040919454
C030034L	NR_015499	RIKEN cDNA C030034L19 gene	4.53342158	0.028748375
Gm3696	NM_001024712	NA	4.327822516	0.092423491
Tnnc1	NM_009393	troponin C, cardiac/slow skeletal	4.321848576	0.108808862
Tec	NM_001113464	tec protein tyrosine kinase	4.284509107	1.23E-05
Col5a2	NM_007737	collagen, type V, alpha 2	4.283108132	0.027839834
Stap1	NM_019992	signal transducing adaptor family member 1	4.231396269	0.103290198
Gpr116	NM_001081178	G protein-coupled receptor 116	4.216887018	0.045242168
Mir128-1	NR_029543	microRNA 128-1	4.184670524	0.108808862
Cyp4f15	NM_134127	cytochrome P450, family 4, subfamily f, polypeptide 15	4.165038616	0.090379122
Pparg	NM_011146	peroxisome proliferator activated receptor gamma	4.10273004	0.019345398
Emp1	NM_010128	epithelial membrane protein 1	4.080323293	0.00727893
Pdgfrb	NM_008809	platelet derived growth factor receptor, beta polypeptide	4.022553736	0.044428841
Bmp6	NM_007556	bone morphogenetic protein 6	4.008843691	0.101707419
Tac1	NM_009311	tachykinin 1	3.999649051	0.00926261
Tfr2	NM_001289507.1	NA	3.966984475	0.01393947
Mroh7	NM_198547.1	NA	3.921054415	0.040802317
Dysf	NM_021469	dysferlin	3.892709639	0.103243216
Klhl6	NM_183390	kelch-like 6 (Drosophila)	3.801579862	0.045363028
Cd74	NM_010545	CD74 antigen (invariant polypeptide of major histocompatibility complex, class II antigen-associated)	3.799278734	0.001950082
Hcls1	NM_008225	hematopoietic cell specific Lyn substrate 1	3.774521989	0.083661933

Naip6	NM_010871	NLR family, apoptosis inhibitory protein 6	3.738722175	0.055858757
Cytip	NM_139200	cytohesin 1 interacting protein	3.728414089	0.026871139
Rbm47	NM_178446	RNA binding motif protein 47	3.639691891	0.027480382
BC035044	NA	NA	3.618047001	0.108808862
Havcr2	NM_134250	hepatitis A virus cellular receptor 2	3.59418802	0.000990744
Zfp750	NM_178763	zinc finger protein 750	3.592940282	0.083661933
Plaur	NM_011113	plasminogen activator, urokinase receptor	3.553413283	0.006554677
Ptger3	NM_011196	prostaglandin E receptor 3 (subtype EP3)	3.540126007	0.040802317
Bcl6b	NM_007528	B-cell CLL/lymphoma 6, member B	3.508937177	0.103290198
Gm6498	NR_003630	glyceraldehyde-3-phosphate dehydrogenase pseudogene	3.501871907	0.059297785
Tnfrsf11a	NM_009399	tumor necrosis factor receptor superfamily, member 11a	3.487932848	0.005834312
Ptafr	NM_001081211	platelet-activating factor receptor	3.437012452	0.060013973
Ptger4	NM_008965	prostaglandin E receptor 4 (subtype EP4)	3.42559694	0.002276021
Rgs1	NM_015811	regulator of G-protein signaling 1	3.411881342	0.002157656
Thbd	NM_009378	thrombomodulin	3.368647699	0.024655659
Tifa	NM_145133	TRAF-interacting protein with forkhead-associated domain	3.298816221	0.001546818
Hhex	NM_008245	hematopoietically expressed homeobox	3.293967047	0.023610027
Clec5a	NM_021364	C-type lectin domain family 5, member a	3.287027003	0.002586939
Cxcl2	NM_009140	chemokine (C-X-C motif) ligand 2	3.281311465	0.004152143
Tktl2	NM_028927	transketolase-like 2	3.19453471	0.045043827
Igf1	NM_184052	insulin-like growth factor 1	3.191236068	0.000476339
Efcab6	NM_029946	EF-hand calcium binding domain 6	3.153368616	0.060865513
Galntl6	NM_175032	UDP-N-acetyl-alpha-D-galactosamine:polypeptide N-acetylgalactosaminyltransferase-like 6	3.130670976	0.029785744
Cd48	NM_007649	CD48 antigen	3.124335837	0.031140506
Gm10125	NR_033552.1	NA	3.066115344	0.108808862
Bcl2a1b	NM_007534	B-cell leukemia/lymphoma 2 related protein A1b	3.052031934	0.030894634
Tlr7	NM_133211	toll-like receptor 7	3.012613166	0.003176829
Mdfic	NM_175088	MyoD family inhibitor domain containing	3.000413319	0.062507406

Clec7a	NM_020008	C-type lectin domain family 7, member a	2.998874501	0.029486386
Thbs1	NM_011580	thrombospondin 1	2.992403087	0.005077278
C730002L(	NA	NA	2.978143453	0.103342177
Cd84	NM_013489	CD84 antigen	2.974677105	0.051248528
Cd163	NM_053094	CD163 antigen	2.9243101	0.043310111
Xirp2	NM_001083919	xin actin-binding repeat containing 2	2.889392445	0.046246529
Gem	NM_010276	GTP binding protein (gene overexpressed in skeletal muscle)	2.86003351	0.006554677
Fyb	NM_011815	FYN binding protein	2.846083059	0.003176829
6230400D	NR_029446	RIKEN cDNA 6230400D17 gene	2.796927695	0.050636828
Htr1a	NM_008308	5-hydroxytryptamine (serotonin) receptor 1A	2.779612438	0.083496921
Brip1	NM_178309	BRCA1 interacting protein C-terminal helicase 1	2.770327857	0.069160805
Cd14	NM_009841	CD14 antigen	2.765121885	0.001449844
Lilrb4	NM_013532	leukocyte immunoglobulin-like receptor, subfamily B, member 4	2.754840654	0.013983452
Tlr1	NM_030682	toll-like receptor 1	2.695662134	0.087360725
Tlr4	NM_021297	toll-like receptor 4	2.688877039	0.029486386
Tlr2	NM_011905	toll-like receptor 2	2.650120794	0.03547538
Ptprc	NM_011210	protein tyrosine phosphatase, receptor type, C	2.646391896	0.030131099
Map3k14	NM_016896	mitogen-activated protein kinase kinase kinase 14	2.617644344	0.065877738
Birc3	NM_007464	baculoviral IAP repeat-containing 3	2.596910183	0.101102861
Gpr34	NM_011823	G protein-coupled receptor 34	2.569654635	0.064189922
Map3k8	NM_007746	mitogen-activated protein kinase kinase kinase 8	2.56525875	0.074343946
Anxa3	NM_013470	annexin A3	2.555351797	0.047777933
Papss2	NM_011864	3'-phosphoadenosine 5'-phosphosulfate synthase 2	2.534684185	0.101344262
Gm10767	NM_001177750.1	NA	2.527897387	0.082569681
Tfpi	NM_011576	tissue factor pathway inhibitor	2.522363268	0.108953854
Gcnt1	NM_173442	glucosaminyl (N-acetyl) transferase 1, core 2	2.516057547	0.026048628

Zfp217	NM_001159683	zinc finger protein 217	2.501735889	0.103290198
Ikzf1	NM_009578	IKAROS family zinc finger 1	2.501261987	0.017585034
Ncf2	NM_010877	neutrophil cytosolic factor 2	2.499118594	0.072774904
C3ar1	NM_009779	complement component 3a receptor 1	2.485119272	0.040802317
E230029C(	NR_015614	RIKEN cDNA E230029C05 gene	2.47104568	0.108083818
Rai14	NM_030690	retinoic acid induced 14	2.462467241	0.006554677
Pcsk2os2	NA	NA	2.441198366	0.106602924
Tnfaip3	NM_009397	tumor necrosis factor, alpha-induced protein 3	2.438394932	5.13E-05
Neurl3	NM_153408	neuralized homolog 3 homolog (Drosophila)	2.435101475	0.089894647
Lair1	NM_178611	leukocyte-associated Ig-like receptor 1	2.431905213	0.004817356
Pik3cd	NM_008840	phosphatidylinositol 3-kinase catalytic delta polypeptide	2.423512691	0.103290198
Ctss	NM_021281	cathepsin S	2.418300802	0.010989006
Adap2	NM_172133	ArfGAP with dual PH domains 2	2.396433379	0.019468765
Cd83	NM_009856	CD83 antigen	2.376335857	0.000184908
Pou2f2	NM_011138	POU domain, class 2, transcription factor 2	2.366876627	0.070290372
Plek	NM_019549	pleckstrin	2.331299776	0.006554677
Itga6	NM_008397	integrin alpha 6	2.32403144	0.00225021
Mertk	NM_008587	c-mer proto-oncogene tyrosine kinase	2.31366549	0.001546818
Cfh	NM_009888	complement component factor h	2.259814638	0.090608072
Ccrl2	NM_017466	chemokine (C-C motif) receptor-like 2	2.246285132	0.070493103
Itga4	NM_010576	integrin alpha 4	2.235147806	0.017637885
Fbxw15	NM_199036	F-box and WD-40 domain protein 15	2.23357624	0.056557518
Pik3cg	NM_020272	phosphoinositide-3-kinase, catalytic, gamma polypeptide	2.23314805	0.00895358
Cd93	NM_010740	CD93 antigen	2.229904252	0.029036623
Il1a	NM_010554	interleukin 1 alpha	2.225654197	0.019345398
Hexb	NM_010422	hexosaminidase B	2.224172546	0.003176829
Arhgap30	NM_001005508	Rho GTPase activating protein 30	2.195583653	0.076713094
Mpeg1	NM_010821	macrophage expressed gene 1	2.195385003	0.003176829
9530091C(	NR_033299	RIKEN cDNA 9530091C08 gene	2.188794798	0.090379122
Cdk6	NM_009873	cyclin-dependent kinase 6	2.178094718	0.040919454
AF251705	NM_134158	cDNA sequence AF251705	2.172794667	0.103290198

Igsf6	NM_030691	immunoglobulin superfamily, member 6	2.15740203	0.013861277
Fcrls	NM_030707	Fc receptor-like S, scavenger receptor	2.146811221	0.081194086
Nxpe3	NM_001134456.1	NA	2.141678296	0.029486386
Cx3cr1	NM_009987	chemokine (C-X3-C) receptor 1	2.141528422	0.004337294
Adrb2	NM_007420	adrenergic receptor, beta 2	2.138178443	0.103290198
Fam105a	NM_198301	family with sequence similarity 105, member A	2.13519949	0.01060591
Deptor	NM_145470.2	NA	2.112302563	0.023610027
Arhgdib	NM_007486	Rho, GDP dissociation inhibitor (GDI) beta	2.110547926	0.026791633
Cd53	NM_007651	CD53 antigen	2.09216435	0.030131099
Aim2	NM_001013779	absent in melanoma 2	2.086174646	0.040332427
Cyp4v3	NM_133969	cytochrome P450, family 4, subfamily v, polypeptide 3	2.052195743	0.095529097
P2ry13	NM_028808	purinergic receptor P2Y, G-protein coupled 13	2.049317749	0.012407292
Hspa1b	NM_010478	heat shock protein 1B	2.00764686	0.039294848
Arhgef6	NM_152801	Rac/Cdc42 guanine nucleotide exchange factor (GEF) 6	1.995659314	0.023730411
Ly86	NM_010745	lymphocyte antigen 86	1.993380193	0.049649098
Ripk2	NM_138952	receptor (TNFRSF)-interacting serine-threonine kinase 2	1.989714393	0.091582765
Gyk	NM_212444	glycerol kinase	1.989515569	0.043583959
Ctsc	NM_009982	cathepsin C	1.988368353	0.052887162
P2ry12	NM_027571	purinergic receptor P2Y, G-protein coupled 12	1.983697781	0.063524414
Mafb	NM_010658	v-maf musculoaponeurotic fibrosarcoma oncogene family, protein B (avian)	1.956595269	0.010989006
Abca9	NM_147220	ATP-binding cassette, sub-family A (ABC1), member 9	1.948654468	0.00926261
Znrf2	NM_199143	zinc and ring finger 2	1.946520825	0.019345398
Zfp36l1	NM_007564	zinc finger protein 36, C3H type-like 1	1.941967816	0.029656196
Inpp4b	NM_001024617	inositol polyphosphate-4-phosphatase, type II	1.924979203	0.070136838

Maf	NM_001025577	avian musculoaponeurotic fibrosarcoma (v-maf) AS42 oncogene homolog	1.913652788	0.047777933
Nrp1	NM_008737	neuropilin 1	1.878016185	0.043583959
Pnpla7	NM_146251	patatin-like phospholipase domain containing 7	1.861329193	0.055868414
Rgs2	NM_009061	regulator of G-protein signaling 2	1.815402044	0.007441329
Cd68	NM_009853	CD68 antigen	1.793023858	0.047182418
Nek6	NM_021606	NIMA (never in mitosis gene a)-related expressed kinase 6	1.78980321	0.029656196
Adcy8	NM_009623	adenylate cyclase 8	1.780718394	0.084492458
Spock3	NM_023689	sparc/osteonectin, cwcv and kazal-like domains proteoglycan 3	1.773136556	0.052787992
Gpc5	NM_175500	glypican 5	1.766514525	0.029486386
Nfkbiz	NM_030612	nuclear factor of kappa light polypeptide gene enhancer in B-cells inhibitor, zeta	1.765616817	0.040802317
Plin2	NM_007408	perilipin 2	1.763222042	0.103290198
Kcnc2	NM_001025581	potassium voltage gated channel, Shaw-related subfamily, member 2	1.759507764	0.091598816
Mlip	NA	NA	1.755486192	0.066088455
Lyn	NM_010747	Yamaguchi sarcoma viral (v-yes-1) oncogene homolog	1.748441931	0.108808862
Kctd12	NM_177715	potassium channel tetramerisation domain containing 12	1.745113914	0.026791633
9130024F1	NR_024326	RIKEN cDNA 9130024F11 gene	1.740193831	0.093247532
Tgfbr1	NM_009370	transforming growth factor, beta receptor I	1.737496557	0.039294848
Snhg11	NM_175692	small nucleolar RNA host gene 11	1.715699865	0.052787992
Hspa1a	NM_010479	heat shock protein 1A	1.68877985	0.036994744
Stk17b	NM_133810	serine/threonine kinase 17b (apoptosis-inducing)	1.68009191	0.050636828
Nwd2	NM_001144990.1	NA	1.676378153	0.049649098
Lactb2	NM_145381	lactamase, beta 2	1.618019864	0.074441737
Tsc22d3	NM_010286	TSC22 domain family, member 3	1.59265972	0.028864281
Amy1	NM_007446	amylase 1, salivary	1.591868772	0.093625384
Mef2c	NM_025282	myocyte enhancer factor 2C	1.585598634	0.043310111

Slc30a10	NM_001033286	solute carrier family 30, member 10	1.55943293	0.103290198
Ociad2	NM_026950	OCIA domain containing 2	1.556571931	0.089894647
Lcp1	NM_008879	lymphocyte cytosolic protein 1	1.536184608	0.103342177
Asph	NM_133723	aspartate-beta-hydroxylase	1.5322978	0.039294848
Cd2ap	NM_009847	CD2-associated protein	1.517237612	0.043583959
Tmem56	NM_178936	transmembrane protein 56	1.489381355	0.088670801
Axl	NM_009465	AXL receptor tyrosine kinase	1.468642017	0.077383796
Man2a1	NM_008549	mannosidase 2, alpha 1	1.414652636	0.082569681
Adamts20	NM_177431	a disintegrin-like and metallopeptidase (reprolysin type) with thrombospondin type 1 motif, 20	1.403952219	0.085329719
Dnajb4	NM_027287	DnaJ (Hsp40) homolog, subfamily B, member 4	1.353302852	0.098872329
Sdcbp	NM_016807	syndecan binding protein	1.264722907	0.090161184
Cep97	NM_028815	centrosomal protein 97	1.242768614	0.073632838
Abca1	NM_013454	ATP-binding cassette, sub-family A (ABC1), member 1	1.202086073	0.078462889
Sgk1	NM_011361	serum/glucocorticoid regulated kinase 1	1.099690559	0.092423491
Arid5b	NM_023598	AT rich interactive domain 5B (MRF1-like)	1.082210213	0.105946651
Slc16a1	NM_009196	solute carrier family 16 (monocarboxylic acid transporters), member 1	1.08164323	0.103290198
Arrdc3	NM_001042591	arrestin domain containing 3	1.067785911	0.045702168
Ccp110	NM_001199022.	NA	1.045252864	0.073107184
Ttll7	NM_027594	tubulin tyrosine ligase-like family, member 7	1.045126337	0.065877738
Scd1	NM_009127	stearoyl-Coenzyme A desaturase 1	0.983349914	0.103290198
Lrrn3	NM_010733	leucine rich repeat protein 3, neuronal	-0.985473618	0.107662718
Ncan	NM_007789	neurocan	-0.988395301	0.106683354
Tnfrsf21	NM_178589	tumor necrosis factor receptor superfamily, member 21	-1.027339254	0.101102861
Idh1	NM_010497	isocitrate dehydrogenase 1 (NADP+), soluble	-1.038767932	0.087360725
Trio	NM_001081302	triple functional domain (PTPRF interacting)	-1.074871169	0.086603314
Sox11	NM_009234	SRY-box containing gene 11	-1.090337012	0.071844195
Sox6	NM_011445	SRY-box containing gene 6	-1.095889434	0.090161184

Stat1	NM_009283	signal transducer and activator of transcription 1	-1.121243115	0.043583959
Chst2	NM_018763	carbohydrate sulfotransferase 2	-1.134594643	0.068066727
Marcksl1	NM_010807	MARCKS-like 1	-1.136017037	0.071138775
Ptprt	NM_021464	protein tyrosine phosphatase, receptor type, T	-1.152333468	0.052887162
Slc1a1	NM_009199	solute carrier family 1 (neuronal/epithelial high affinity glutamate transporter, system Xag), member 1	-1.17239853	0.051248528
Lamc1	NM_010683	laminin, gamma 1	-1.185397742	0.084214867
Map1b	NM_005909	NA	-1.193007711	0.101065555
Fabp5	NM_010634	fatty acid binding protein 5, epidermal	-1.206828282	0.040332427
Atat1	NM_001254952.1	NA	-1.236099141	0.065877738
Lrrc16a	NM_026825	leucine rich repeat containing 16A	-1.239230333	0.093247532
Neu4	NM_173772	sialidase 4	-1.250058885	0.092408269
Reep1	NM_178608	receptor accessory protein 1	-1.252183712	0.042972727
Cyfip2	NM_133769	cytoplasmic FMR1 interacting protein 2	-1.255254301	0.049649098
Myc	NM_010849	myelocytomatosis oncogene	-1.2656092	0.108953854
Klhl5	NM_175174	kelch-like 5 (Drosophila)	-1.270448367	0.041844204
3-Sep	NM_011889	septin 3	-1.274133257	0.06234243
Samd4b	NM_175021	sterile alpha motif domain containing 4B	-1.276486186	0.108808862
Bri3bp	NM_029752	Bri3 binding protein	-1.287289134	0.074065468
Gltp	NM_019821	glycolipid transfer protein	-1.291781843	0.100989168
Zadh2	NM_146090	zinc binding alcohol dehydrogenase, domain containing 2	-1.293933375	0.108808862
Tns3	NM_001083587	tensin 3	-1.300655	0.044042082
Gpr165	NM_029536	G protein-coupled receptor 165	-1.302188736	0.099193861
Tmem108	NM_178638	transmembrane protein 108	-1.311541029	0.059140574
Aldh1l2	NM_153543	aldehyde dehydrogenase 1 family, member L2	-1.314847949	0.041844204
Parp12	NM_172893	poly (ADP-ribose) polymerase family, member 12	-1.318309937	0.093247532
Dynll2	NM_026556	dynein light chain LC8-type 2	-1.324533277	0.055528985
Nova2	NM_001029877	neuro-oncological ventral antigen 2	-1.330111692	0.103342177

Nmnat2	NM_175460	nicotinamide nucleotide adenylyltransferase 2	-1.336019729	0.064189922
Lsamp	NM_175548	limbic system-associated membrane protein	-1.36313735	0.060881523
Arhgef7	NM_017402	Rho guanine nucleotide exchange factor (GEF7)	-1.369006827	0.071206273
Tmem163	NM_028135	transmembrane protein 163	-1.369856117	0.047102007
S100b	NM_009115	S100 protein, beta polypeptide, neural	-1.381254404	0.090161184
Rimklb	NM_027664	ribosomal modification protein rimK-like family member B	-1.382117489	0.041844204
Armcx2	NM_026139	armadillo repeat containing, X-linked 2	-1.386472004	0.108808862
Sulf2	NM_028072	sulfatase 2	-1.395524545	0.029486386
Natd1	NM_152914.2	NA	-1.40320458	0.091582765
Kank1	NM_181404	KN motif and ankyrin repeat domains 1	-1.414211493	0.092423491
Stat2	NM_019963	signal transducer and activator of transcription 2	-1.415261099	0.035451108
Cachd1	NM_198037	cache domain containing 1	-1.416048649	0.082974355
Itpr2	NM_019923	inositol 1,4,5-triphosphate receptor 2	-1.454214805	0.037603524
Eps8	NM_007945	epidermal growth factor receptor pathway substrate 8	-1.469143258	0.03547538
Lbh	NM_029999	limb-bud and heart	-1.474357079	0.083496921
Ppfibp1	NM_026221	PTPRF interacting protein, binding protein 1 (liprin beta 1)	-1.48485944	0.042889872
Gap43	NM_008083	growth associated protein 43	-1.487365941	0.040802317
D630045J1	NM_194061	RIKEN cDNA D630045J12 gene	-1.498885196	0.004666537
Mpzl1	NM_001083897	myelin protein zero-like 1	-1.52408578	0.072503522
Prom1	NM_008935	prominin 1	-1.526564205	0.039294848
Tmem176	NM_025326	transmembrane protein 176A	-1.53124212	0.103290198
Fyn	NM_008054	Fyn proto-oncogene	-1.542038383	0.005555138
Nfasc	NM_182716	neurofascin	-1.548324004	0.083775824
Bcas1	NM_029815	breast carcinoma amplified sequence 1	-1.550747274	0.020759879
Dlgap4	NM_146128	discs, large homolog-associated protein 4 (Drosophila)	-1.564600949	0.093181547
Irs1	NM_010570	insulin receptor substrate 1	-1.567947613	0.040919454
Arhgap35	NM_004491.4	NA	-1.584483426	0.006554677

Atp6v0a2	NM_011596	ATPase, H+ transporting, lysosomal V0 subunit A2	-1.587825344	0.026791633
Sema5b	NM_013661	sema domain, seven thrombospondin repeats (type 1 and type 1-like), transmembrane domain (TM) and short cytoplasmic domain, (semaphorin) 5B	-1.590310149	0.023730411
Igsf3	NM_207205	immunoglobulin superfamily, member 3	-1.593426695	0.049649098
Ddx58	NM_172689	DEAD (Asp-Glu-Ala-Asp) box polypeptide 58	-1.593752111	0.029656196
Igdcc4	NM_020043	immunoglobulin superfamily, DCC subclass, member 4	-1.602044735	0.099224558
Rnf122	NM_175136	ring finger protein 122	-1.604993961	0.031140506
Masp1	NM_008555	mannan-binding lectin serine peptidase 1	-1.607908517	0.103508983
Tnr	NM_022312	tenascin R	-1.615109719	0.037603524
Casp3	NM_009810	caspase 3	-1.615480035	0.004036048
Plekha6	NM_182930	pleckstrin homology domain containing, family A member 6	-1.619549889	0.090041351
Sh3rf1	NM_021506	SH3 domain containing ring finger 1	-1.628682193	0.106683354
Igsf10	NM_001162884	immunoglobulin superfamily, member 10	-1.633506602	0.018569279
Tcf7l2	NM_009333	transcription factor 7-like 2, T-cell specific, HMG-box	-1.633592483	0.002586939
Pde9a	NM_008804	phosphodiesterase 9A	-1.658259913	0.060865513
AI414108	NR_027907	expressed sequence AI414108	-1.658330942	0.062882038
Socs3	NM_007707	suppressor of cytokine signaling 3	-1.661634423	0.099373528
Sez6l	NM_019982	seizure related 6 homolog like	-1.685862446	0.060881523
Prdx2	NM_011563	peroxiredoxin 2	-1.689976932	0.107792468
Adamts17	NM_001033877	a disintegrin-like and metallopeptidase (reprolysin type) with thrombospondin type 1 motif, 17	-1.69113508	0.109454738
Inppl1	NM_010567	inositol polyphosphate phosphatase-like 1	-1.706183276	0.107944847
Chst3	NM_016803	carbohydrate (chondroitin 6/keratan) sulfotransferase 3	-1.709636351	0.065877738
Bcan	NM_007529	brevican	-1.732370237	0.066853751
Gpr17	NM_001025381	G protein-coupled receptor 17	-1.735249888	0.106688329

Slc39a1	NM_013901	solute carrier family 39 (zinc transporter), member 1	-1.738559219	0.041515601
Nhsl2	NM_001163610	NHS-like 2	-1.747195215	0.015172992
Lims2	NM_144862	LIM and senescent cell antigen like domains 2	-1.74880791	0.041663006
Mycl	NM_008506	v-myc myelocytomatosis viral oncogene homolog 1, lung carcinoma derived (avian)	-1.750733932	0.06234243
Pik3r3	NM_181585	phosphatidylinositol 3 kinase, regulatory subunit, polypeptide 3 (p55)	-1.75302521	0.001717044
D430019H	NM_001252508	RIKEN cDNA D430019H16 gene	-1.753123372	0.046246529
C1ql1	NM_011795	complement component 1, q subcomponent-like 1	-1.753293344	0.105946651
Rab33a	NM_011228	RAB33A, member of RAS oncogene family	-1.773841983	0.05867893
Notch1	NM_008714	Notch gene homolog 1 (Drosophila)	-1.789233875	0.072503522
Alox5	NM_009662	arachidonate 5-lipoxygenase	-1.790569946	0.092408269
Gpr37l1	NM_134438	G protein-coupled receptor 37-like 1	-1.810813518	0.072503522
Sox4	NM_009238	SRY-box containing gene 4	-1.845841689	0.108953854
Capn6	NM_007603	calpain 6	-1.846962453	0.037603524
Zfp579	NM_026741	zinc finger protein 579	-1.850077283	0.083661933
Proser3	NM_183321.1	NA	-1.873672573	0.106683354
Tubb2b	NM_023716	tubulin, beta 2B	-1.873777114	0.029486386
Ptpn14	NM_008976	protein tyrosine phosphatase, non-receptor type 14	-1.889033834	0.076297
Orai3	NM_198424	ORAI calcium release-activated calcium modulator 3	-1.897956475	0.093872544
Gpd1	NM_010271	glycerol-3-phosphate dehydrogenase 1 (soluble)	-1.900928559	0.040919454
Tuba1a	NM_011653	tubulin, alpha 1A	-1.910000175	0.044498669
Frmd4a	NM_172475	FERM domain containing 4A	-1.913679283	0.00131348
Ifit3	NM_010501	interferon-induced protein with tetratricopeptide repeats 3	-1.919950592	0.072503522
Hsd17b7	NM_010476	hydroxysteroid (17-beta) dehydrogenase 7	-1.957049275	0.000269231
Grik3	NM_001081097	glutamate receptor, ionotropic, kainate 3	-1.959254539	0.043583959
Col9a3	NM_009936	collagen, type IX, alpha 3	-1.97320811	0.001371605

Sv2c	NM_029210	synaptic vesicle glycoprotein 2c	-1.980937148	0.040919454
Slco5a1	NM_172841	solute carrier organic anion transporter family, member 5A1	-2.000958068	0.046869912
Col11a1	NM_007729	collagen, type XI, alpha 1	-2.008999482	0.006764762
Cdkn1c	NM_009876	cyclin-dependent kinase inhibitor 1C (P57)	-2.012039043	0.023833094
Fgfrl1	NM_054071	fibroblast growth factor receptor-like 1	-2.019094563	0.052787992
6430503K(	NA	NA	-2.020036369	0.107333026
Gareml	NM_001191033.1	NA	-2.054907608	0.03547538
Cnksr3	NM_172546	Cnksr family member 3	-2.073422266	0.019468765
Vash1	NM_177354	vasohibin 1	-2.087846837	0.06920456
Mical1	NM_138315	microtubule associated monoxygenase, calponin and LIM domain containing 1	-2.1099586	0.046285252
Gp1bb	NM_010327	glycoprotein Ib, beta polypeptide	-2.132071747	0.040802317
Cmpk2	NM_020557	cytidine monophosphate (UMP-CMP) kinase 2, mitochondrial	-2.134344146	0.00085028
1810041L1	NM_001163145	RIKEN cDNA 1810041L15 gene	-2.137381379	0.013983452
Hpgd	NM_008278	hydroxyprostaglandin dehydrogenase 15 (NAD)	-2.143943728	0.001035418
Fam84a	NM_029007	family with sequence similarity 84, member A	-2.172582024	0.103290198
5730559C:	NM_028872	RIKEN cDNA 5730559C18 gene	-2.215698973	0.069926956
Cnih2	NM_009920	cornichon homolog 2 (Drosophila)	-2.230661305	0.090161184
Usp18	NM_011909	ubiquitin specific peptidase 18	-2.239017017	0.023610027
Parvb	NM_133167	parvin, beta	-2.280595802	0.001546818
A930003O	NR_027362	RIKEN cDNA A930003O13 gene	-2.283847707	0.026791633
Rassf10	NM_175279	Ras association (RalGDS/AF-6) domain family (N terminal) member 10	-2.298533057	0.028145626
Trpc4	NR_046161	transient receptor potential cation channel, subfamily C, member 4	-2.353992388	0.005098262
Slc14a1	NM_028122	solute carrier family 14 (urea transporter), member 1	-2.395454858	0.005768312
Obsl1	NM_178884	obscurin-like 1	-2.40130539	0.10712552
Emx2os	NR_002863	empty spiracles homolog 2 (Drosophila) opposite strand	-2.43096442	0.070493103

Serpina3n	NM_009252	serine (or cysteine) peptidase inhibitor, clade A, member 3N	-2.458426449	1.19E-06
Igfbp7	NM_008048	insulin-like growth factor binding protein 7	-2.47827436	0.029486386
Panx1	NM_019482	pannexin 1	-2.502994353	0.029486386
Hinfp	NM_172162	histone H4 transcription factor	-2.505963362	0.081650873
Slc29a4	NM_146257	solute carrier family 29 (nucleoside transporters), member 4	-2.560384816	0.051389161
Pycr1	NM_144795	pyrroline-5-carboxylate reductase 1	-2.602380764	0.084598442
Rnd2	NM_009708	Rho family GTPase 2	-2.603075461	0.077383796
Mkrn3	NM_011746	makorin, ring finger protein, 3	-2.712149579	0.043583959
Kif19a	NM_001102615	kinesin family member 19A	-2.746671268	0.092583283
Gpr124	NM_054044	G protein-coupled receptor 124	-2.79101916	0.077859633
Gng4	NM_010317	guanine nucleotide binding protein (G protein), gamma 4	-2.855436611	1.20E-09
Sfrp1	NM_013834	secreted frizzled-related protein 1	-2.882905266	5.30E-08
Kcnj12	NM_010603	potassium inwardly-rectifying channel, subfamily J, member 12	-2.916907626	0.070890257
Klk8	NM_008940	kallikrein related-peptidase 8	-2.949352301	0.059063679
Tarbp2	NM_009319	TAR (HIV) RNA binding protein 2	-2.970943541	0.045855627
Clca1	NM_009899	chloride channel calcium activated 1	-3.014353356	0.071059705
Chrna7	NM_007390	cholinergic receptor, nicotinic, alpha polypeptide 7	-3.044121491	0.103290198
Spef1	NM_027641	sperm flagellar 1	-3.106153188	0.071937924
Col20a1	NM_028518	collagen, type XX, alpha 1	-3.160681413	2.99E-05
Efna3	NM_010108	ephrin A3	-3.279796284	0.105946651
C2cd4c	NM_198614	C2 calcium-dependent domain containing 4C	-3.299710589	0.044428841
Epcam	NM_008532	epithelial cell adhesion molecule	-3.301555372	0.054296527
Sfrp2	NM_009144	secreted frizzled-related protein 2	-3.537276148	0.057243188
Npy	NM_023456	neuropeptide Y	-3.549932867	0.051248528
Mdga1	NM_001081160	MAM domain containing glycosylphosphatidylinositol anchor 1	-3.567261267	0.006554677
Plcd1	NM_019676	phospholipase C, delta 1	-3.573455595	0.017637885
Dlx1as	NR_002854	distal-less homeobox 1, antisense	-3.647613386	0.013396784

Dyrk3	NM_145508	dual-specificity tyrosine-(Y)-phosphorylation regulated kinase 3	-3.679237551	0.034300764
Vwc2	NM_177033	von Willebrand factor C domain containing 2	-3.808534123	0.001950082
Kdm4d	NM_173433	lysine (K)-specific demethylase 4D	-3.965590737	0.029486386
Nxf2	NM_031259	nuclear RNA export factor 2	-4.729585348	0.090161184
Grpr	NM_008177	gastrin releasing peptide receptor	-4.825226756	0.019213878
Sypl2	NM_008596	synaptophysin-like 2	-5.126713493	0.085329719
Lefty2	NM_177099	left-right determination factor 2	-5.436269475	0.082858631
Dsp	NM_023842	desmoplakin	-5.472365287	0.003521921
Fasl	NM_010177	Fas ligand (TNF superfamily, member 6)	-5.478616819	0.052770673
Dpf3	NM_058212	D4, zinc and double PHD fingers, family 3	-6.069671465	0.011747404
Vmn2r2	NM_001104592	vomeronasal 2, receptor 2	-6.311822263	0.107944847
Lrrc10b	NM_001111140	leucine rich repeat containing 10B	-6.79134608	0.062358662
Irx2	NM_010574	Iroquois related homeobox 2 (Drosophila)	-7.37525677	0.103290198
Obox5	NM_145709	oocyte specific homeobox 5	-7.677931749	0.059063679
Tusc5	NM_177709	tumor suppressor candidate 5	-7.691067918	0.106688329
Vax1	NM_009501	ventral anterior homeobox containing gene 1	-8.380374412	0.103290198
2610206C	NA	NA	-8.400411189	0.052887162
Apol7a	NM_029419	apolipoprotein L 7a	-8.59684903	0.042926826
Npbwr1	NM_010342	neuropeptides B/W receptor 1	-8.798691452	0.014799167
Ucn2	NM_145077	urocortin 2	-8.921727784	0.040802317
2900057B	NA	NA	-9.271069356	0.106292712
D130009I1	NR_015593	RIKEN cDNA D130009I18 gene	-9.795648941	0.044652762
Olfr457	NM_146987	olfactory receptor 457	-9.838435004	0.063730579

Supplementary Table 9

Sources for Genome Wide Assocation Analysis

Study name	Species	Platform	Array type	Sample #	unique gene IDs (official gene symbol)	Note	Reference
Developing Cortical Efferent Neurons	Mouse	microarray	affy_moe430a	19	12249	CEL files	Arlotta, P., Molyneaux, B.J., Chen, J., Inoue, J., Kominami, R. & Macklis, J,D. Neuronal subtype-specific genes that control corticospinal motor neuron development in vivo. *Neuron* . **45**, 207-21. (2005)
Mouse Cortical Neurons: P7, P16, P28	Mouse	microarray	affy_mouse430_2	7	16240	CEL files	Cahoy, J.D. *et al* . A transcriptome database for astrocytes, neurons, and oligodendrocytes: a new resource for understanding brain development and function. *J Neurosci* **8**, 264-78 (2008).
Growth cone	Mouse	microarray	affy_mouse430_2	5	16240	CEL files	Zivraj, K.H. *et al* . Subcellular profiling reveals distinct and developmentally regulated repertoire of growth cone mRNAs. *J Neurosci* **30**, 15464-78 (2010).
Clitical Period Mouse (P28)	Mouse	microarray	affy_mg_u74av2	3	7912	CEL files	Lyckman, A.W., *et al* . Gene expression patterns in visual cortex during the critical period: synaptic stabilization and reversal by visual deprivation. Proc Natl Acad Sci U S A **105**, 9409-14 (2008)
	Mouse	microarray	affy_mgu_74bv2	3	6176	CEL files	
	Mouse	microarray	affy_mgu_74cv2 combined	3	3009	CEL files all samples replicates	

Retinal ganglion transection or crush	Rat	microarray	affy_rat230_2	35	10046	CEL files (one outlier:CRUCH_12H_B)	Agudo, M., *et al*. Time course profiling of the retinal transcriptome after optic nerve transection and optic nerve crush. *Mol Vis* **14**, 1050-63 (2008).
Exercise and hippo memory enhancement	Rat	microarray	Agilent-014879 4x44k (	4	35671	txt files (two channel arrays)	Inoue. K., Unpublished GEO data set. http://www.ncbi.nlm.nih.gov/geo/query/acc.cgi?acc=GSE45813
Motor cortex SCI	Rat	exon array	affy_ragene_1_0_st_v1	72	12503	CEL files	Jaerve, A., Schiwy, N., Schmitz, C., Mueller, H.W. Differential effect of aging on axon sprouting and regenerative growth in spinal cord injury. *Exp Neurol* **231**, 284-94 (2011)
Fear conditioning medial PFC	Mouse	Hiseq 2000	mm10	4	24060	SRA files	Bero, A.W., *et al*. Early remodeling of the neocortex upon episodic memory encoding. *Proc Natl Acad Sci U S* A 111, 11852-7 (2014)
Contralateral cortex stroke	Rat	BeadChip	ratRef-12 v1.0	25	21908	excel file (5 batches normalized), remove _"predicted" in gene symbol	Zai, L., *et al*. Inosine alters gene expression and axonal projections in neurons contralateral to a cortical infarct and improves skilled use of the impaired limb. *J Neurosci* **29**, 8187-97 (2009).

Supplementary Table 10

Primary Antibodies

Antibody	Species and type	Dilution	Source	Cat. #
GDF10	Rabbit polyclonal	1:100	Abgent	AP2069a
GDF10	Rabbit polyclonal	1:100	Life Technlogies (same epitope as above)	PA-11927
Tuj1	Mouse monoclonal	1:150	Covance Inc.	MMS-435P
Map2	Chicken polyclonal	1:150	Abcam	ab5392
NeuN	Mouse polyclonal	1:1000	Chemicon	MAB377B
SMI-312	Mouse monoclonal	1:1000	Abcam	ab24574
GFAP	Rat monoclonal	1:1000	Invitrogen	13-0300
CD31/PECAM-1	Rat monoclonal	1:500	BD Biosciences	553370
Iba1/AIF1	Goat polyoclonal	1:100	Abcam	ab5076
pSmad2/3	Goat polyclonal	1:50	Santa Cruz Biotechnology	sc-11769
pSmad2/3 (in vivo)	Rabbit monoclonal	1:200	Cell Signaling	8828
pSmad1/5/8	Rabbit polyclonal	1:100	Chemicon	AB3848
Tgfbr 2	Rabbit polyclonal	1:100	Santa Cruz Biotechnology	sc-1700
Tgfbr 3	Goat polyclonal	1:200	Santa Cruz Biotechnology	sc-6199
Smad1	Rabbit polyclonal	1:100	Invitrogen	38-5400
Smad2	Goat polyclonal	1:100	Santa Cruz Biotechnology	sc-6200
Smad3	Rabbit monoclonal	1:100	Abcam	ab40854
Smad5	Goat polyclonal	1:100	Santa Cruz Biotechnology	sc-7443
CD11b/c	Mouse monoclonal	1:500	Abcam	ab1211
VGLUT2	Guinea Pig Polyclonal	1:500	Millipore	AB2251
Homer1	Rabbit polyclonal	1:200	Synaptic Systems	160 003

Supplementary Table 11

Multiple Comparsions ANOVA and Tukey-Kramer Test for Differences Between Means in Figure 5

	GFAP				PEACM				IBA1			
	Mice #	vations	F	P	Mice #	vations	F	P	Mice #	vations	F	P
Normal control vs Stroke only	4	27	12.66496	0.00081	4	27	11.80752	0.00117	5	31	12.79323	0.00068
Normal control vs Scrambled+Stroke	4	27	13.32856	0.00053	4	27	95.60264	#######	5	31	10.86801	0.00163
Normal control vs siRNA+Stroke	5	27	6.63489	0.01272	5	27	12.29059	0.00091	5	31	0.00378	0.95115
Normal control vs GDF10+Stroke	4	27	41.55122	0.00852	4	27	57.00595	0.00765	5	31	64.65966	########
Normal contro lvs Protein control+Stroke	4	27	10.81345	0.00158	4	27	29.18284	0.03762	5	31	17.14702	0.00011
Stroke only vs Scrambled+Stroke	4	27	0.01008	0.92036	4	27	3.71511	0.05836	6	34	0.07899	0.77958
Stroke only vs siRNA+Stroke	4	27	3.03175	0.08724	4	27	1.92318	0.1711	6	34	9.74432	0.00268
Stroke only vs GDF10+Stroke	4	27	15.09757	0.00025	4	27	19.0559	0.00004	6	34	14.34361	0.00034
Stroke only vs Protein control+Stroke	4	27	0.01319	0.90891	4	27	1.80447	0.18351	6	34	0.47757	0.49198
Scrambled+Stroke vs siRNA+Stroke	6	39	6.13768	0.01805	6	39	14.80578	0.00031	5	32	8.88401	0.00408
Scrambled+Stroke vs GDF10+Stroke	6	39	21.27314	0.00002	6	39	17.95102	0.00006	5	32	8.60974	0.00466
Scrambled+Stroke vs Protein control+Stroke	6	39	0.00044	0.98329	6	39	0.04855	0.82616	5	32	0.10882	0.74259
siRNA+Stroke vs GDF10+Stroke	5	30	30.36185	0.00976	5	30	38.13568	0.04148	5	33	47.84595	0.04758
siRNA+Stroke vs Protein control+Stroke	5	30	2.64333	0.1083	5	30	10.34389	0.00194	5	33	13.39042	0.00051
Protein control+Stroke vs GDF10+Stroke	7	45	22.26683	0.0001	7	45	16.56525	0.0001	5	33	8.33919	0.00529